Measurement of the W boson mass with the LHCb detector

CERN seminar
29 June 2021

Mika Vesterinen,
University of Warwick,
on behalf of the LHCb Collaboration

LHCb-PAPER-2021-024 *in preparation*
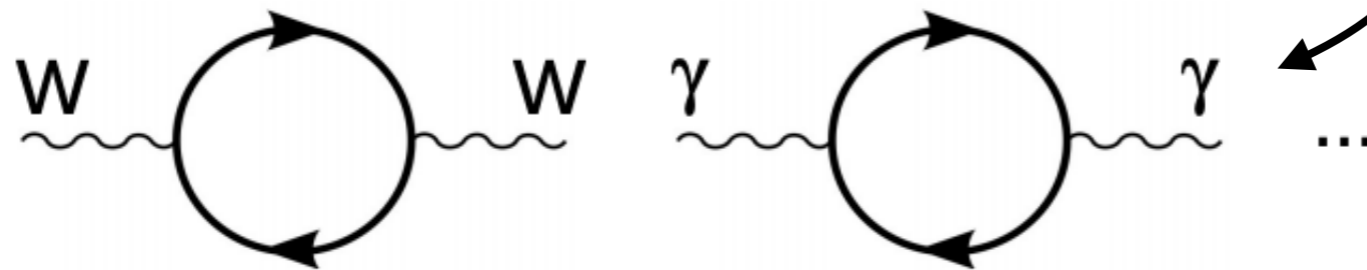
Scientific context
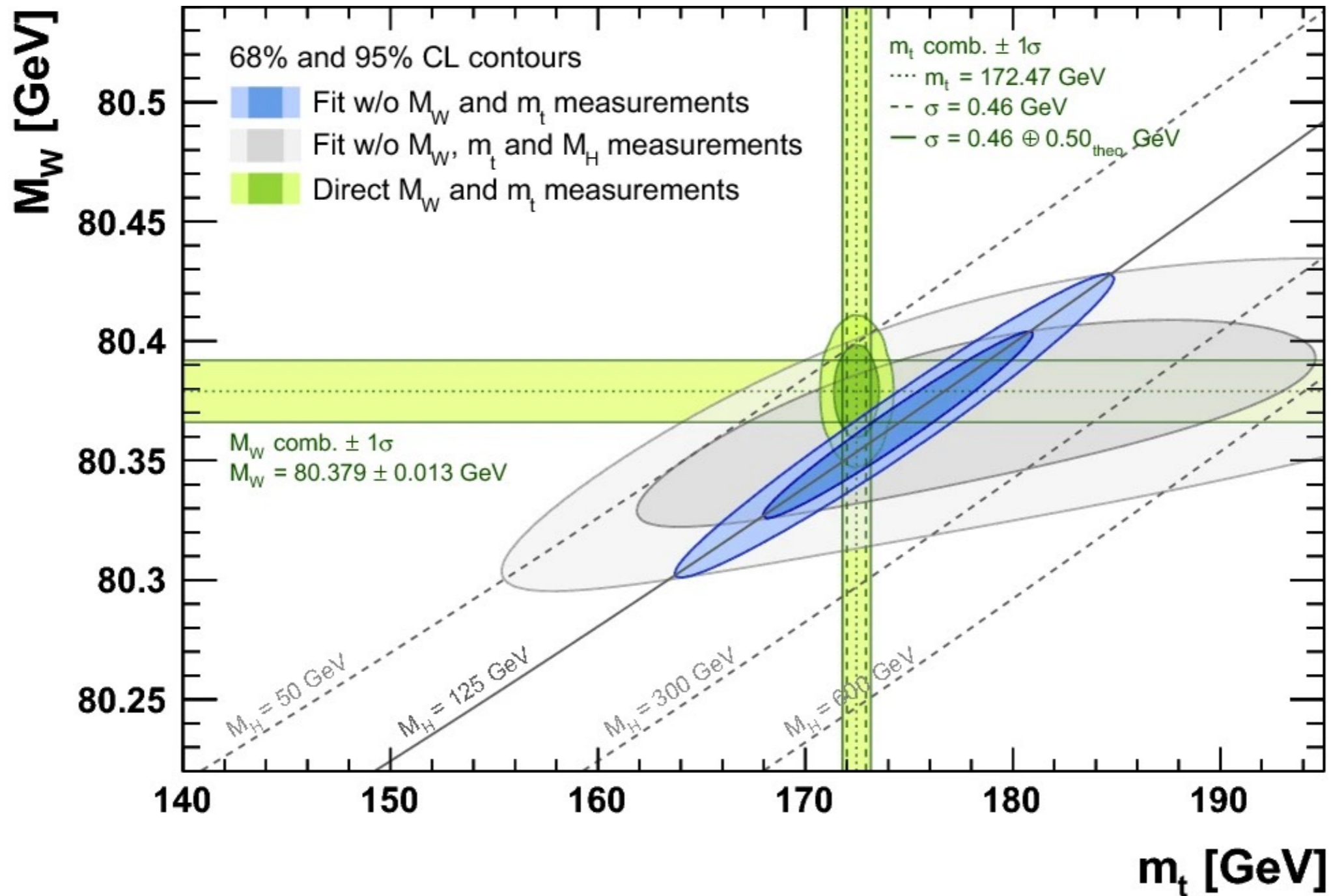

Three parameters (g, g', v) in electroweak theory.

Given m_Z, α and G_F, the W mass is predictable

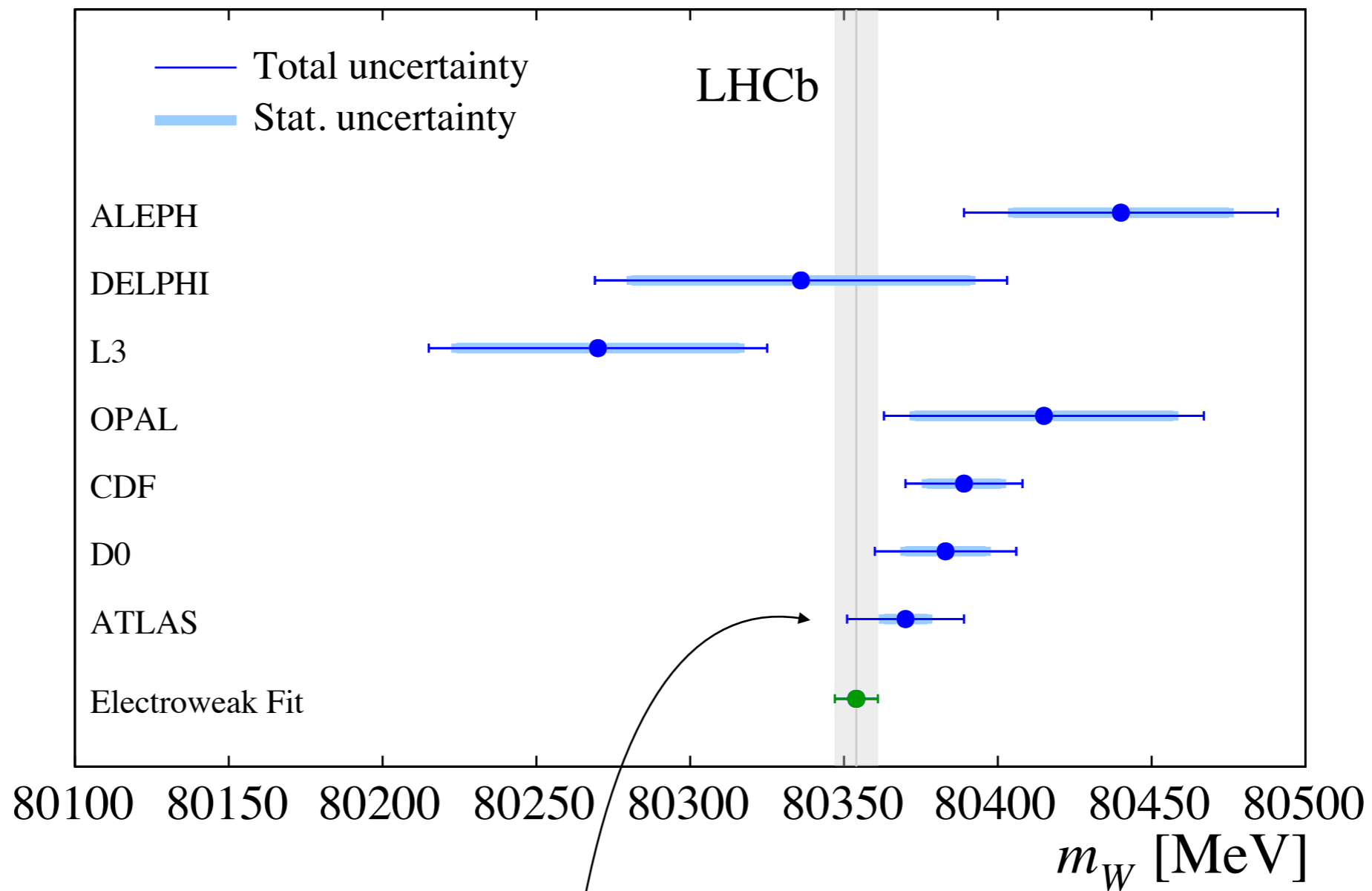$$m_W^2 \left(1 - \frac{m_W^2}{m_Z^2}\right) = \frac{\pi\alpha}{\sqrt{2}G_F}(1 + \Delta)$$

Global electroweak fit by the gFitter group [EPJC 78, 675 (2018)](#)

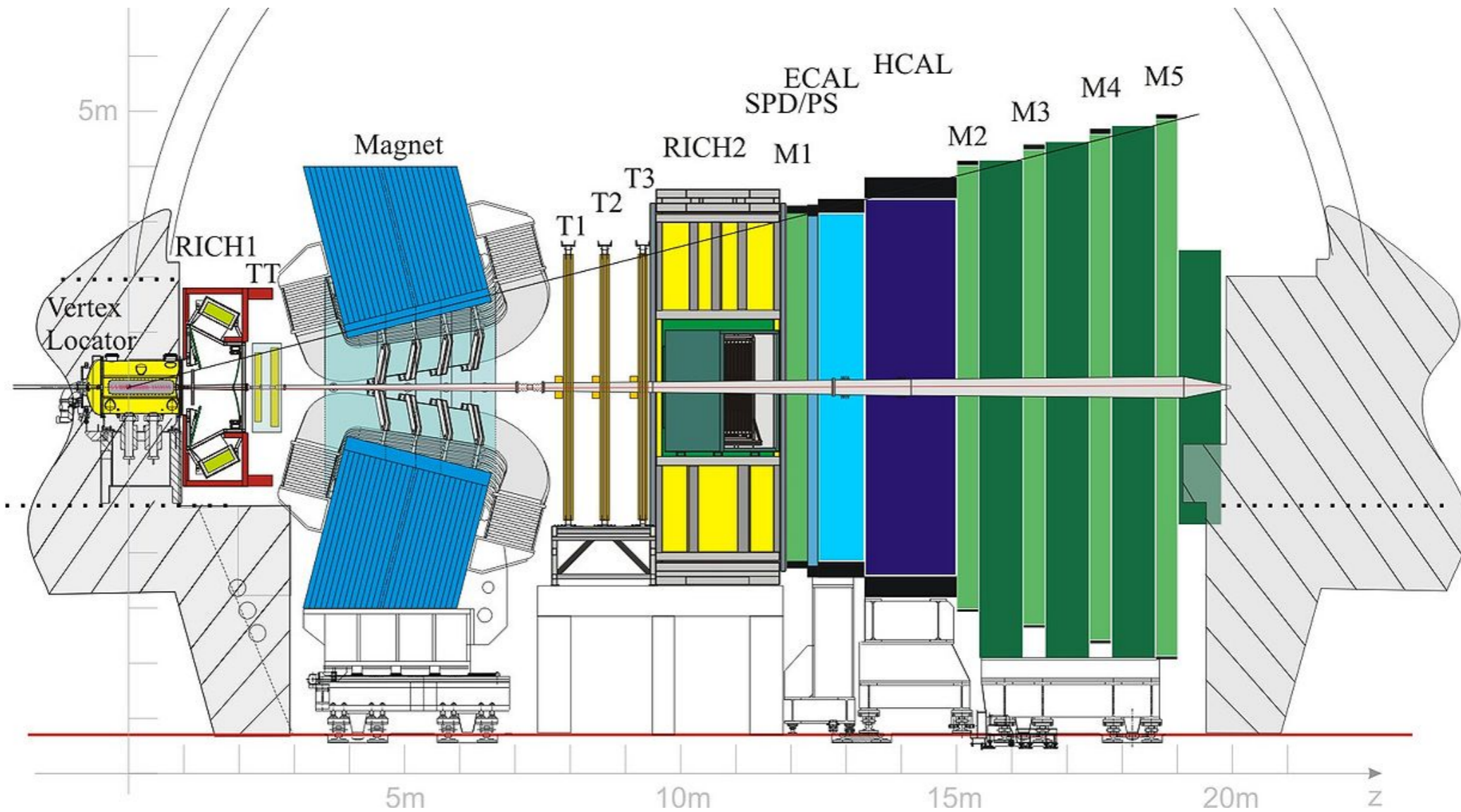Sensitivity to BSM physics is primarily limited by precision of direct measurements of m_W.

$m_W^{\text{pred}} = 80354 \pm 7 \text{ MeV}$

LHCb

ALEPH

DELPHI

L3

OPAL

CDF

D0

ATLAS

Electroweak Fit

Total uncertainty
Stat. uncertainty

m_W [MeV]

Most recent measurement by ATLAS (EPJC 78 (2018) 110) with 19 MeV uncertainty.

4

LHCb experiment

Small angle spectrometer, covering the pseudorapidity region $2 < \eta < 5$, primarily designed for precision study of b- and c-hadrons.

Unique opportunity for wide physics programme at large rapidity (y).

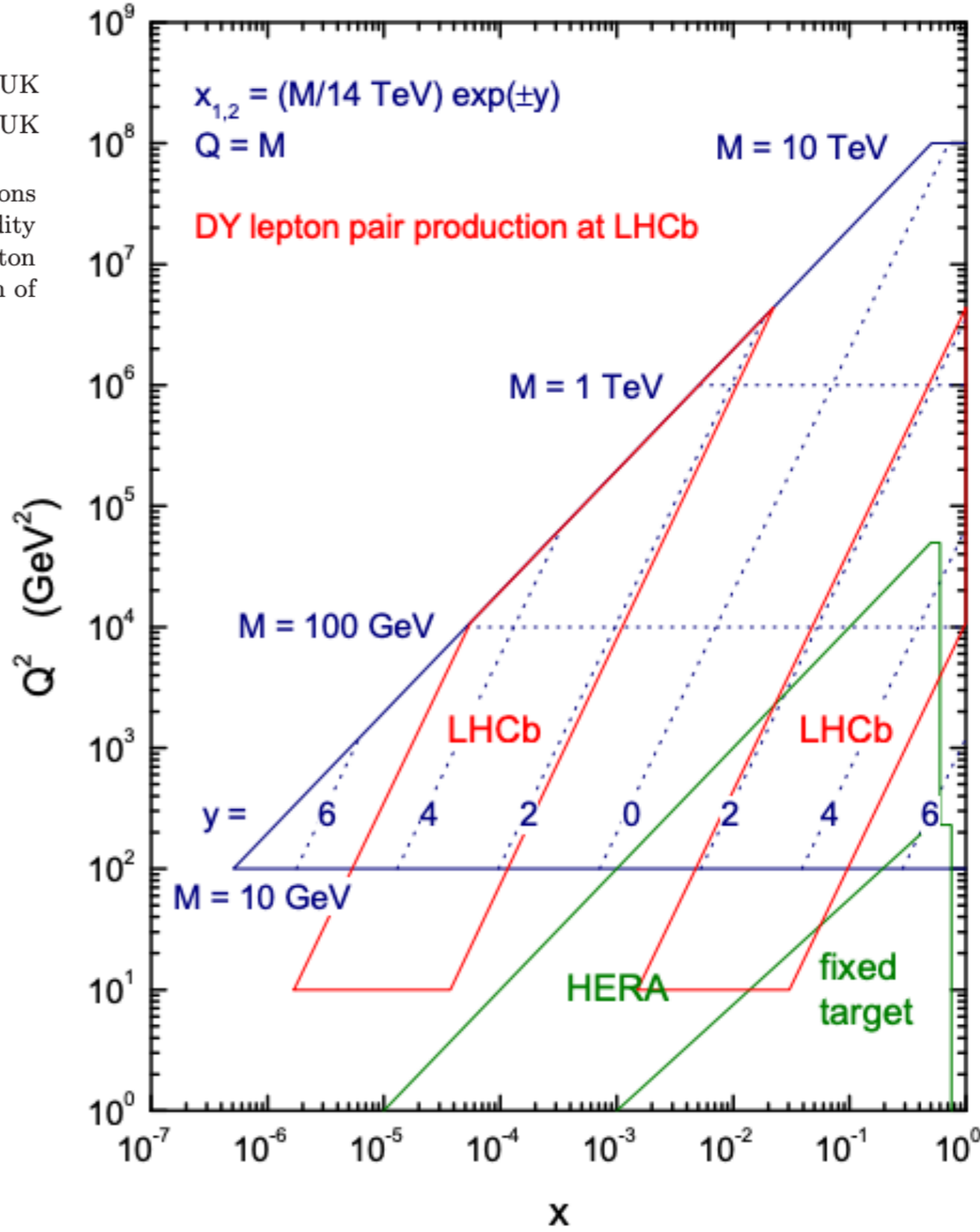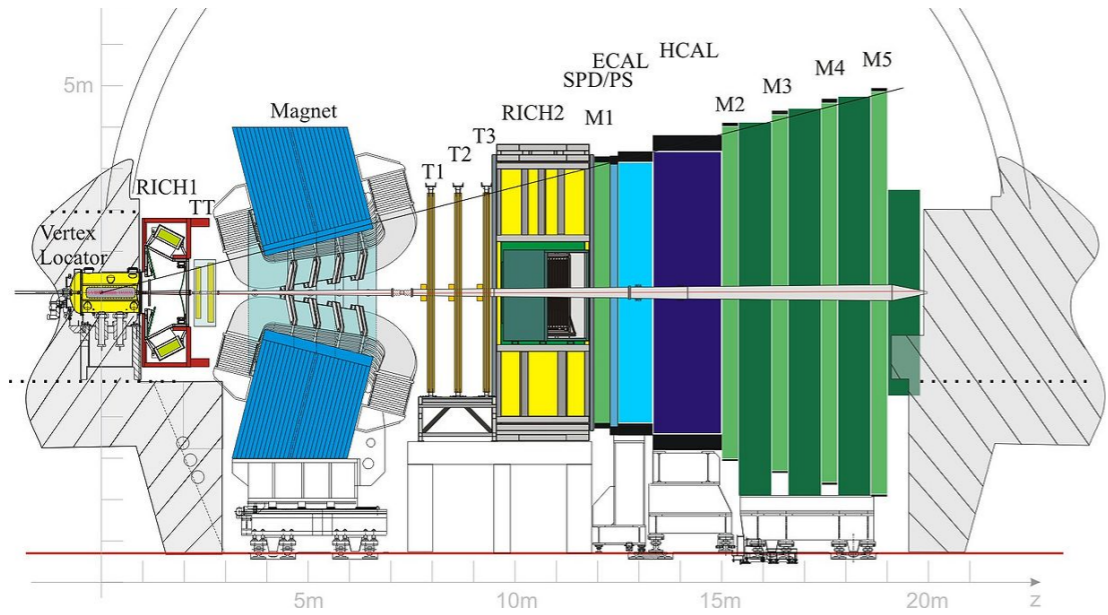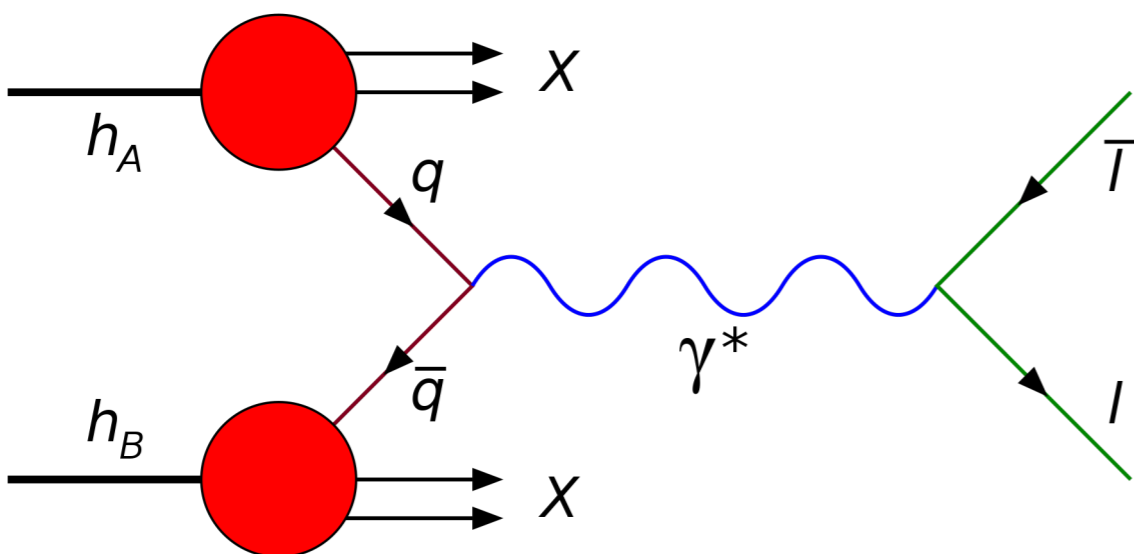# Vector boson production in LHCb and Parton Density Functions

Parton Distributions and QCD at LHCb

R.S. Thorne[1], A.D. Martin[2], W.J. Stirling[2] and G. Watt[1]

1- Department of Physics and Astronomy, University College London, WC1E 6BT, UK
2- Institute for Particle Physics Phenomenology, University of Durham, DH1 3LE, UK

We consider the impact that can be made on our understanding of parton distributions (PDFs) and QCD from early measurements at the LHCb experiment. The high rapidity values make the experiment uniquely suited to a detailed study of small-x parton distributions and hence will make a significant contribution towards the clarification of both experimental and theoretical uncertainties on PDFs and their applications.

Vector boson production in LHCb and Parton Density Functions

Some figures from one of many examples* of LHCb measurements of vector boson production

JHEP 01 (2016) 155
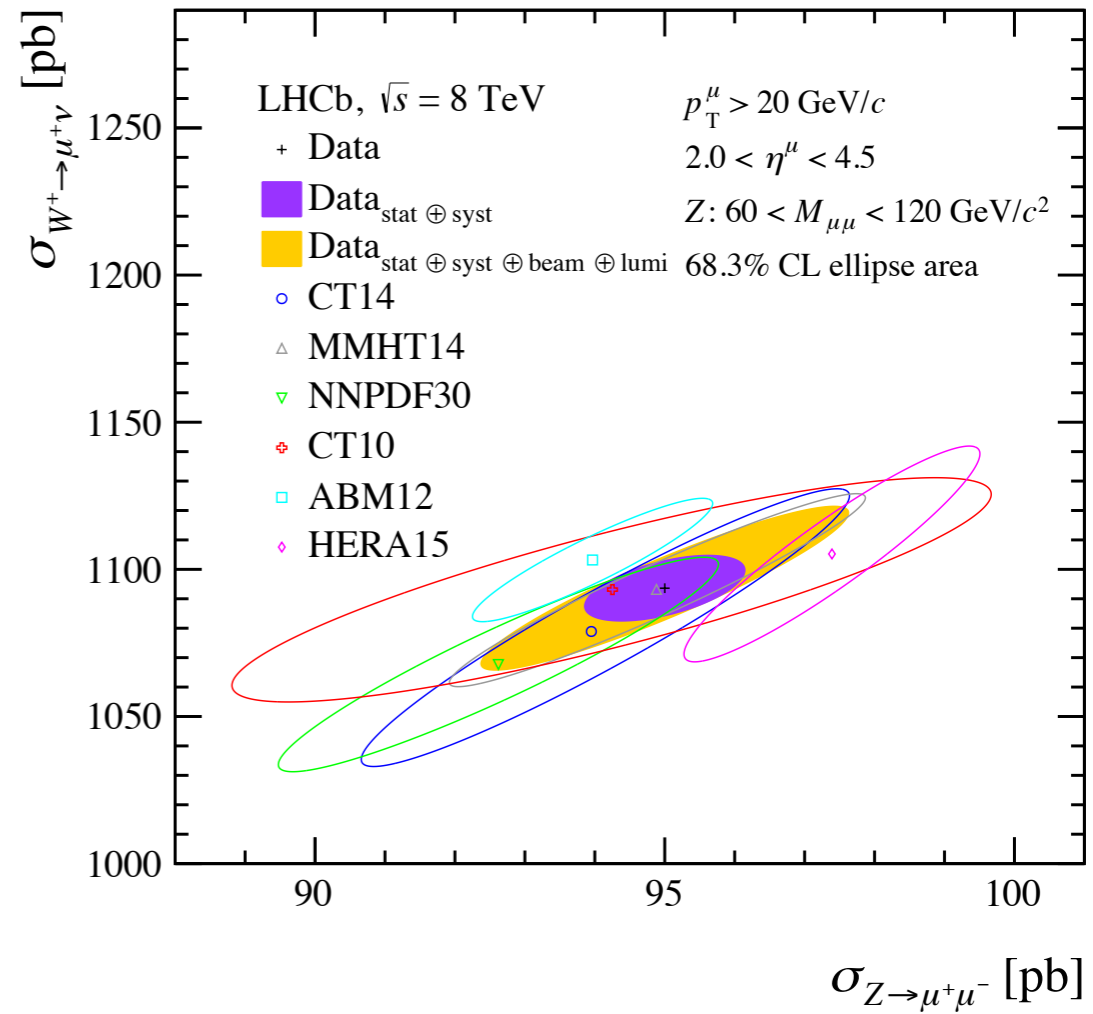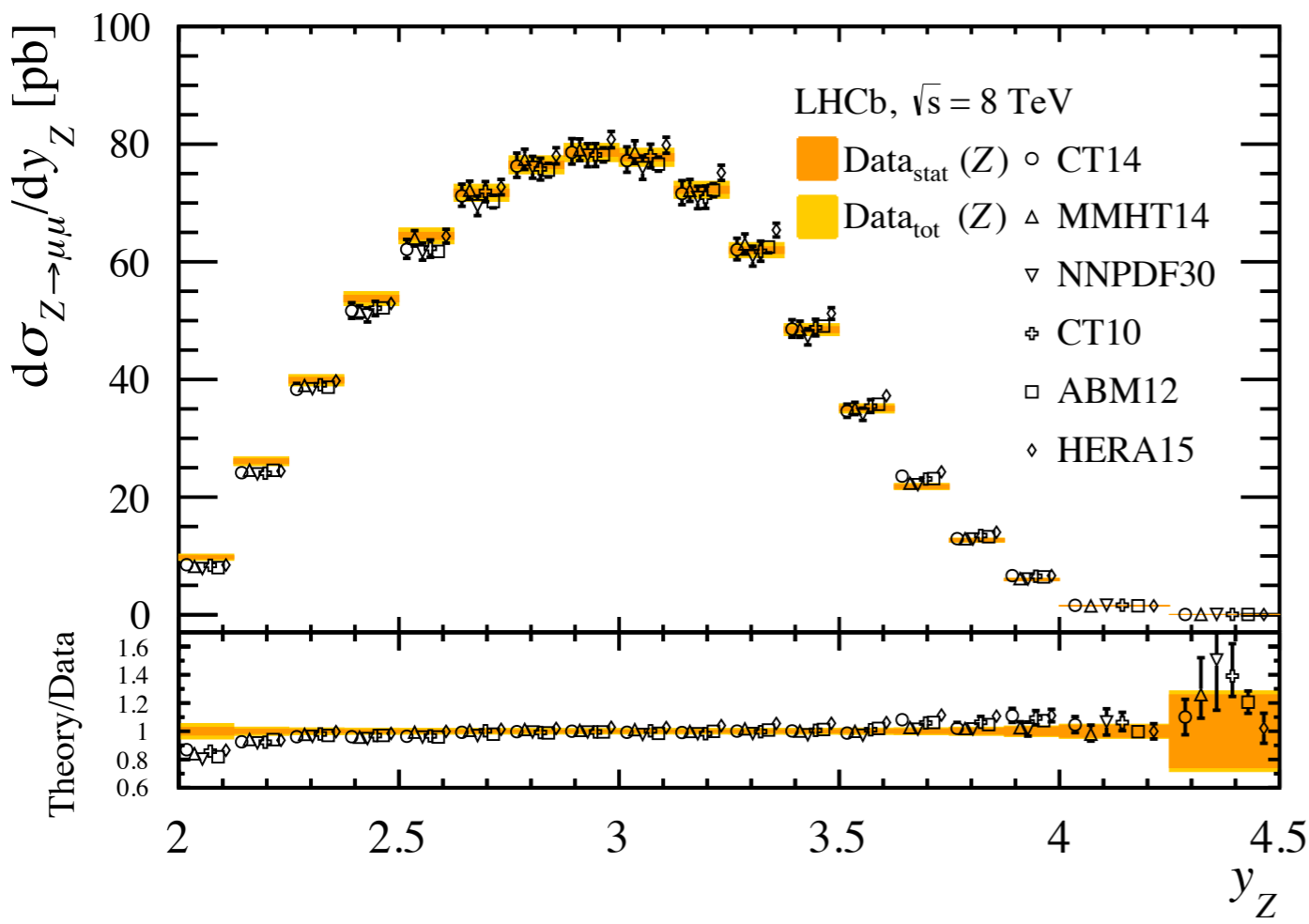
The LHCb data have been particularly constraining on the valence quark distributions at high-x in recent global PDF fits.

*Full list of LHCb publications in "QCD electroweak and exotica"

The W mass, the LHC and LHCb

Measurements of m_W by CDF and D0 were highlights of the Tevatron programme.

Long-standing concerns about W production being more difficult to model in proton-proton collisions than in proton-antiproton collisions.

A particular concern is the dependence on PDFs, which is related to the detector acceptance.
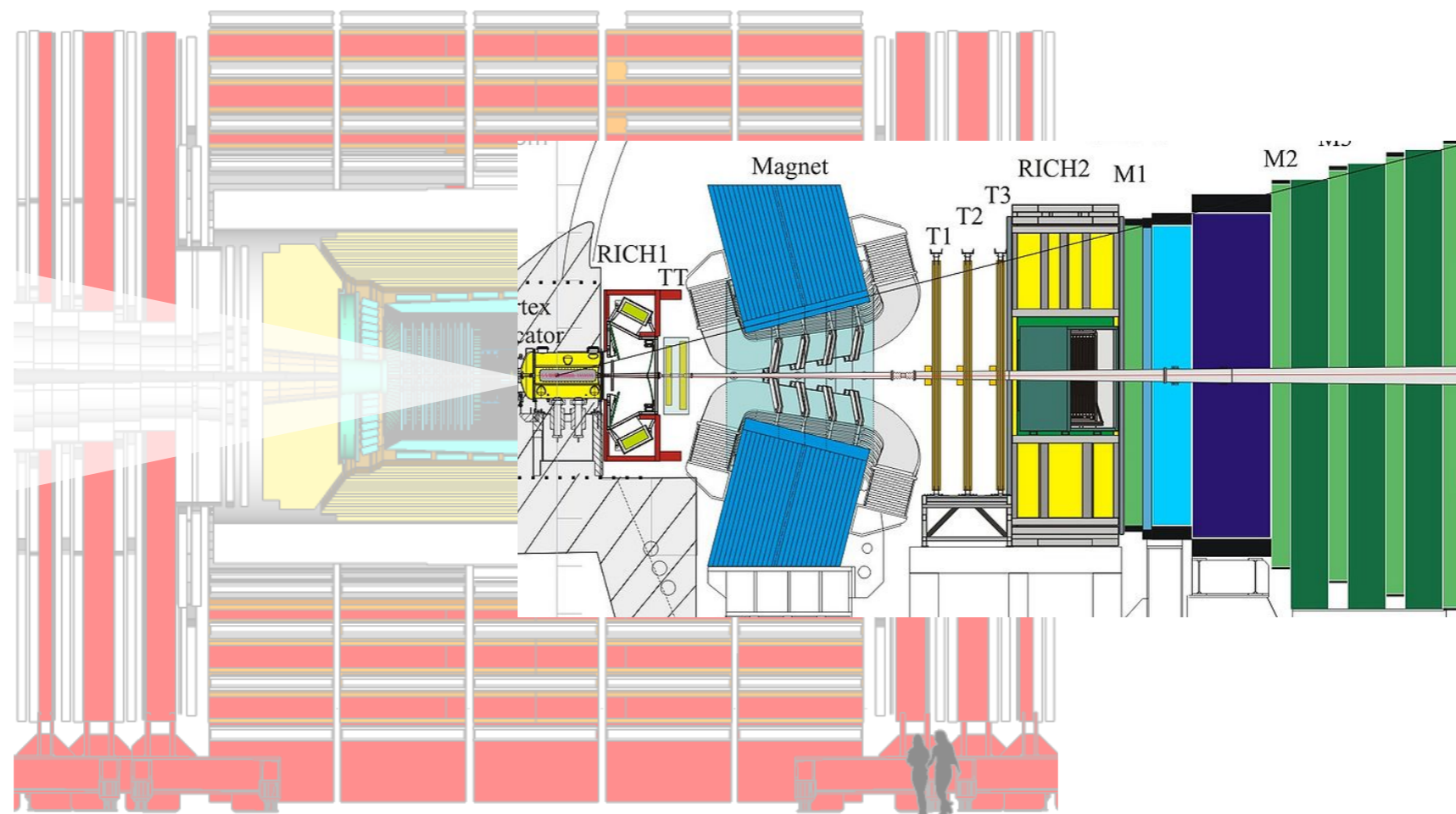
Prospects for muon p_T based m_W measurement by LHCb

EPJC 75 (2015) 12, 601

Partial *anti*correlation of the PDF uncertainty between LHCb and ATLAS/CMS-like measurements of m_W.

Statistical uncertainty with LHCb's Run-2 (2015-2018) dataset would be better than 10 MeV.

Follow up LHCb-specific studies: EPJC (2019) 79: 497, 1907.09958 (2019), EPJC 81 (2021) 3, 251

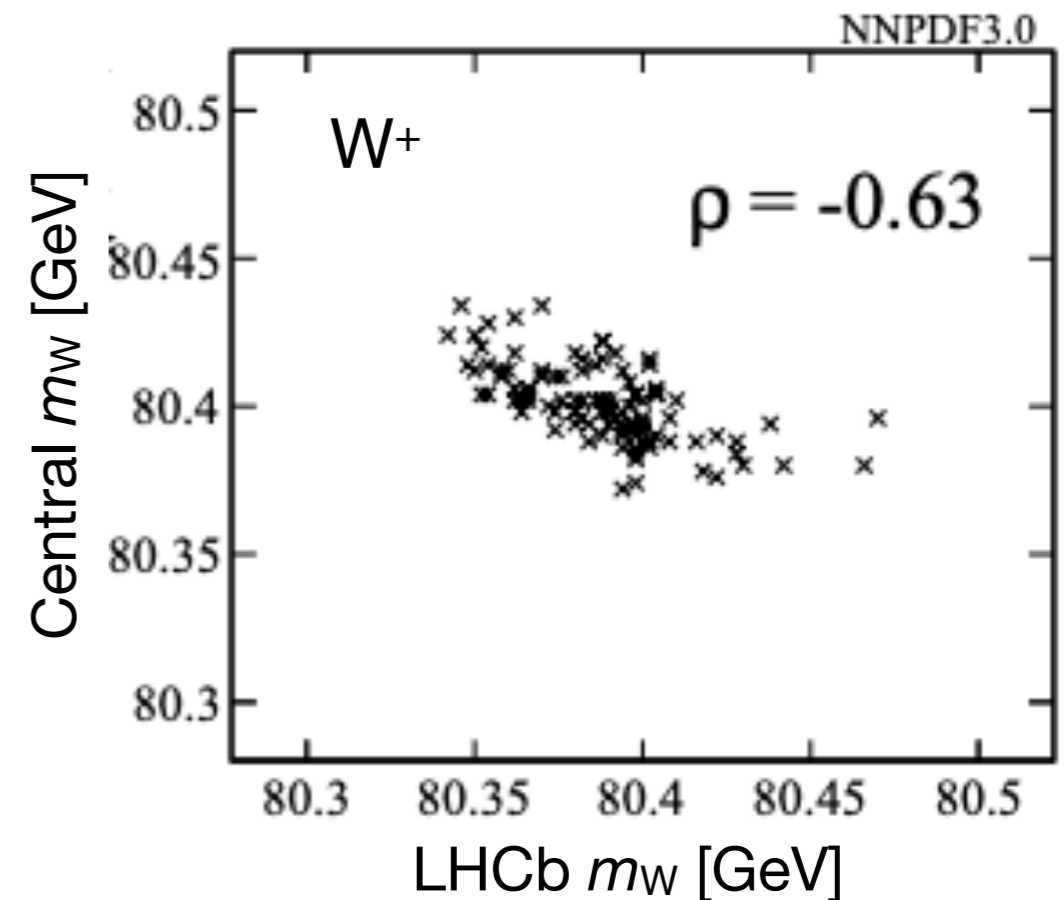# Prospects for muon p_T based m_W measurement by LHCb

EPJC 75 (2015) 12, 601

Partial *anti*correlation of the PDF uncertainty between LHCb and ATLAS/CMS-like measurements of m_W.

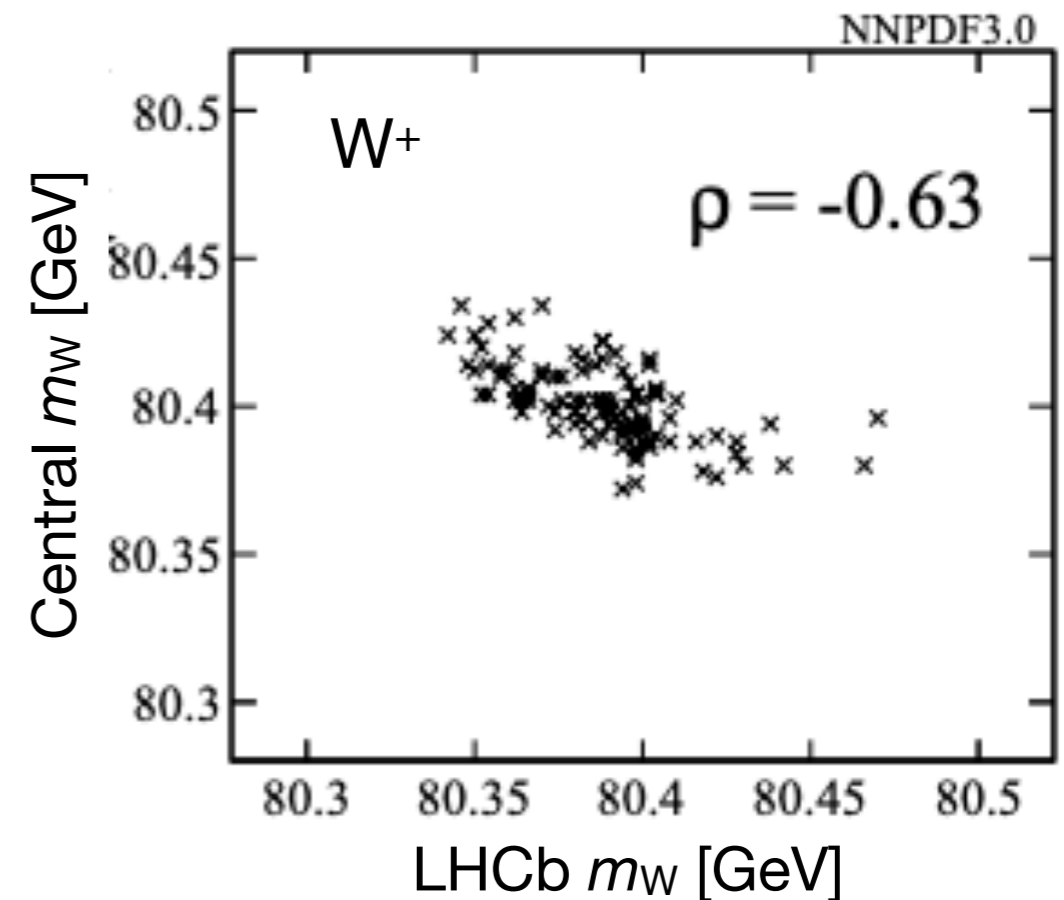Statistical uncertainty with LHCb's Run-2 (2015-2018) dataset would be better than 10 MeV.

An important word of caution from the authors:

5 Uncertainties stemming from the p_T^W modelling

Another source of theoretical uncertainty that we have overlooked so far is the p_T^W model. This strongly affects the preparation of the templates that are used to fit the data and eventually to extract m_W. The presence, at low lepton-pair transverse momenta, of large logarithmically enhanced QCD corrections and the role, in the same kinematic region, of non-perturbative effects have been discussed in Refs. [30,

Follow up LHCb-specific studies: EPJC (2019) 79: 497, 1907.09958 (2019), EPJC 81 (2021) 3, 251

LHCb's dataset and strategy for m_W
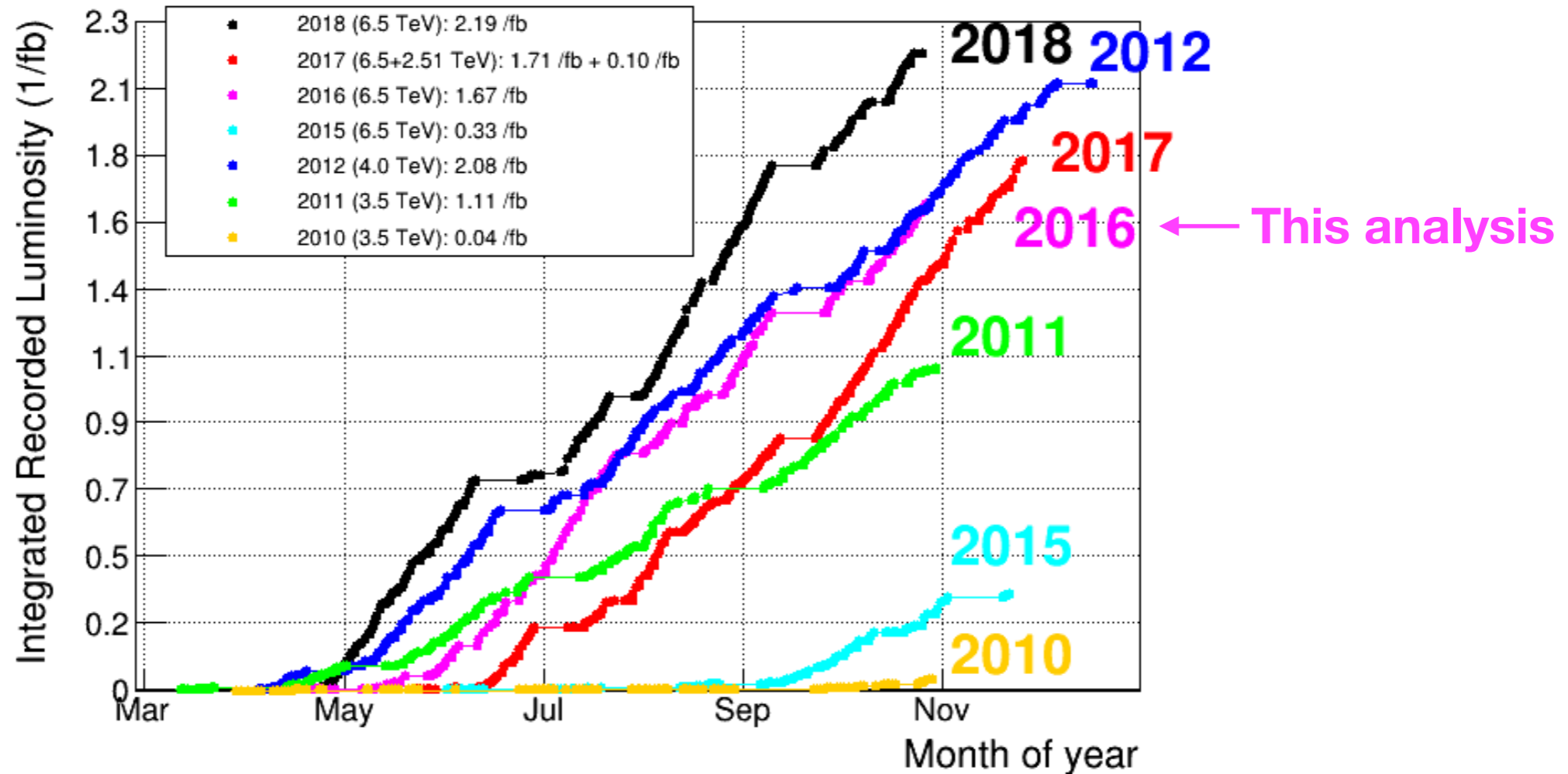
Strategic decision to perform a pathfinder measurement of m_W based on the 2016 dataset (1.7 fb⁻¹) and benefit from the ongoing evolution* of the theory tools in the exploitation of the full Run-II dataset (6 fb⁻¹).

The measured m_W value was blinded until the internal review had concluded.

Selection of W→μν signal candidates

Identified muon candidate matched to single muon trigger path.

Hadronic background suppressed to the percent level by an isolation[1] requirement, which is about 80% efficient for the signal.

Second-muon[2] veto suppressed Z→μμ background by a factor of ~2.

Roughly 2.4 million events remain in the region $28 < p_T < 52$ GeV and $2.2 < \eta < 4.4$ that is used in the m_W fit.

[1]Our isolation variable is the p_T sum of all particle-flow objects within a cone of $\Delta R < 0.4$ around the muon.
[2]With $p_T > 20$ GeV and $2 < \eta < 4.5$.

The simulation

The complete events and detector interactions are initially simulated with Pythia [1,2] and GEANT [3], respectively.

A variety of models are used to fully reweight the events to/beyond next-to-leading-order accuracy.

[1] Pythia version 8.186 Comput. Phys. Commun. 191 (2015) 159
[2] LHCb specific tune J. Phys.: Conf. Ser. 331 032047
[3] The LHCb Simulation Application, Gauss: Design, Evolution and Experience J. Phys.: Conf. Ser. 331 032023

Measurement strategy: fitting the muon q/p$_T$ distribution

W^- fit region

LHCb simulation
Preliminary

m_W

—— +300 MeV

—— -300 MeV

W^+ fit region

$$q/p_T \approx \frac{2}{m_W}$$

Normalised events per GeV^{-1}

Ratio

q/p_T [1/GeV]
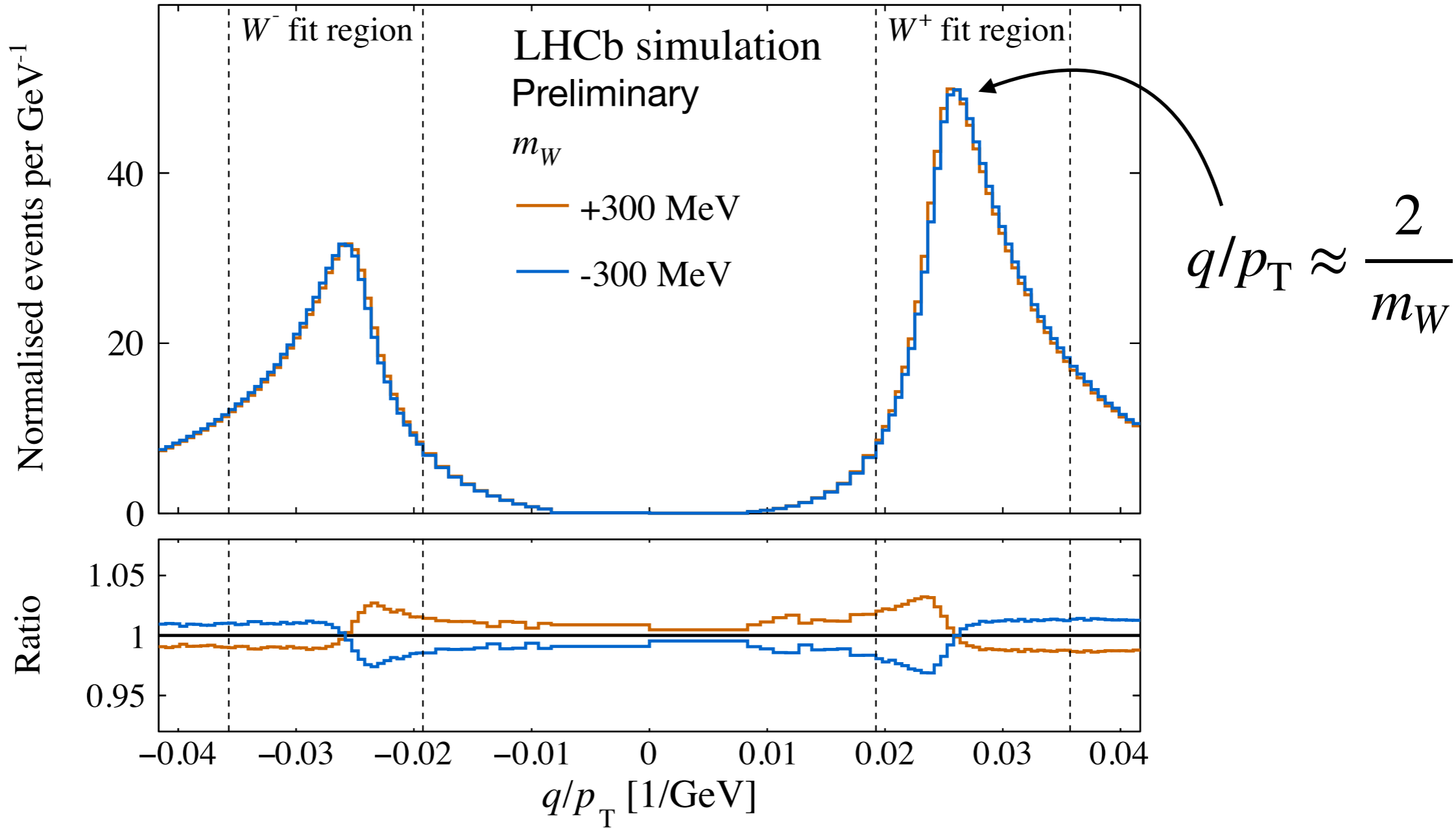
The m$_W$ hypothesis is adjusted with event-by-event weights based on a ratio of relativistic Breit-Wigner functions with mass dependent widths.

Challenges for the fit model

Detector response

Muon momentum measurement.

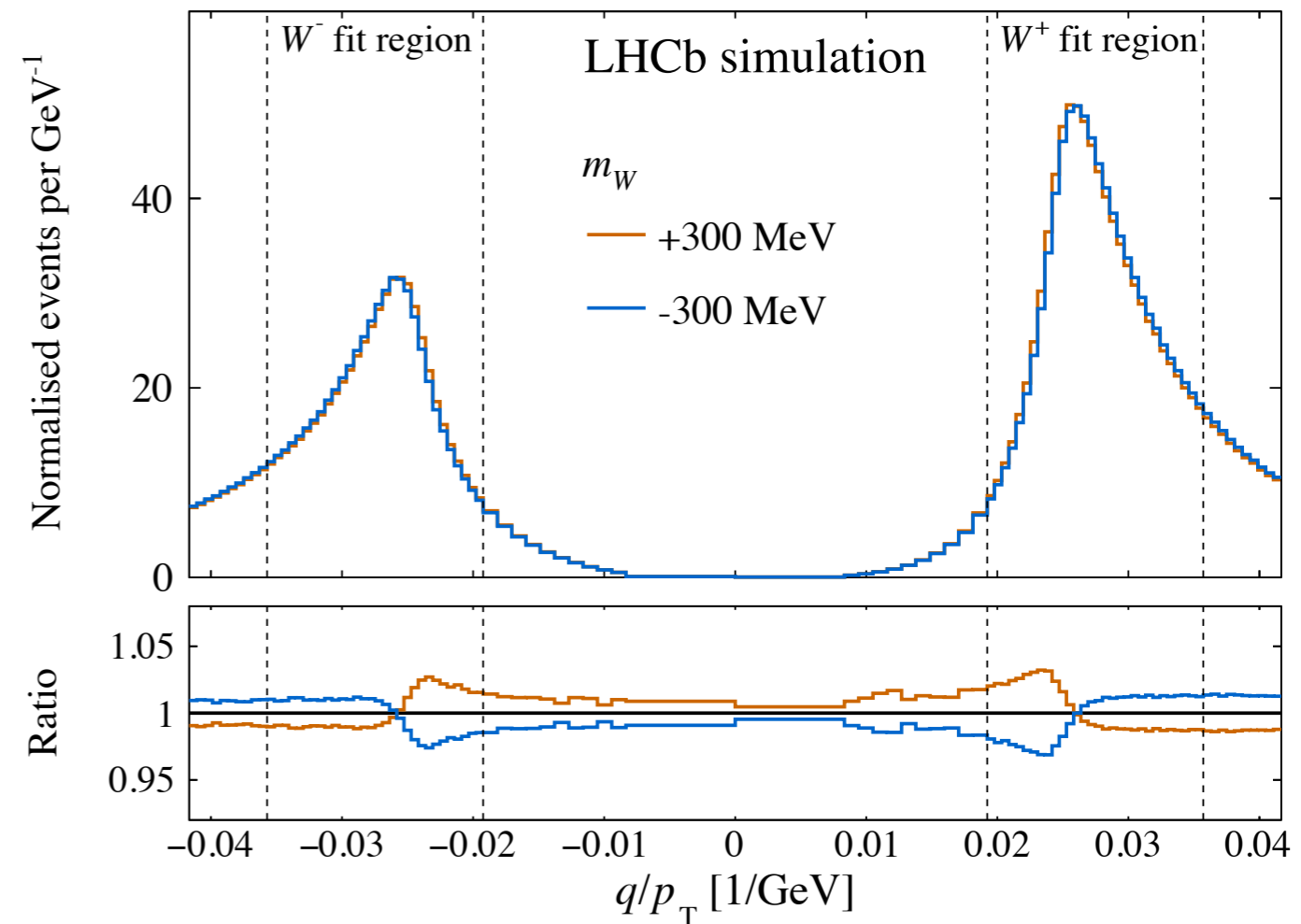Muon reconstruction and selection efficiency.

Electroweak (Z→μμ/ττ, W→τν, diboson, top…) and hadronic backgrounds.

W boson production

Modelling of the W p_T distribution is of particular concern.

Also the PDFs, boson polarisation and electroweak corrections.

Simultaneously fitting the W and Z data

Due to the similarity of W and Z production and the role of the Z background in the W sample it is decided to extract m_W in a simultaneous fit of W and Z data (roughly 200k events).

The Z data are binned in

$$\phi^* \equiv \tan\left(\frac{\pi - \Delta\phi}{2}\right)/\cosh\left(\frac{\Delta\eta}{2}\right) \sim \frac{p_T}{M}$$

EPJC 71:1600 (2011)

Muon momentum calibration and modelling strategy

1. Custom alignment of the tracking system for high p_T physics
    LHCb-FIGURE-2020-009

2. Finer analysis-level q/p corrections with the *pseudomass* method
    EPJC 81 (2021) 3, 251 applied to data and simulation.

3. Final *smearing* of the muon momenta in simulation, with
    parameters determined from a simultaneous fit of Z, J/Ψ, Υ(1S)
    data (and simulation).

Charge-dependent curvature biases
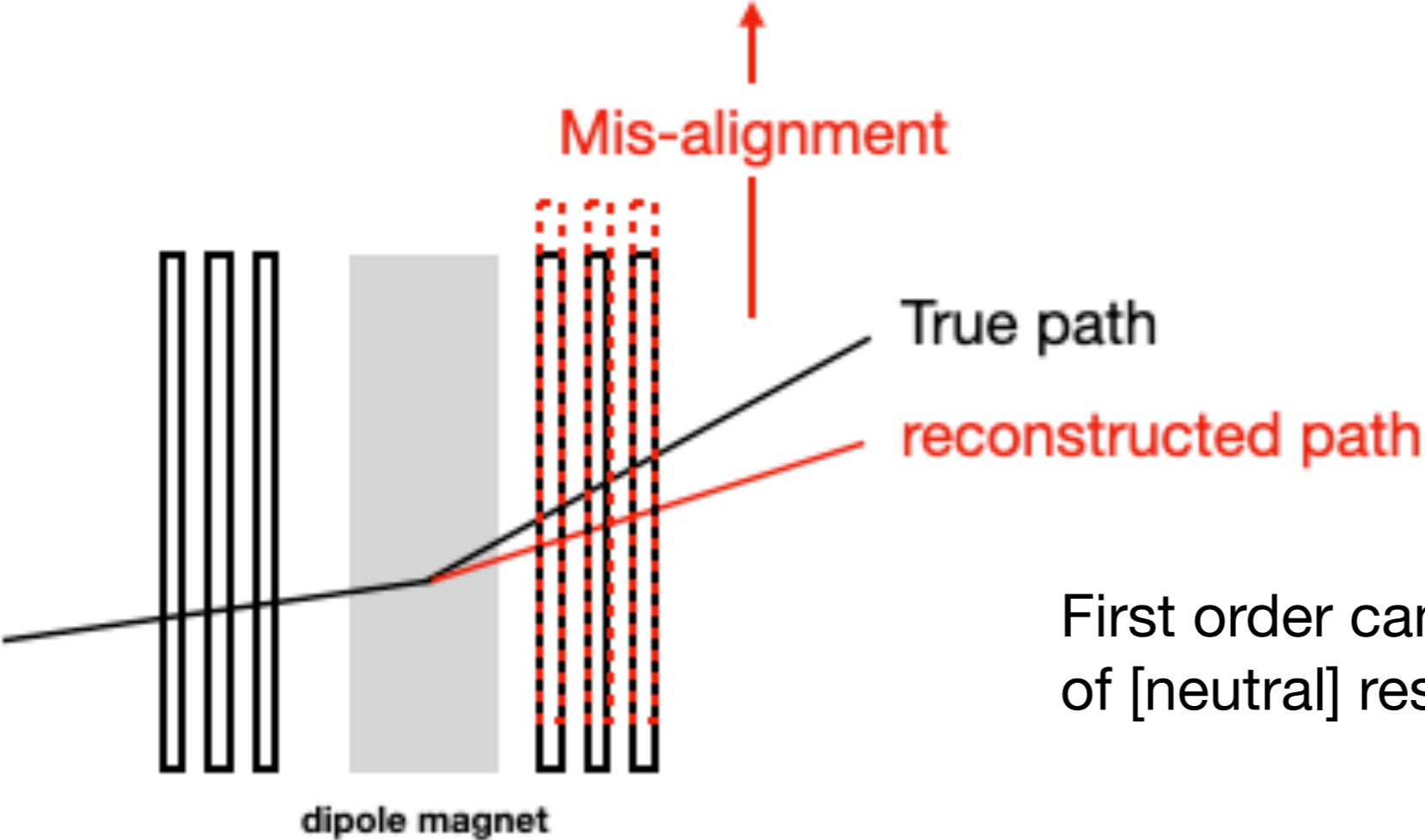
Mis-alignment

True path

reconstructed path

dipole magnet

First order cancellation in masses of [neutral] resonances e.g. Z→μμ.

Charge-dependent curvature biases

First order cancellation in masses of [neutral] resonances e.g. Z→μμ.
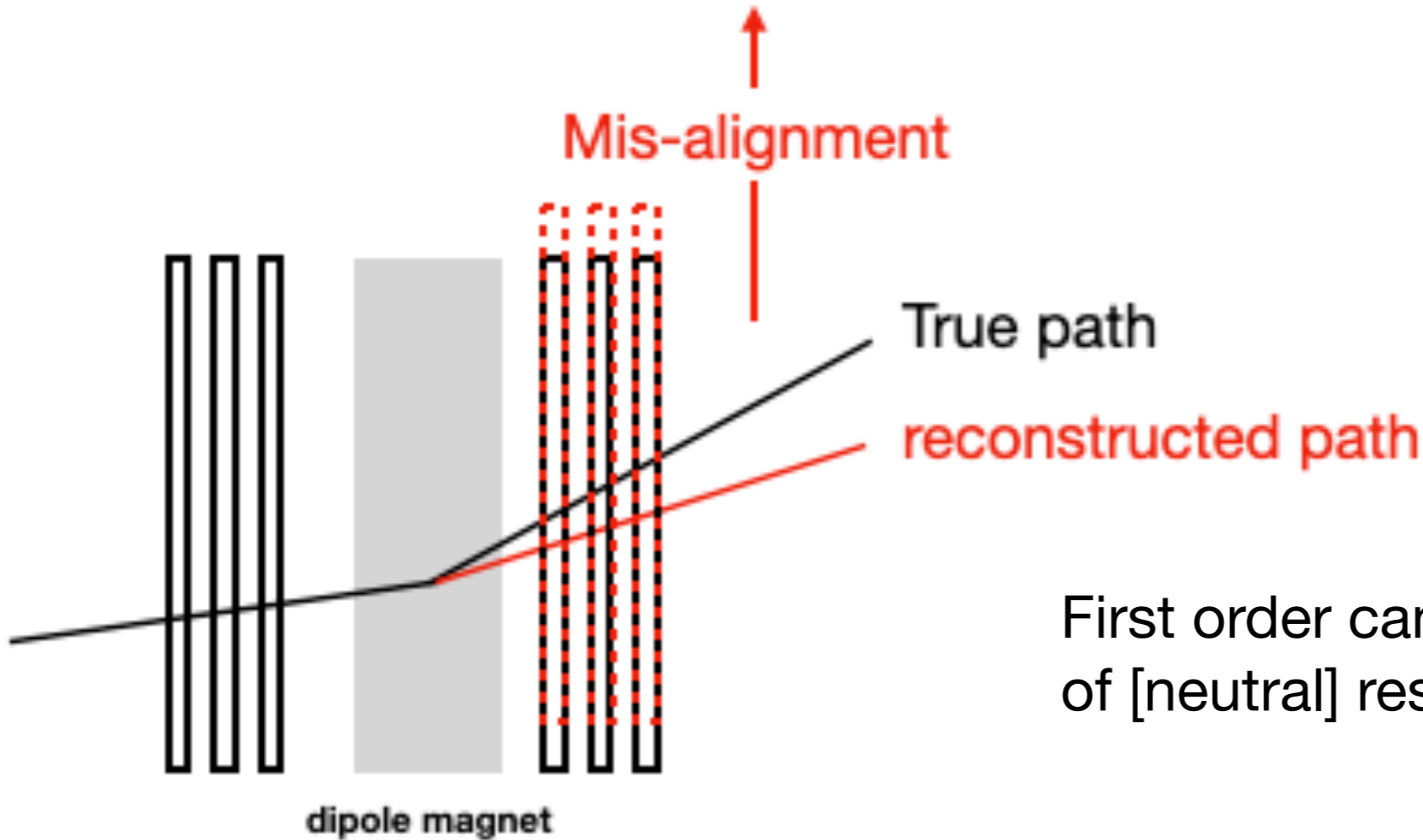
Our definition of the *pseudomass**

$$M^{\pm} = \sqrt{2p^{\pm}p_T^{\pm}\frac{p^{\mp}}{p_T^{\mp}}(1 - \cos\theta)},$$

EPJC 81 (2021) 3, 251

*Inspired by the use of the pseudomass with a slightly different definition in a D0 analysis PRD 91, 072002 (2015)

Charge-dependent curvature biases

Mis-alignment

True path

reconstructed path

dipole magnet
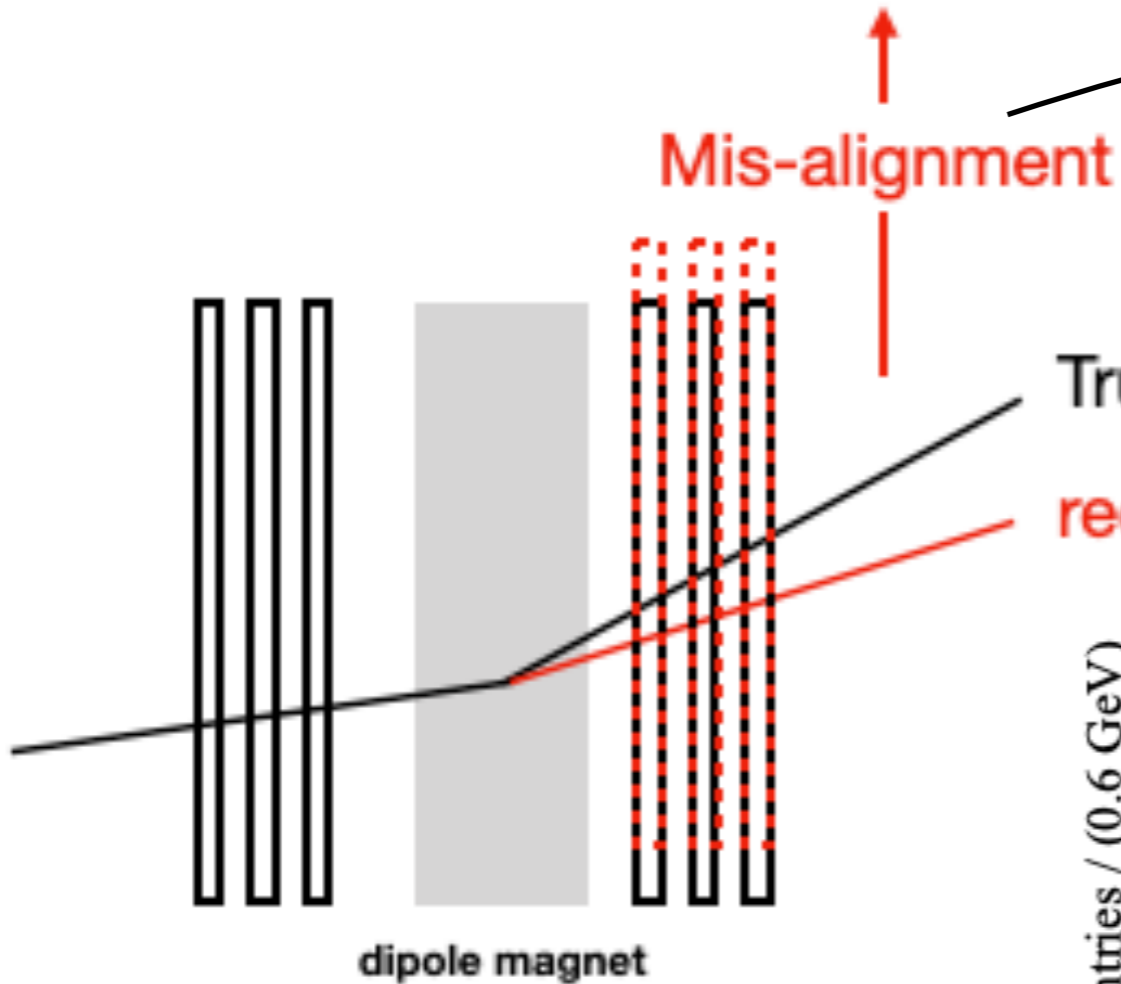
Hypothetical 50 micron displacement in simplified simulation of Z →μμ events

EPJC 81 (2021) 3, 251

M^+ M^-

Our definition of the *pseudomass**

$$M^{\pm} = \sqrt{2p^{\pm}p_T^{\pm}\frac{p^{\mp}}{p_T^{\mp}}(1-\cos\theta)},$$
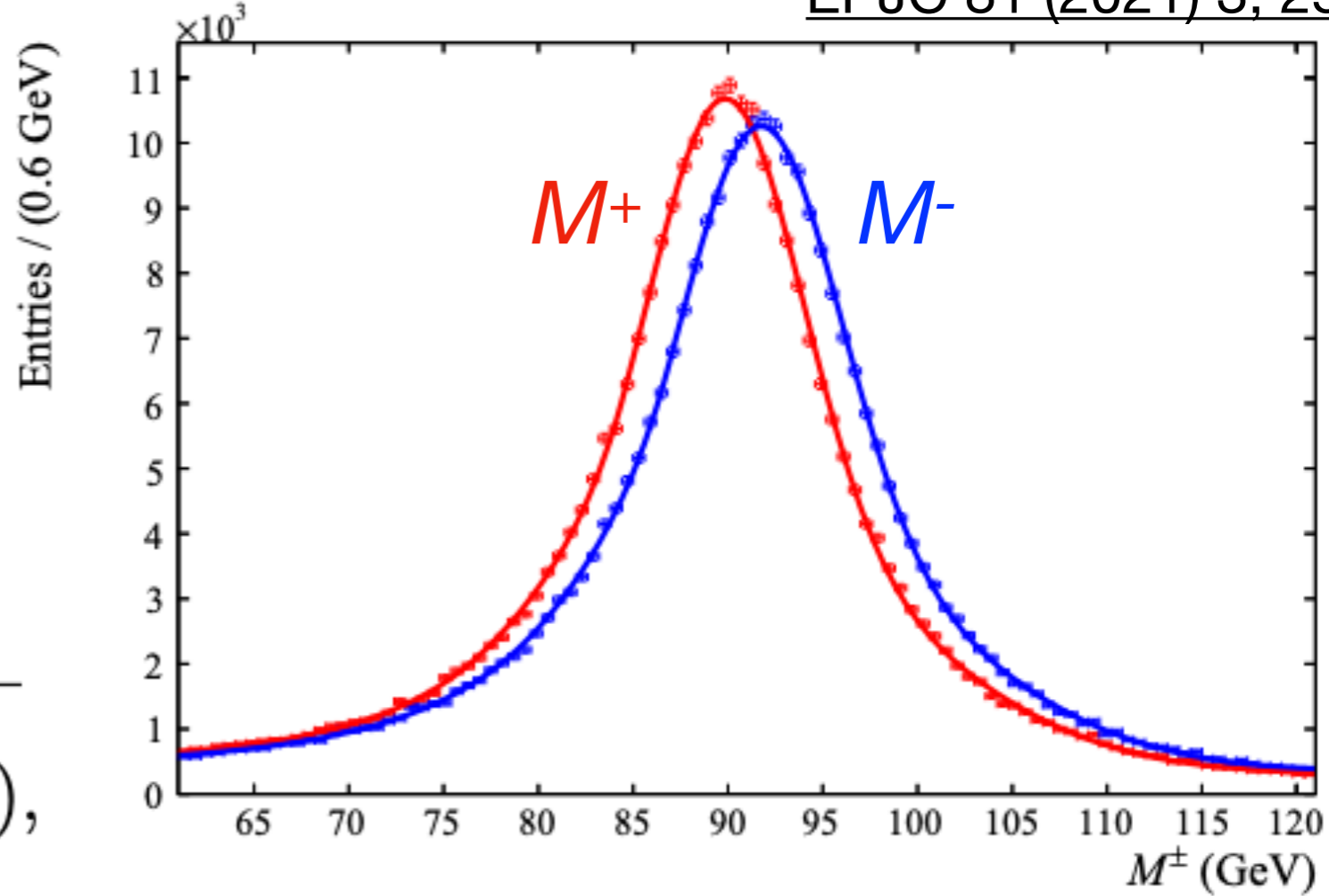
Entries / (0.6 GeV)

$\times 10^3$

$M^{\pm}$ (GeV)

*Inspired by the use of the pseudomass with a slightly different definition in a D0 analysis PRD 91, 072002 (2015)

Charge-dependent curvature biases

Fit the pseudomass asymmetries (between M+ and M- peak positions) in fine detector "regions" (mostly* bins in η and φ) and translate these to curvature corrections (shifts in q/p).
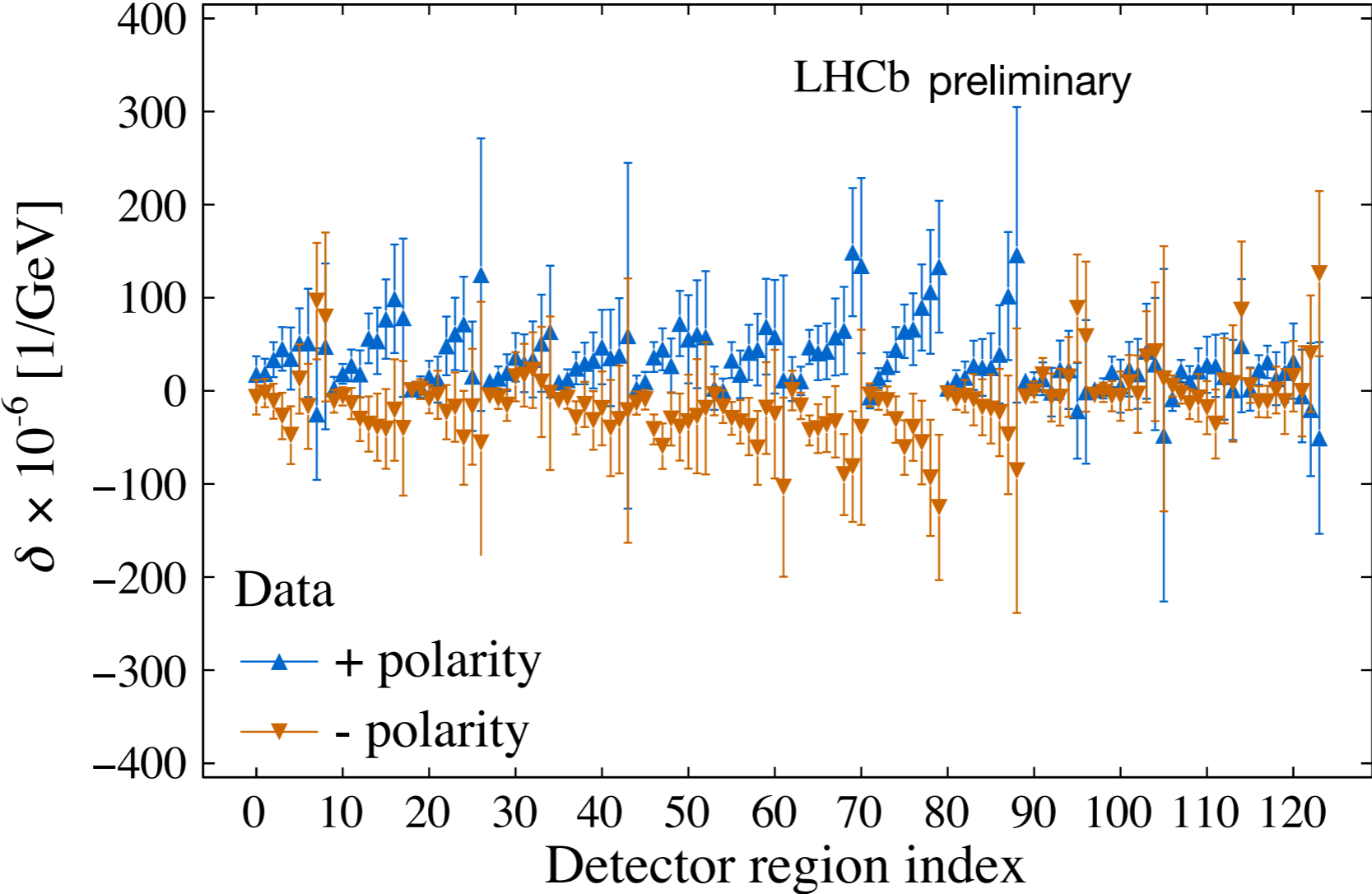
*With a further distinction between tracks that go through the straw-tube versus silicon-strip parts of the tracking stations downstream of the magnet.

Momentum smearing fit

$$\frac{q}{p} \rightarrow \frac{q}{p \cdot \mathcal{N}(1 + \alpha, \sigma_{\text{MS}})} + \mathcal{N}\left(\delta, \frac{\sigma_\delta}{\cosh \eta}\right)$$

Simultaneous fit of Z, Υ(1S) and J/Ψ data (and simulation)

36 fit categories (based on species, magnet polarity, η of the two muons).

Projections after the fit, aggregating categories:

$$\chi^2_{\text{total}}/\text{ndf} = 1862/2082$$
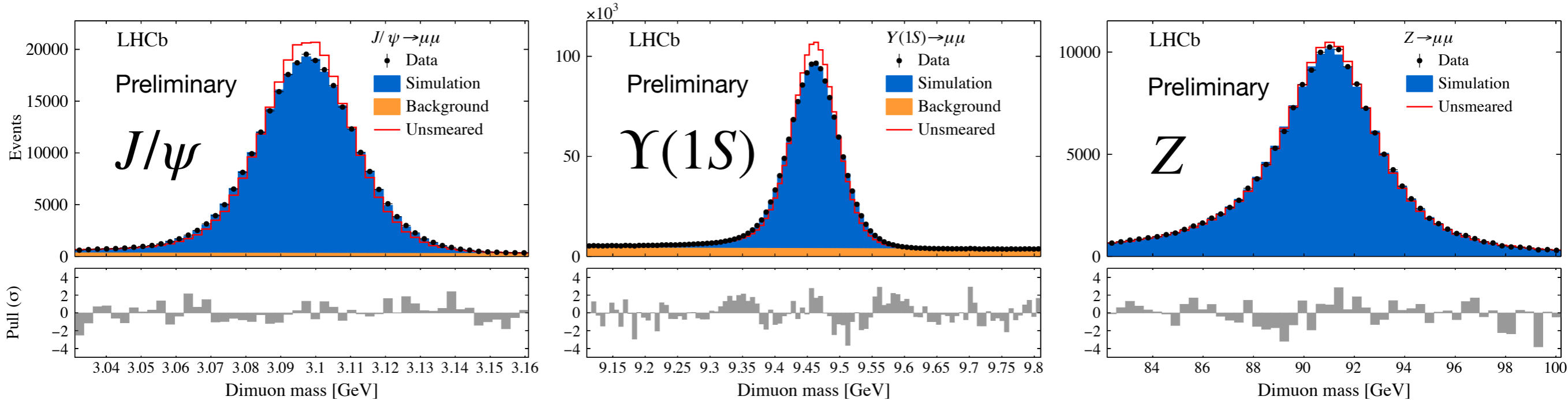
Statistical and systematic uncertainties including; variations in the PDG resonance masses, detector material budget, final state radiation and the form of the smearing function.

Selection efficiency modelling

The muon trigger, identification and tracking efficiencies are measured in data and simulation with the same methods.

The simulated events are subsequently corrected with event-by-event weights.

The largest corrections are to the muon trigger efficiency, which is measured using a combination of Z→μμ and Y(1S)→μμ events in bins of muon η and φ.

p_T dependent parameterisations of the trigger efficiency ratios

$\epsilon_{\text{data}}/\epsilon_{\text{simulation}}$

$-1 < \phi/\pi < -1/2$ $-1/2 < \phi/\pi < 0$ $0 < \phi/\pi < 1/2$ $1/2 < \phi/\pi < 1$

LHCb preliminary

$1.5 < \eta < 1.9$
$1.9 < \eta < 2.2$
$2.2 < \eta < 2.5$
$2.5 < \eta < 2.8$
$2.8 < \eta < 3.0$
$3.0 < \eta < 3.3$
$3.3 < \eta < 3.6$
$3.6 < \eta < 3.9$
$3.9 < \eta < 4.1$
$4.1 < \eta < 4.4$
$4.4 < \eta < 5.0$

$\Upsilon(1S) \to \mu\mu$

$Z \to \mu\mu$

$1/p_T$ [1/GeV]
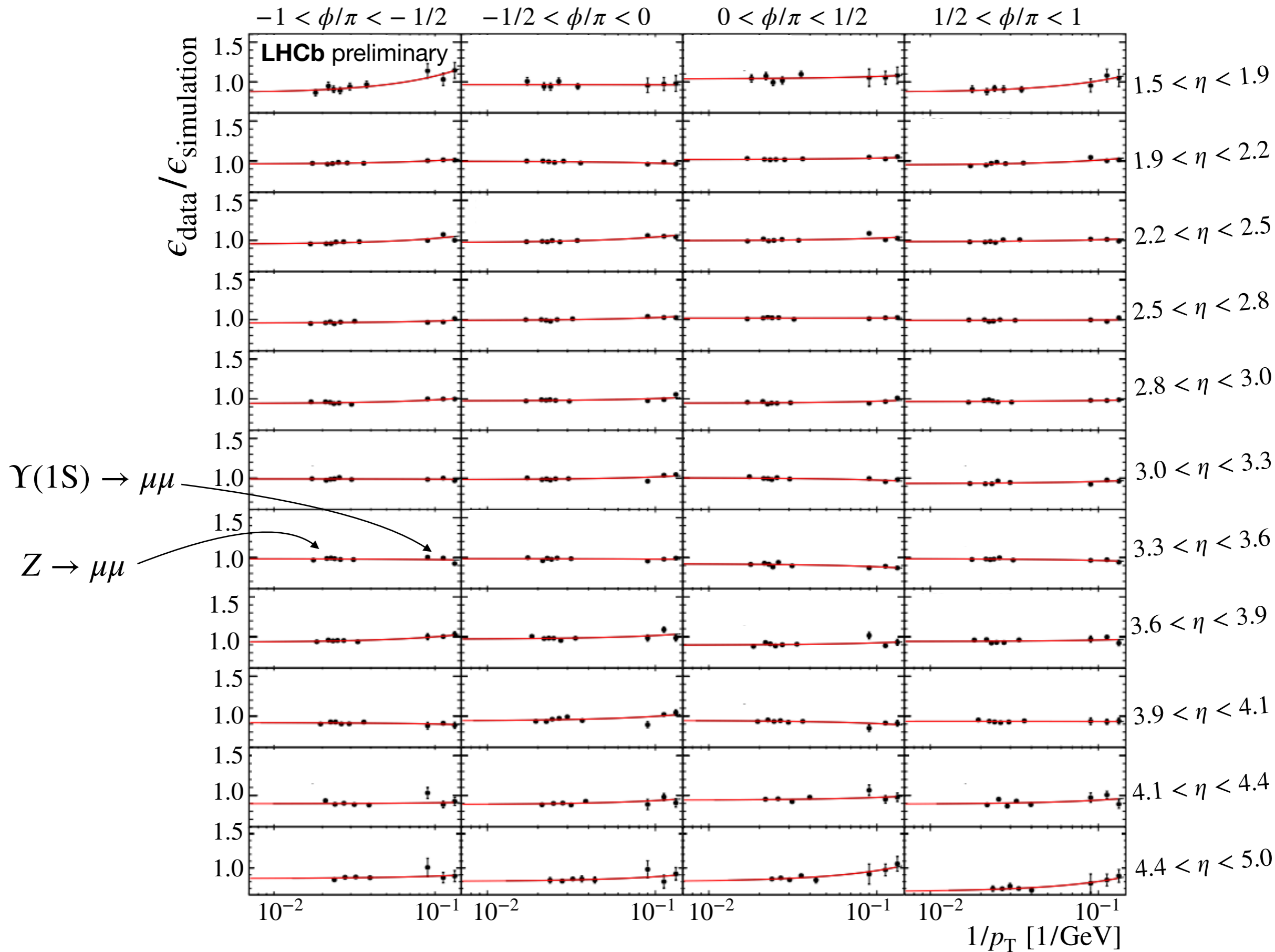
Selection efficiency modelling

Similar methods for the tracking and muon identification efficiencies.

Tracking and ID efficiency corrections also apply to the Z→μμ background (~6% of the W candidates) that survives the second-muon-veto.

Uncertainties include:

Limited Z and Y(1S) statistics.

Variations in the binning, selections and parameterisations.

Modelling the efficiency of the isolation cut

Measured with Z→µµ events in bins of η and the projection of the boson p_T onto the muon.

$$u = \frac{\vec{p}_T^V \cdot \vec{p}_T^\mu}{p_T^\mu}$$
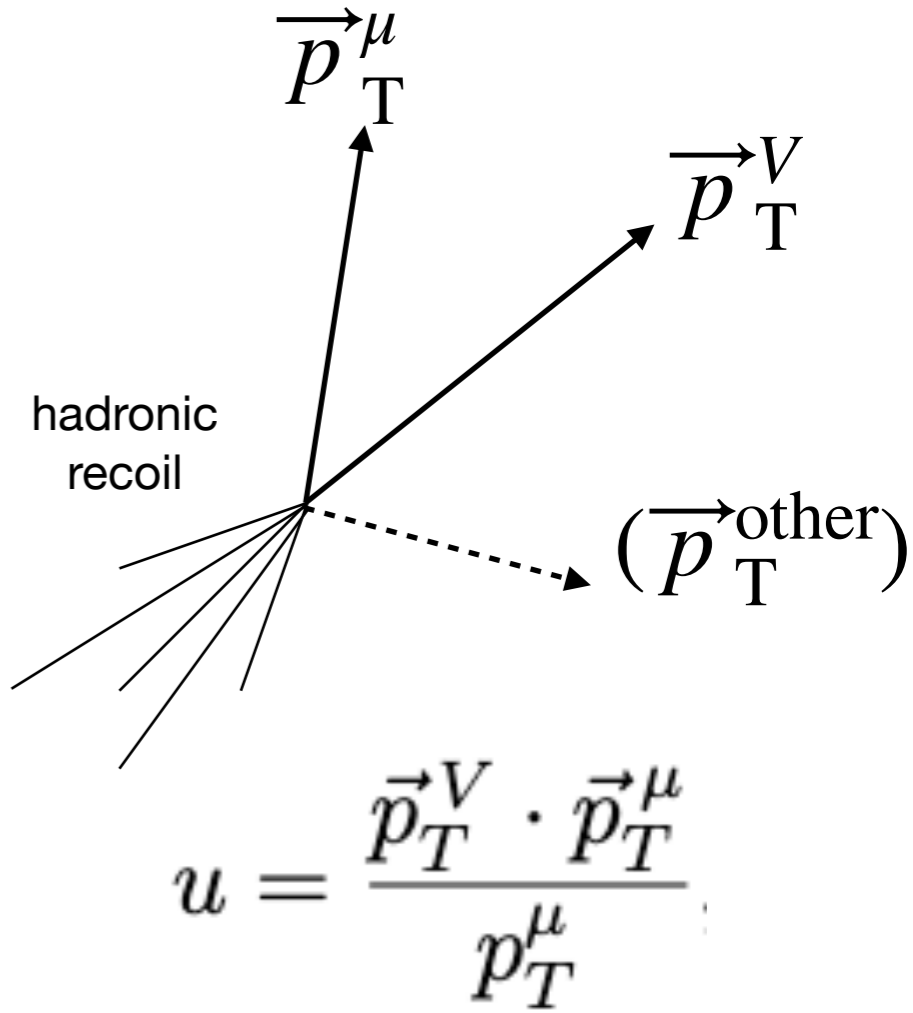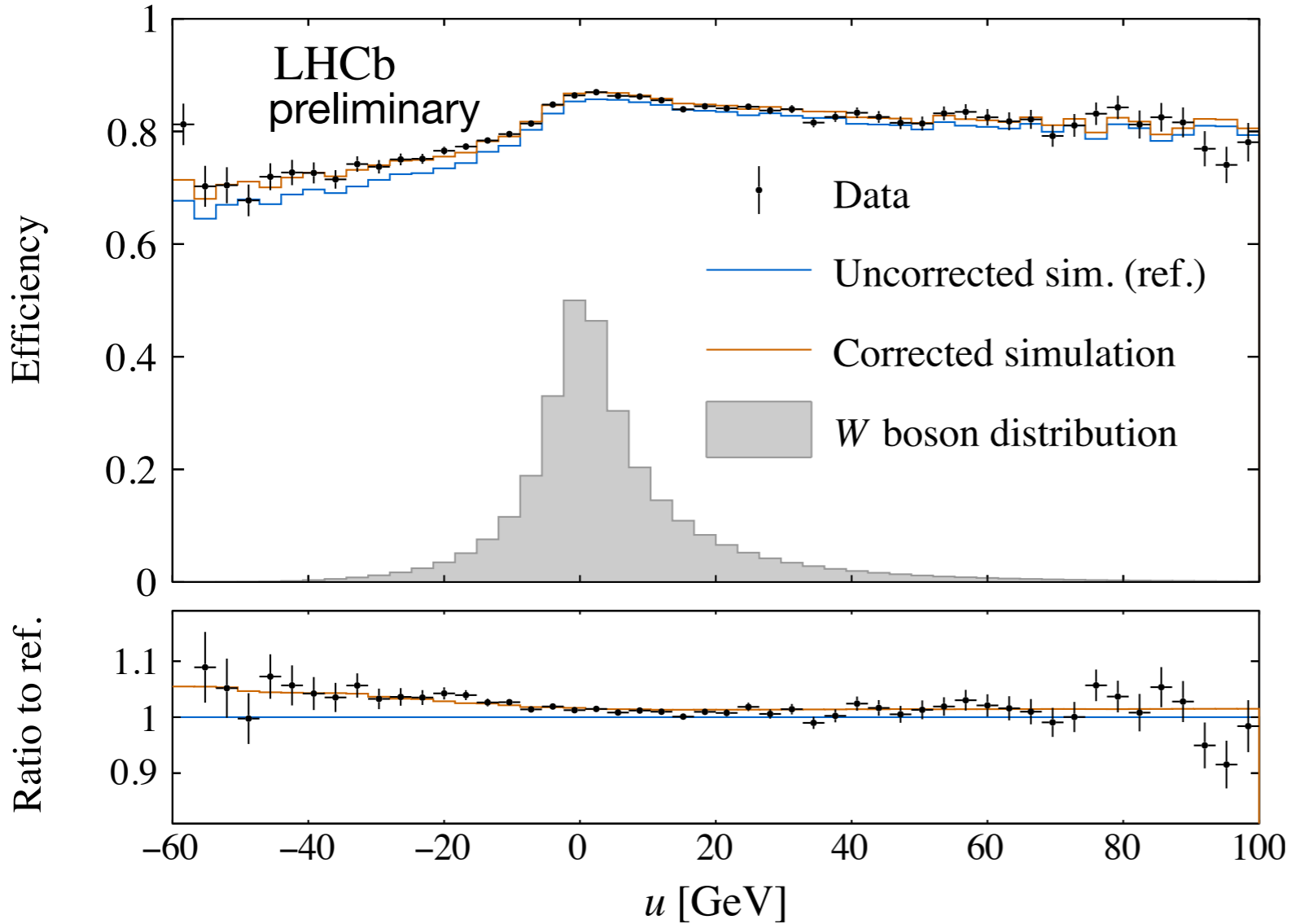
Uncertainty on this part of the model includes the statistics of the Z samples and the dependence of the results on the binning and other method details.

Backgrounds in the W→μν sample

1) Electroweak backgrounds and heavy flavour hadrons are modelled with the same simulation as used for the signal.

2) Hadronic background
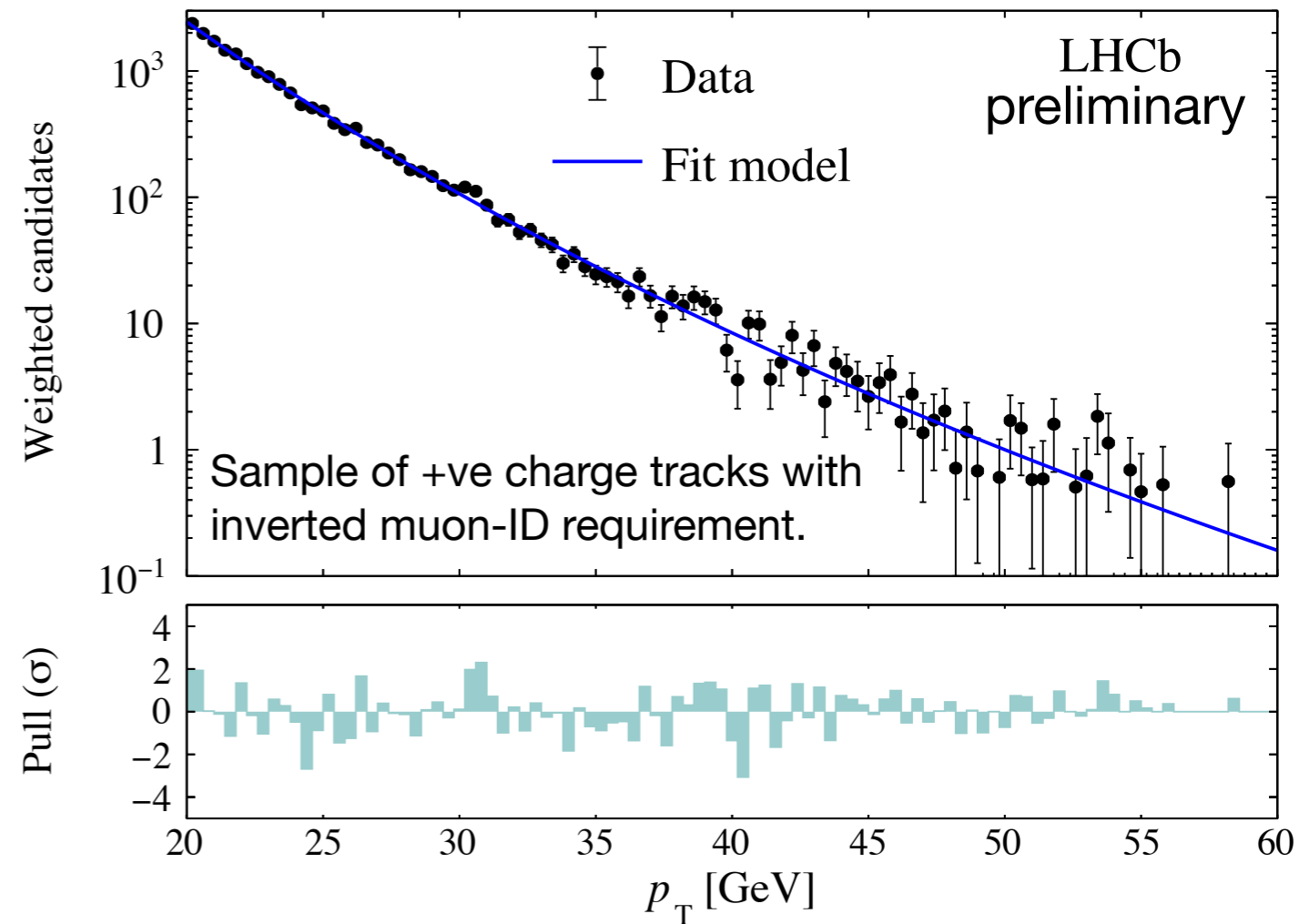
A parametric model for in-flight decays of pions and kaons is trained on a sample of hadrons with weights to account for the variation of the decay-length acceptance on the Lorentz boost.

The p_T shape and the charge asymmetry is fixed but the total fraction is left to float in the m_W fit. Variations in the details of this background model result in a systematic uncertainty of only 2.3 MeV.

Vector boson production model

lepton plane

hadron plane
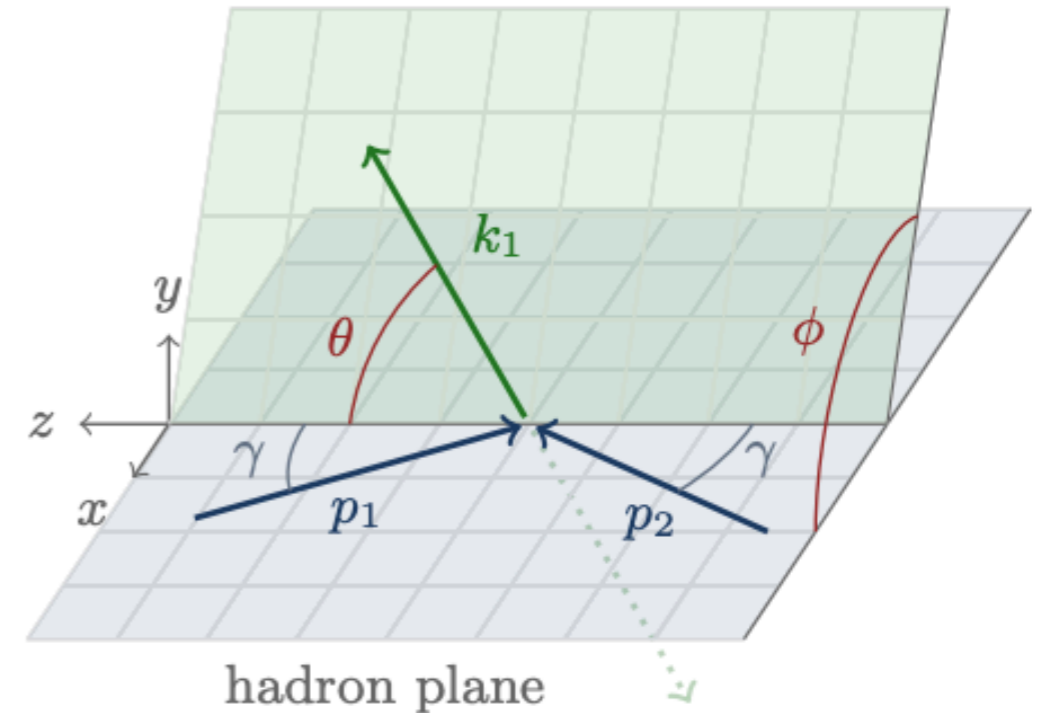
Born-level form of W→µν kinematics:

$$\frac{\mathrm{d}\sigma}{\mathrm{d}p_{\mathrm{T}}^{W}\,\mathrm{d}y\,\mathrm{d}M\,\mathrm{d}\cos\theta\,\mathrm{d}\phi} = \frac{3}{16\pi}\frac{\mathrm{d}\sigma^{\mathrm{unpol.}}}{\mathrm{d}p_{\mathrm{T}}^{V}\,\mathrm{d}y\,\mathrm{d}M}$$

$$\left\{(1+\cos^2\theta) + A_0\frac{1}{2}(1-3\cos^2\theta) + A_1\sin 2\theta\cos\phi\right.$$

$$+ A_2\frac{1}{2}\sin^2\theta\cos 2\phi + A_3\sin\theta\cos\phi + A_4\cos\theta$$

$$\left.+ A_5\sin^2\theta\sin 2\phi + A_6\sin 2\theta\sin\phi + A_7\sin\theta\sin\phi\right\},$$

Electroweak corrections must also be considered.

28

Choice of PDFs

Measurement based on three recent global PDF sets

1. **NNPDF31** EPJC 77 (2017) 10, 663

2. **CT18** PRD 103 (2021) 1, 014013

3. **MSHT20** EPJC 81 (2021) 4, 341

We report measurements with full PDF uncertainties based on the three sets individually but the main result is a simple arithmetic average of the three m_W determinations.

These sets supersede the PDF4LHC recommendations J. Phys. G: Nucl. Part. Phys. 43 023001 (2016) but we expect that new recommendations are in the pipeline and these can influence our future analysis of the remaining LHCb data.

The W boson p_T distribution

Complete **event generation** with parton-showers matched to NLO matrix elements
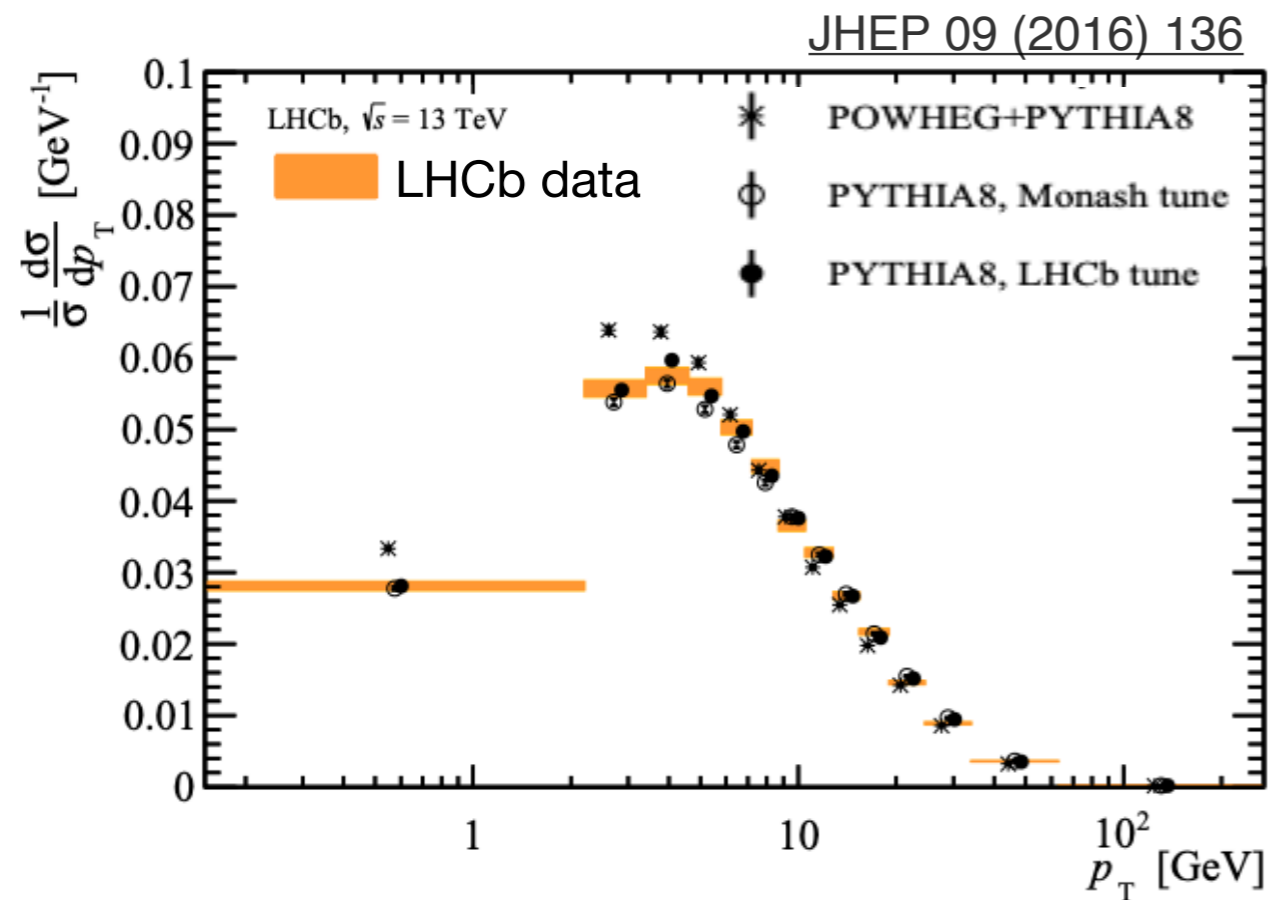
Tuning required to compensate for limited perturbative accuracy.

Cross-section calculation** at up to N³LL (logarithmic) accuracy, e.g. DYTurbo*:
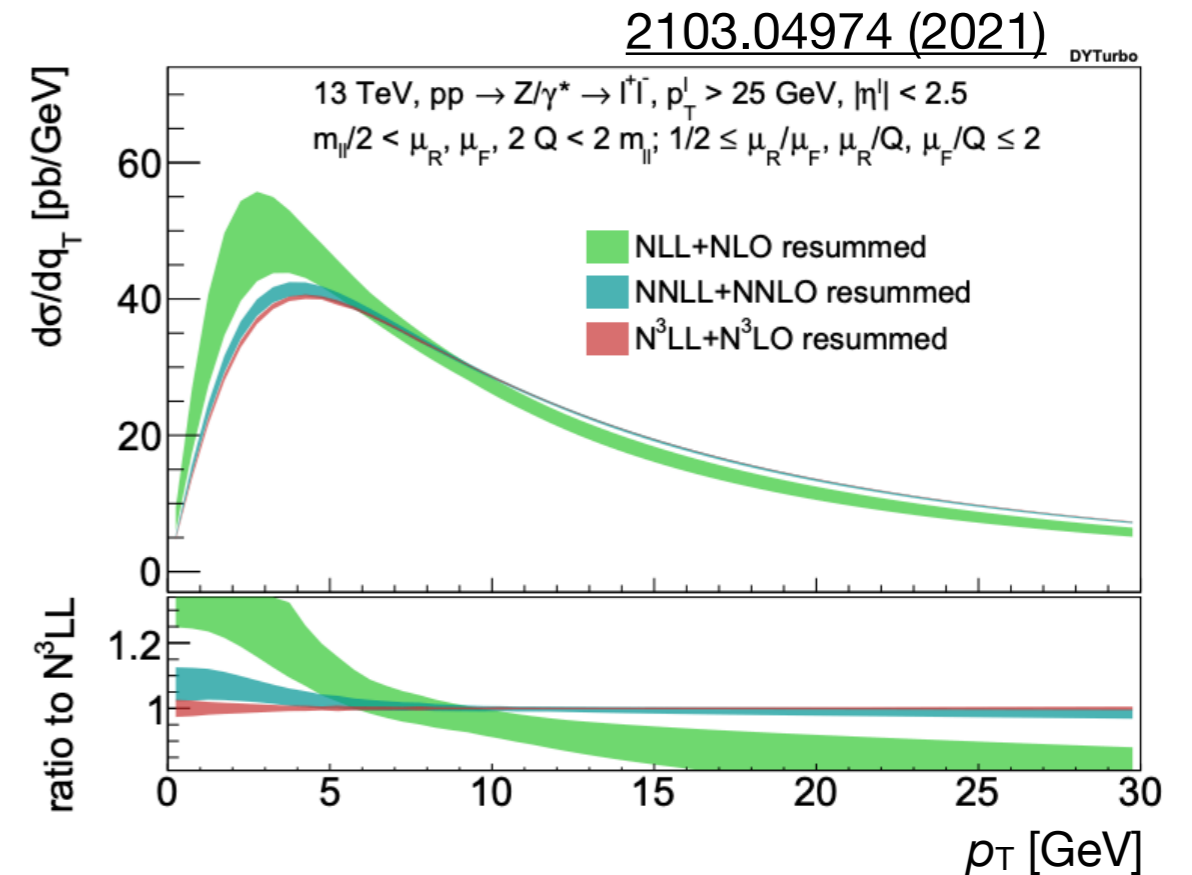
Ultimate perturbative accuracy but debated flexibility to fit the data.

*As one example out of the work of *many* groups working in this area! Similarly for the event-generator codes.

Tuning and validation with Z p_T data
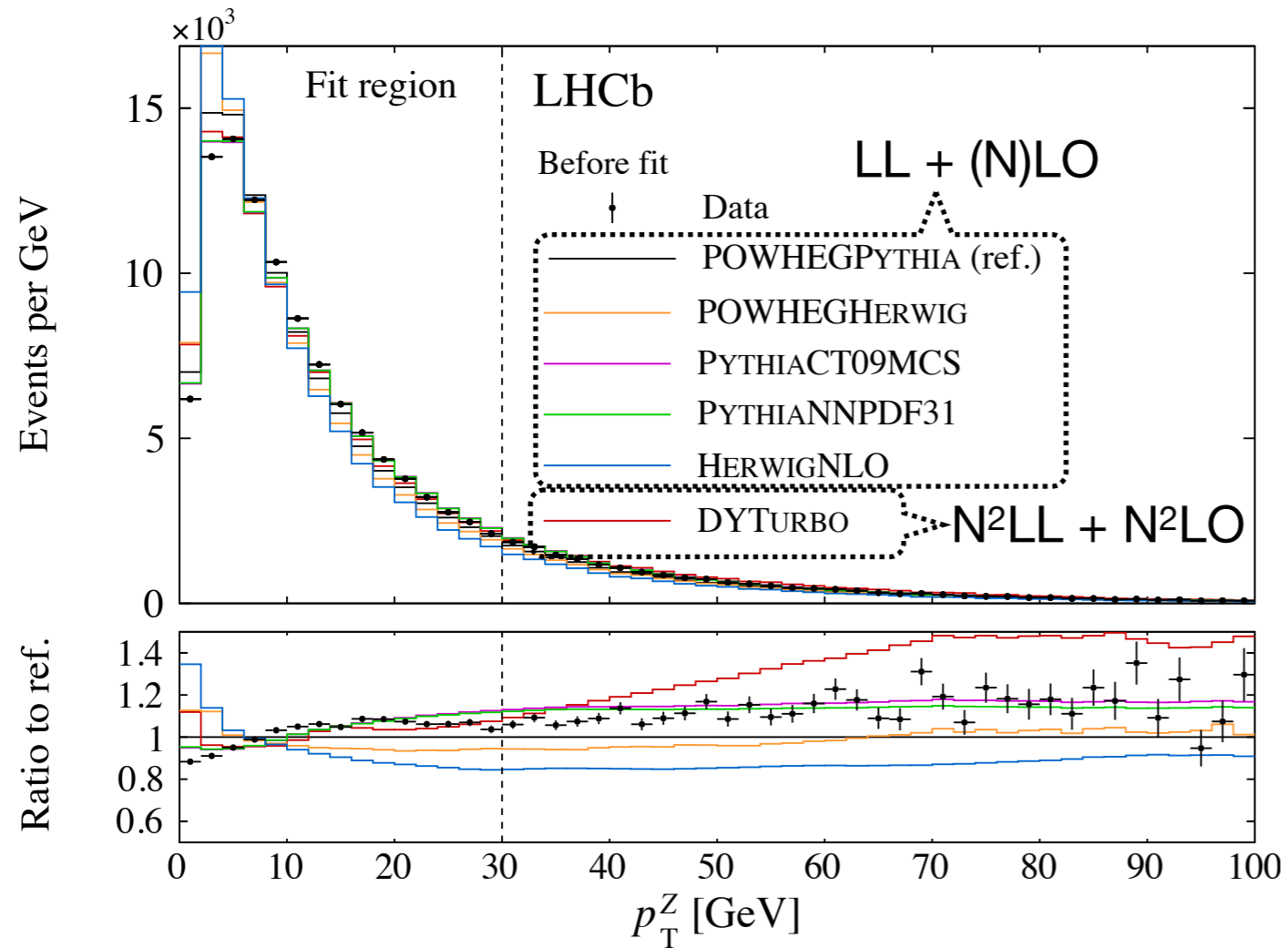
DYTurbo (at N²LL+N²LO) does *OK* out-of-the-box for p_T < 30 GeV

Varied success with the event generators, but they can still be tuned…

Tuning and validation with Z p$_T$ data

Tuning of α$_s$ and intrinsic k$_T$
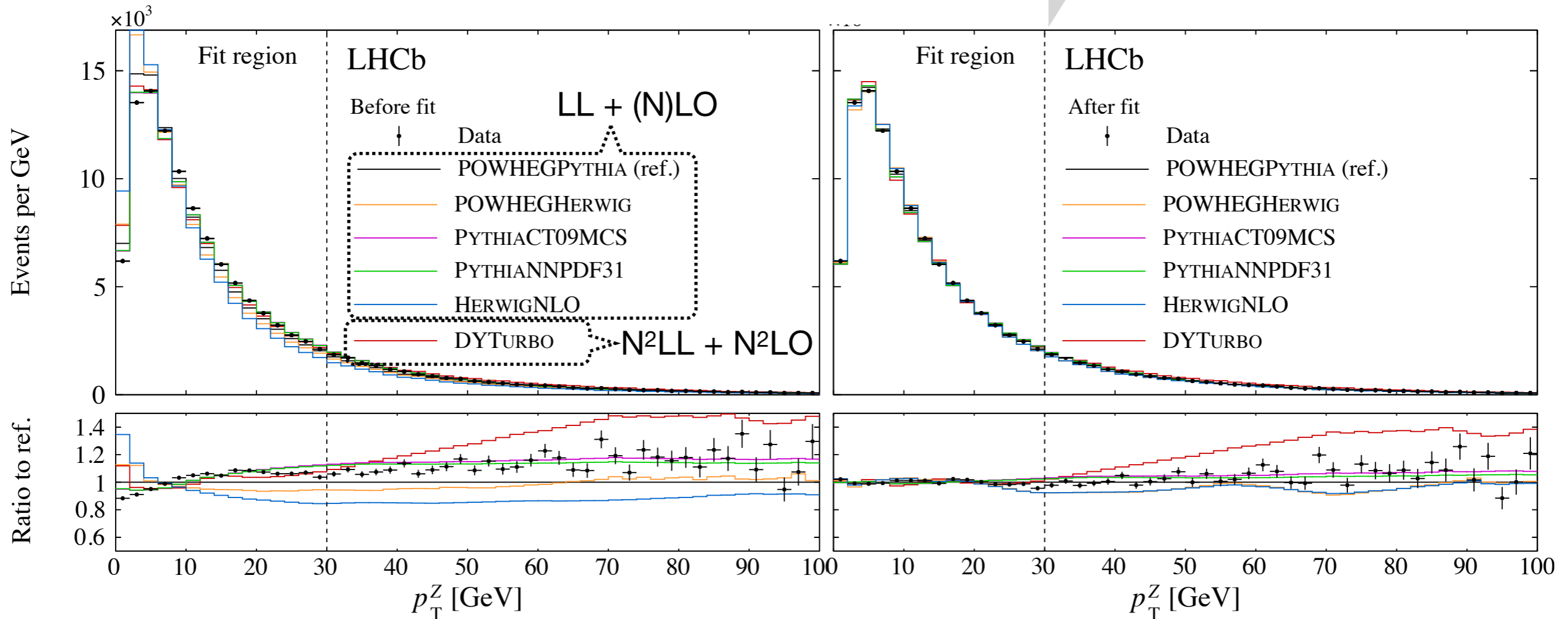

DYTurbo (at N²LL+N²LO) does *OK* out-of-the-box for p$_T$ < 30 GeV

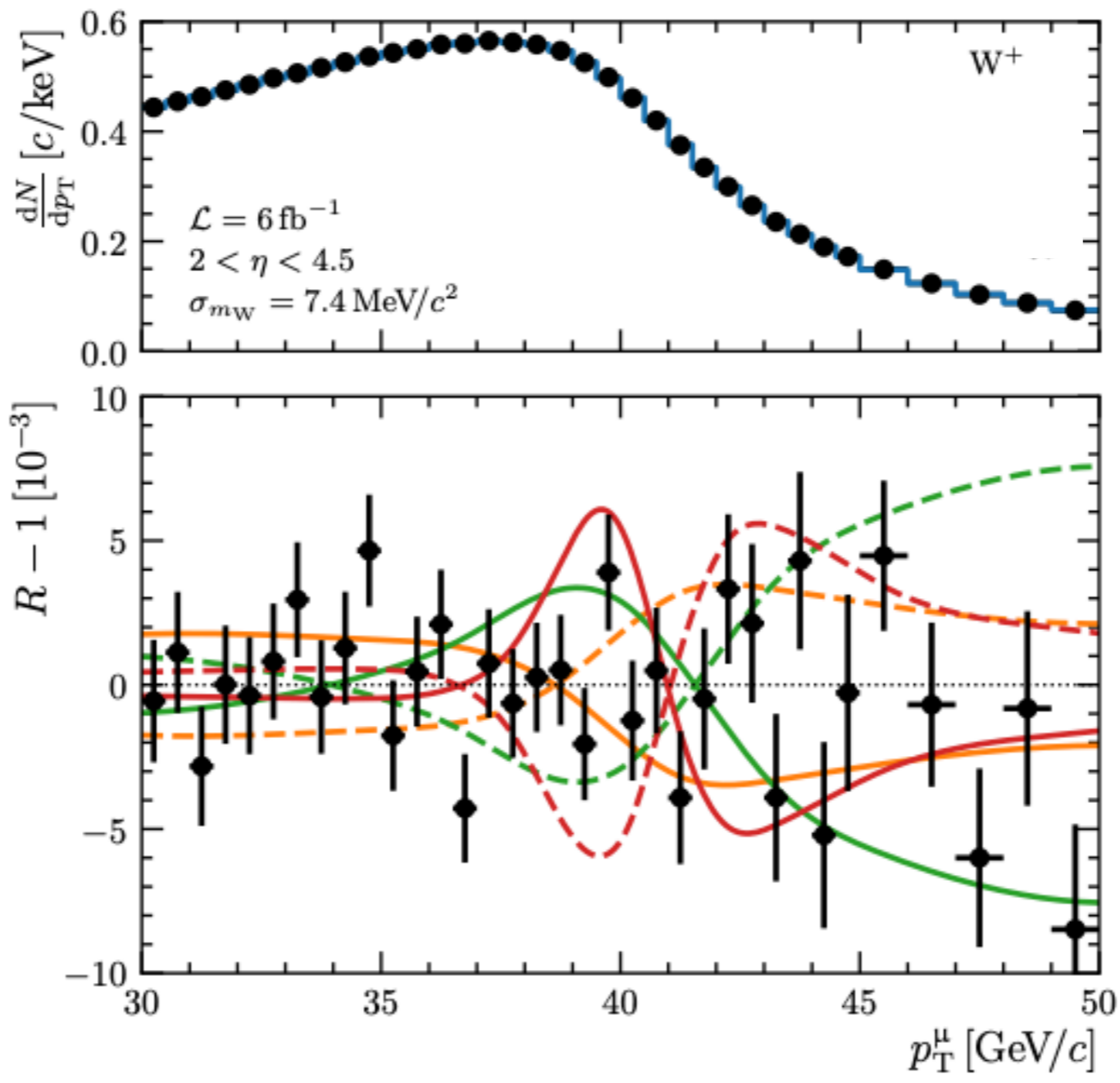Varied success with the event generators, but they can still be tuned…

POWHEGPythia gives the best description after tuning and is therefore the basis of our central model.

⚠️ Would the resulting predictions of W p$_T$ distribution be reliable?

Avoiding this issue with a W-specific tune

1907.09958 (2019)

±5σ variations

— m_{W}
— α_s
— $k_{\mathrm{T}}^{\mathrm{intr.}}$

Angular coefficients

$$\frac{\mathrm{d}\sigma}{\mathrm{d}p_{\mathrm{T}}^{W}\mathrm{d}y\mathrm{d}M\mathrm{d}\cos\theta\mathrm{d}\phi} = \frac{3}{16\pi}\frac{\mathrm{d}\sigma^{\mathrm{unpol.}}}{\mathrm{d}p_{\mathrm{T}}^{V}\mathrm{d}y\mathrm{d}M}$$

$$\{(1+\cos^2\theta) + A_0\frac{1}{2}(1-3\cos^2\theta) + A_1\sin 2\theta\cos\phi$$

$$+ A_2\frac{1}{2}\sin^2\theta\cos 2\phi + A_3\sin\theta\cos\phi + A_4\cos\theta$$

$$+ A_5\sin^2\theta\sin 2\phi + A_6\sin 2\theta\sin\phi + A_7\sin\theta\sin\phi\},$$
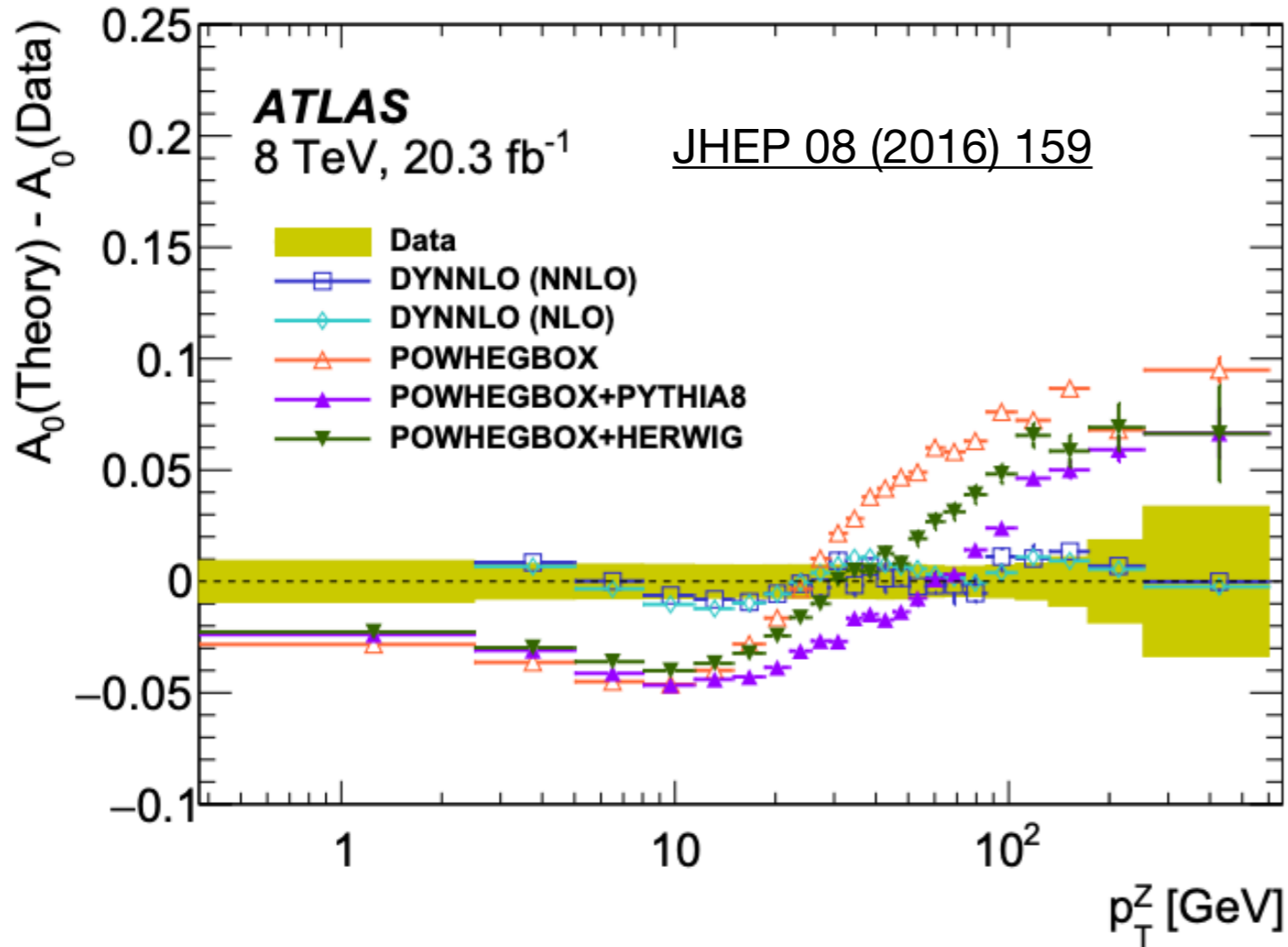
Event generators (e.g. POWHEG) have various difficulties.

Choose to use predictions at $O(\alpha_s^2)$ from DYTurbo.

The angular coefficients are essentially [helicity] cross-section *ratios*: do we correlate the scale variations?

Angular coefficients

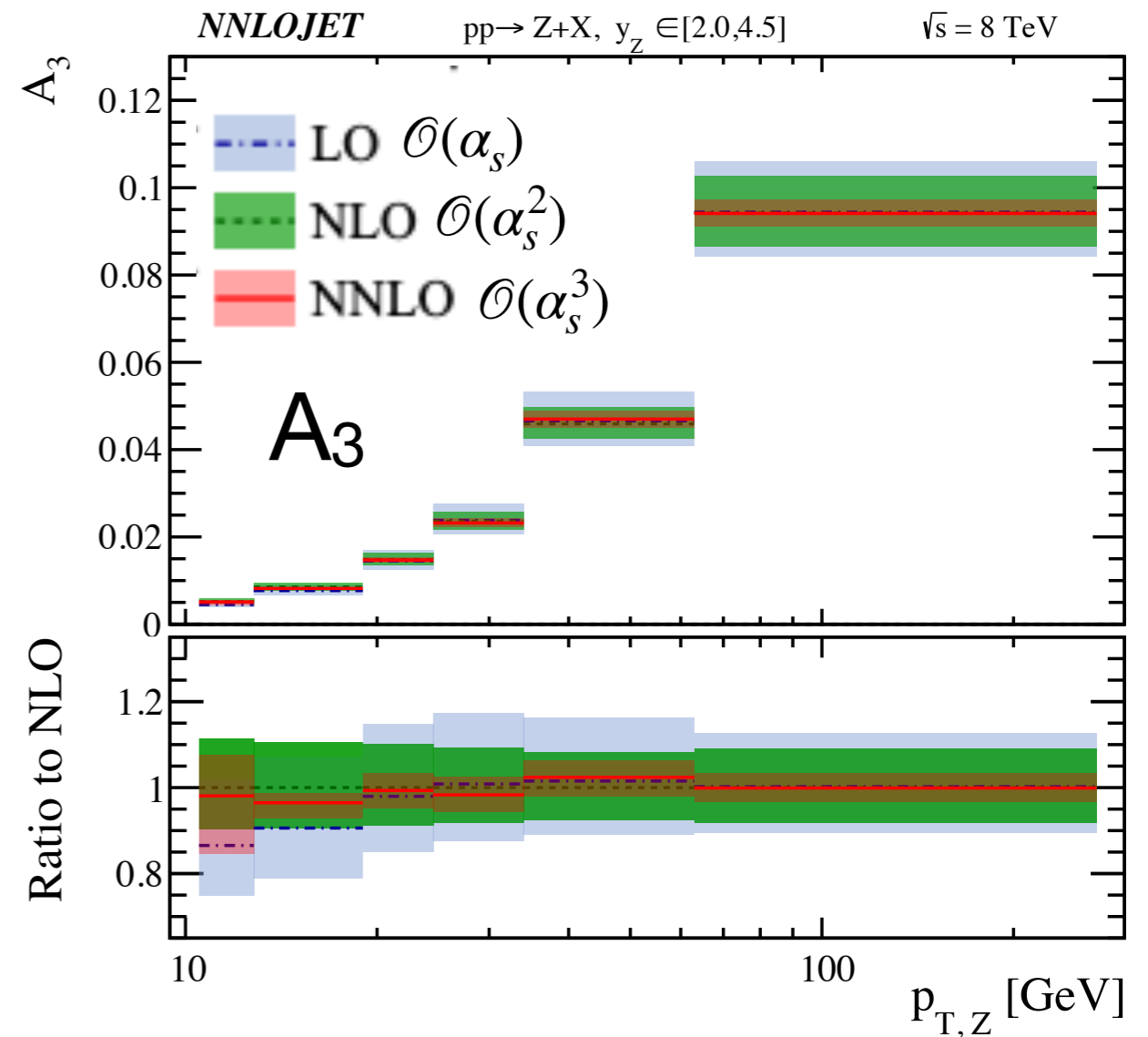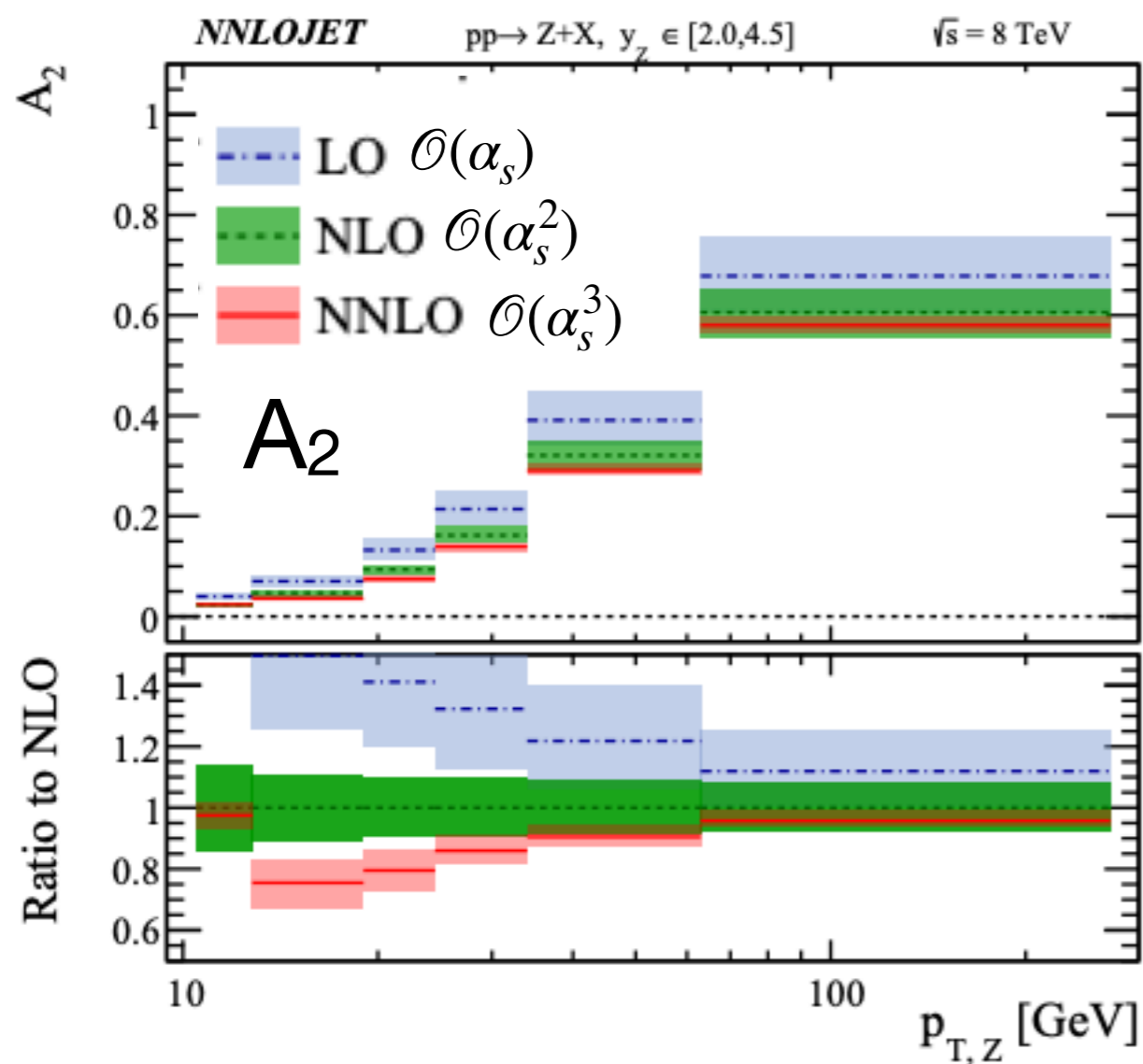We follow the preference of JHEP 11 (2017) 003: *uncorrelated* prescription with 31 point scale variation.

Our special treatment of A₃

$$\frac{\mathrm{d}\sigma}{\mathrm{d}p_T^W\,\mathrm{d}y\,\mathrm{d}M\,\mathrm{d}\cos\theta\,\mathrm{d}\phi} = \frac{3}{16\pi}\frac{\mathrm{d}\sigma^{\mathrm{U+L}}}{\mathrm{d}p_T^V\,\mathrm{d}y\,\mathrm{d}M}$$

$$\left\{ (1+\cos^2\theta) + A_0\frac{1}{2}(1-3\cos^2\theta) + A_1\sin 2\theta\cos\phi \right.$$

$$+ A_2\frac{1}{2}\sin^2\theta\cos 2\phi + \boxed{A_3\sin\theta\cos\phi} + A_4\cos\theta$$

$$\left. + A_5\sin^2\theta\sin 2\phi + A_6\sin 2\theta\sin\phi + A_7\sin\theta\sin\phi \right\},$$
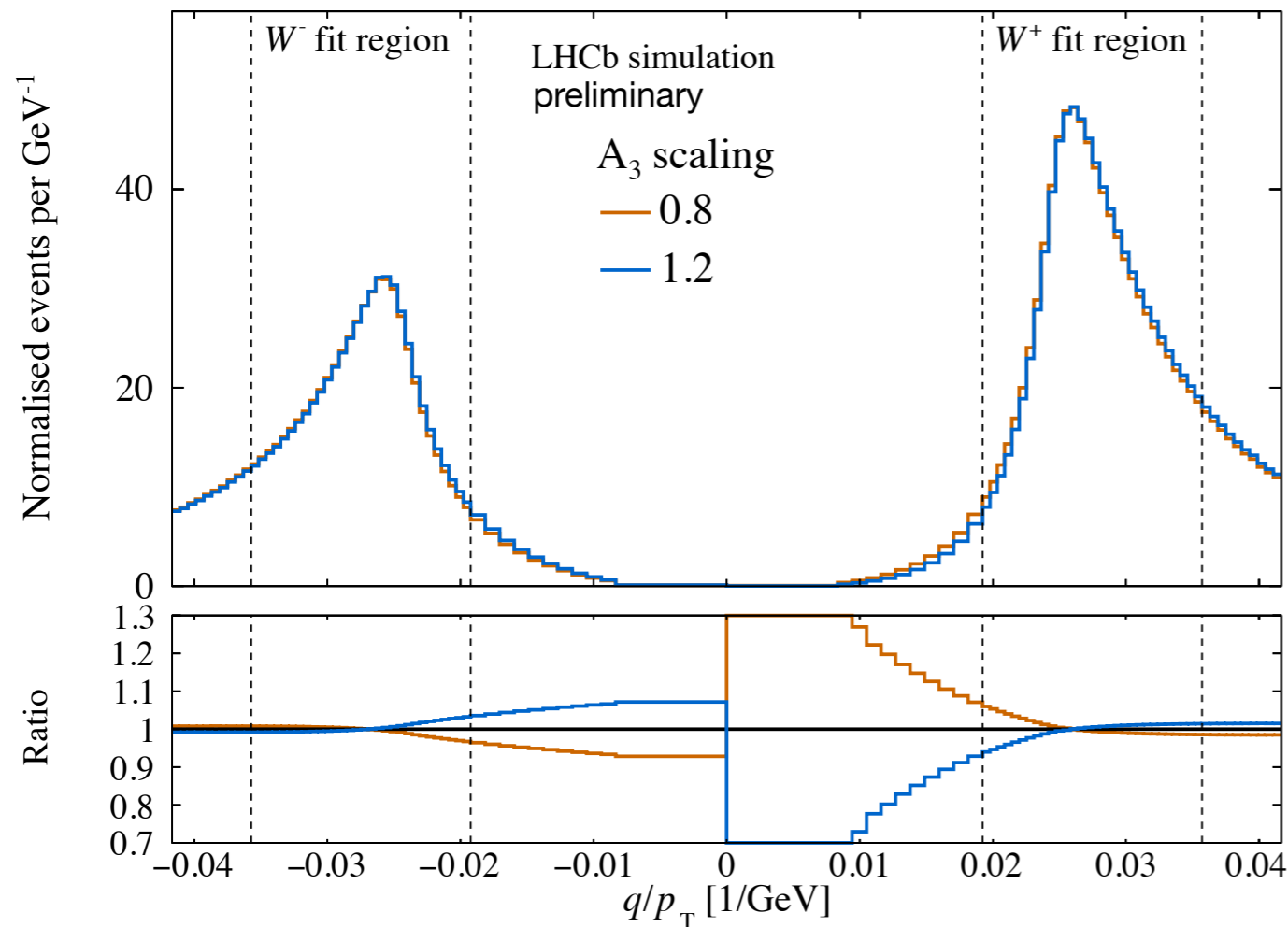
The resulting uncertainty on m_W would be around 20-30 MeV.

Dominant sensitivity traced to the A_3 parameter.

Our solution is to float a single A_3 scale factor, which reduces the uncertainty to below 10 MeV.

[Pseudo]data challenges
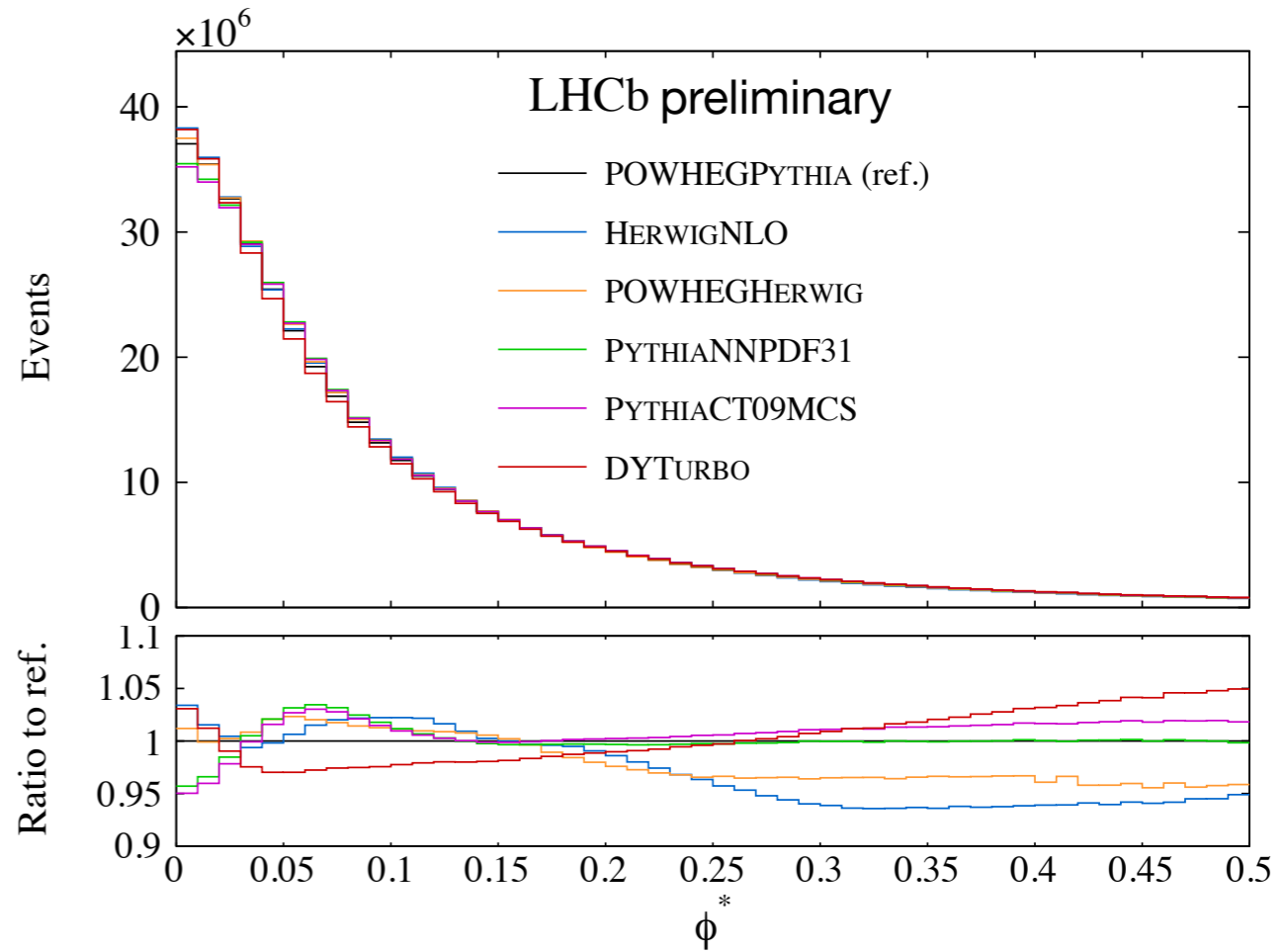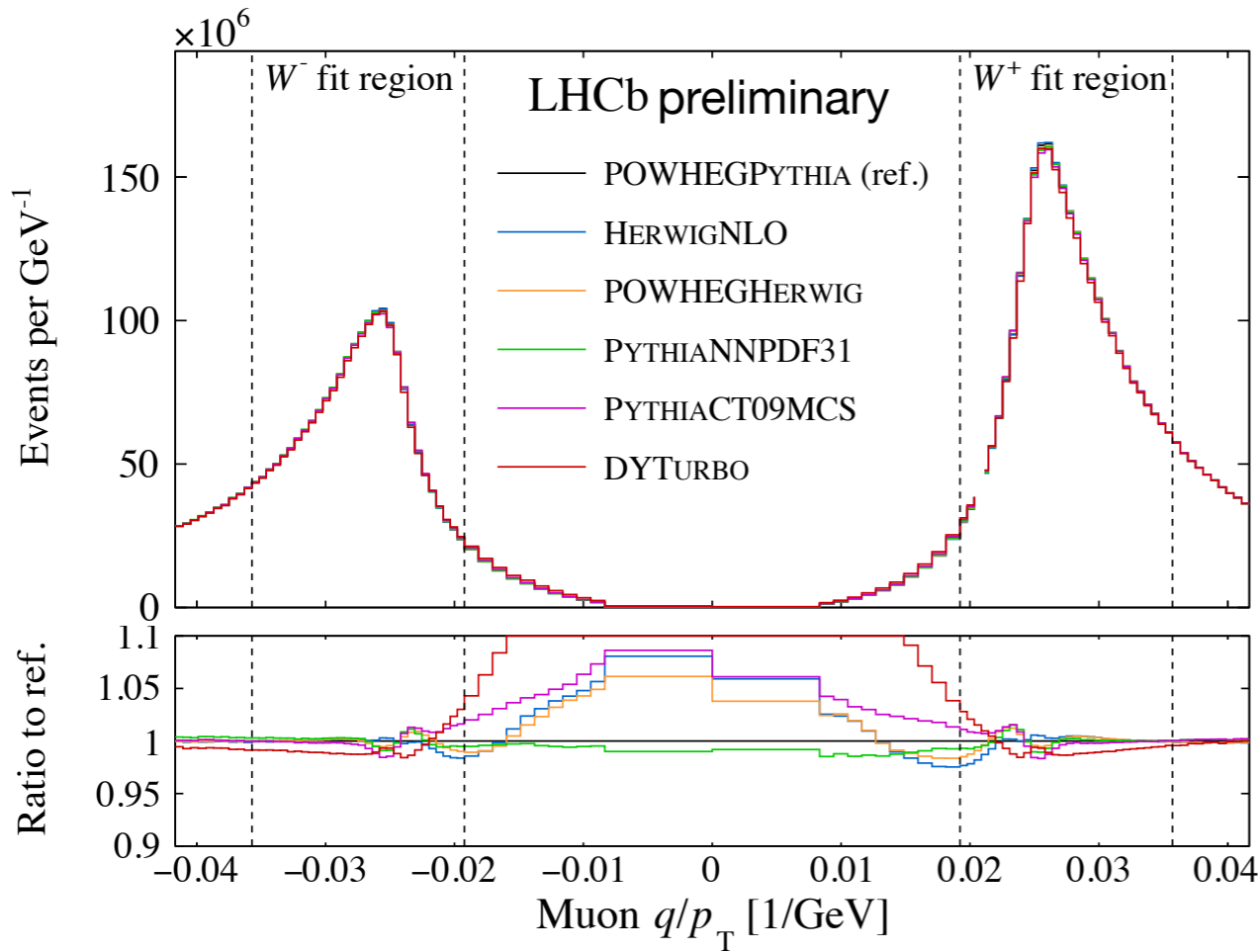
Can our [POWHEG+Pythia] model adapt itself to pseudo data corresponding to *other* models of the W/Z pT distributions?

[Pseudo]data challenges
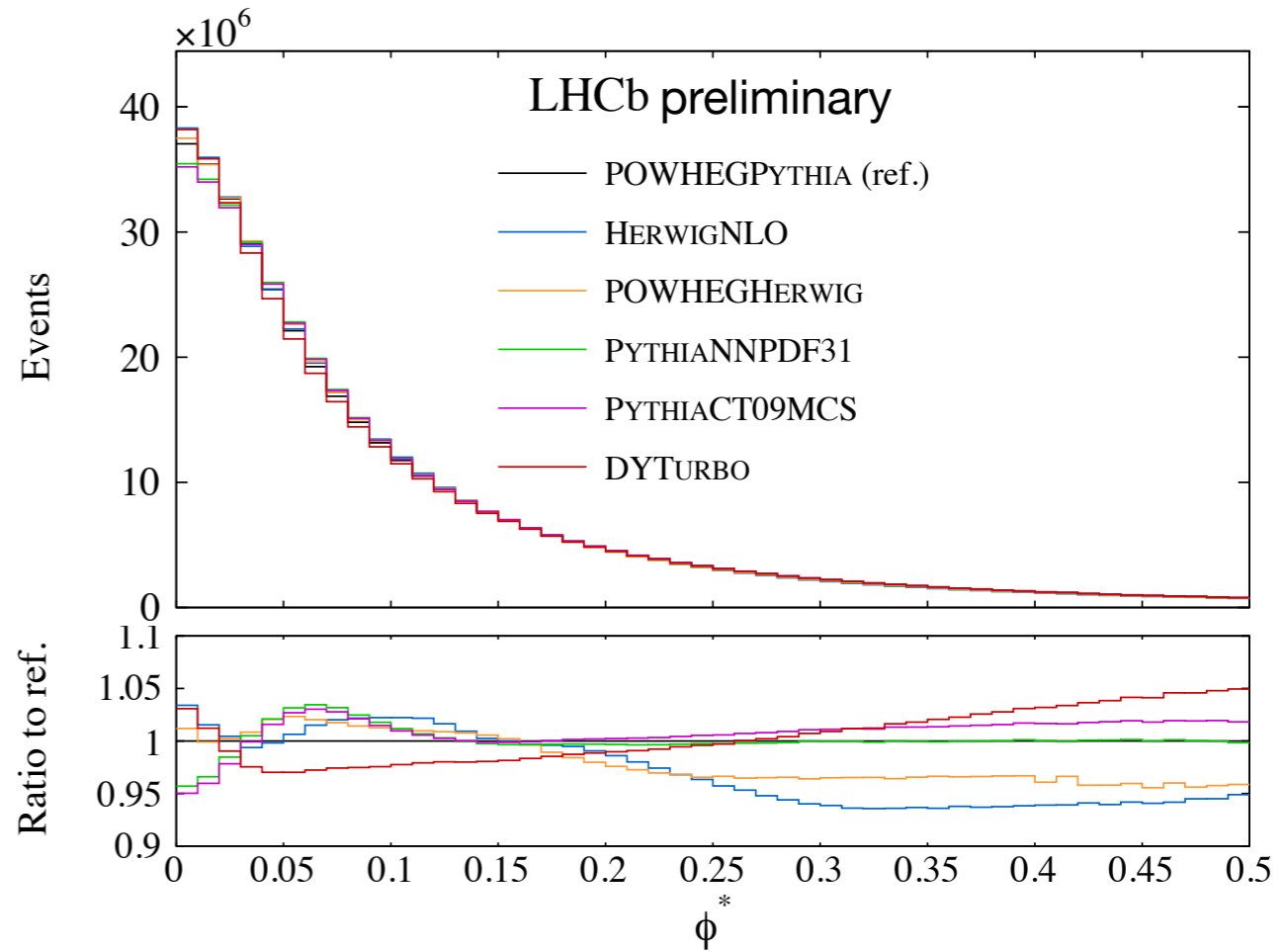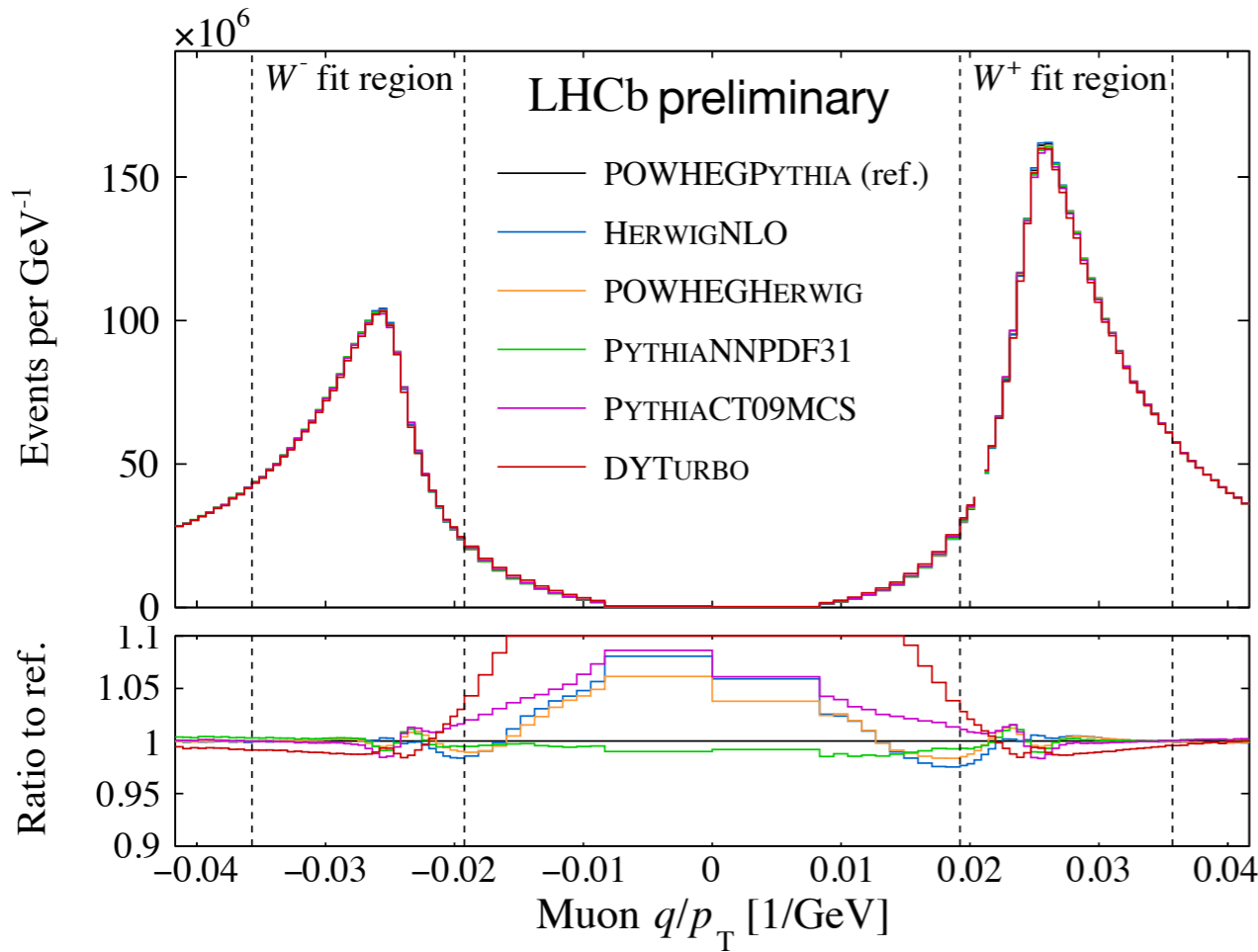
Can our [POWHEG+Pythia] model adapt itself to pseudo data corresponding to *other* models of the W/Z p$_T$ distributions?

Data config.	χ^2_W	χ^2_Z	δm_W [MeV]
POWHEGPYTHIA	64.8	34.2	–
HERWIGNLO	71.9	600.4	1.6
POWHEGHERWIG	64.0	118.6	2.7
PYTHIA 8, CT09MCS	71.0	215.8	-2.4
PYTHIA 8, NNPDF31	66.9	156.2	-10.4
DYTURBO	81.5	334.3	-0.8

✅ No more than 10 MeV bias on m$_W$!

Electroweak corrections

Pythia, Photos and Herwig models of QED final state radiation considered.

Central result based on the average of the three, while the uncertainty is based on the envelope over the three individual models.
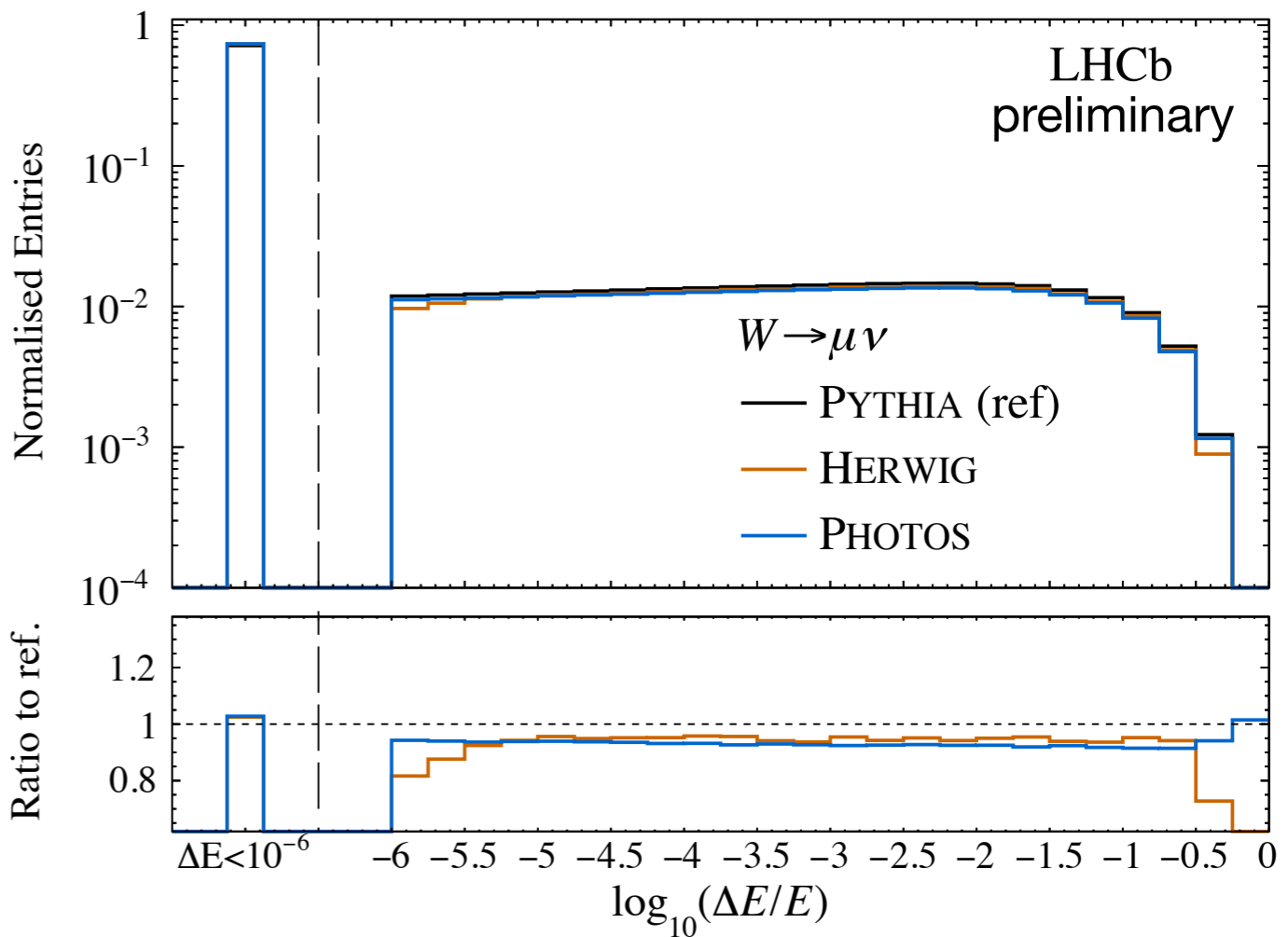
The reweighting variable where ΔE is the difference in energy between the final-state lepton pair before and after QED FSR.

The effect of additional missing electroweak corrections is assessed by fitting pseudodata from POWHEGew JHEP 04 (2012) 037 with and without EW corrections. The difference in m_W is insignificant so the statistical uncertainty of 5 MeV is assigned.

The central fit
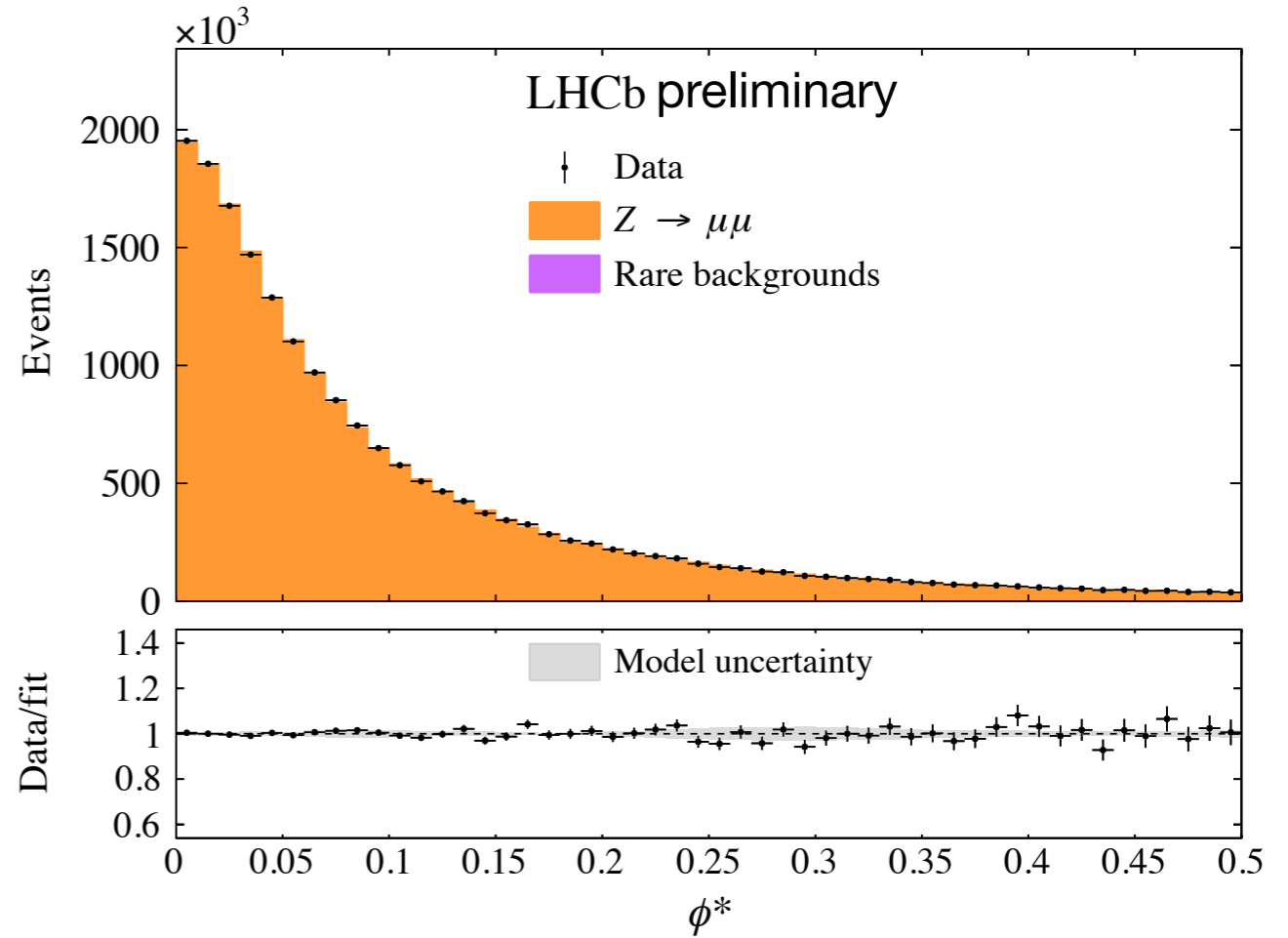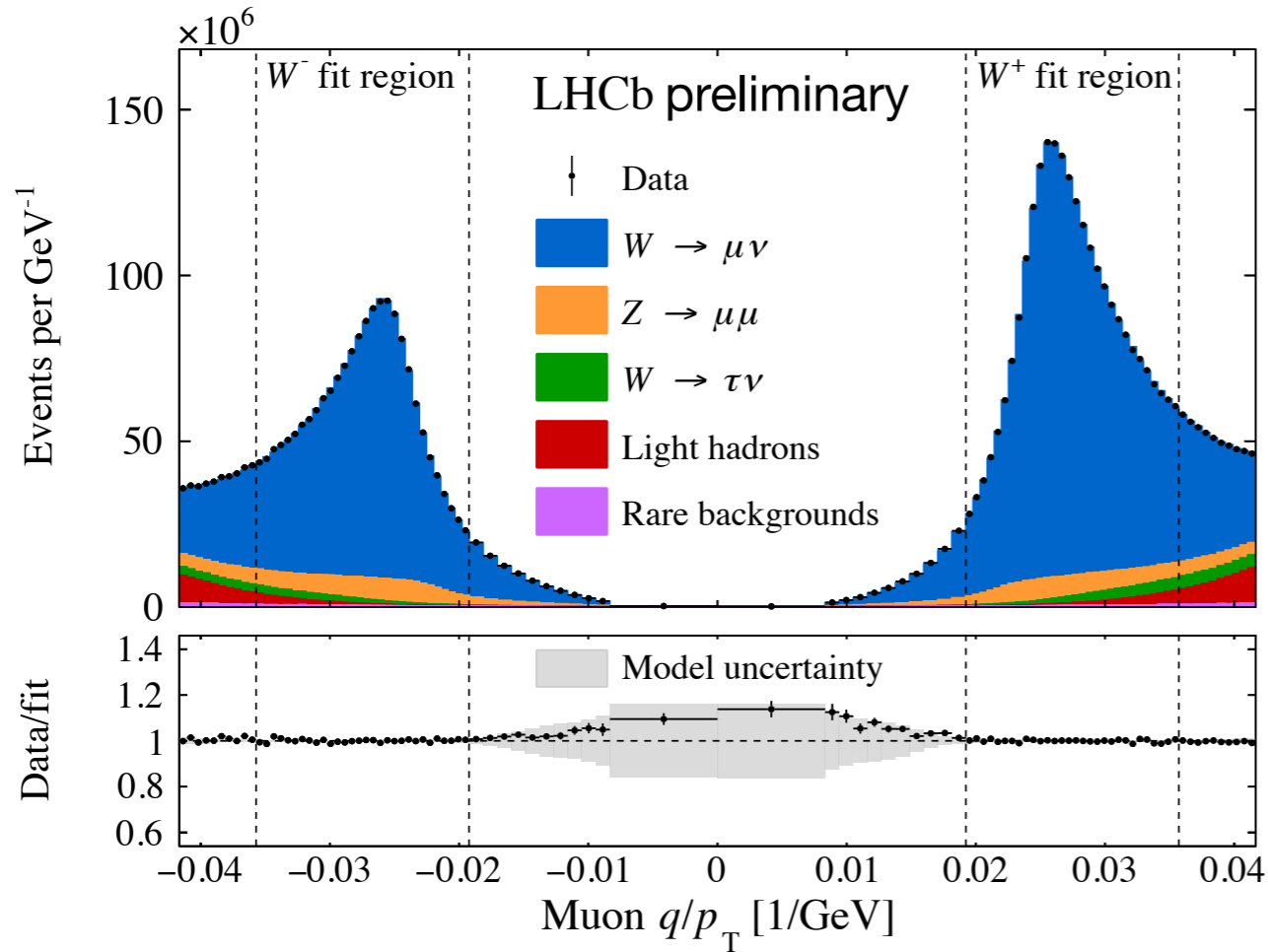
Floating parameter	Postfit value
Fraction of $W^+ \to \mu^+\nu$	0.5293 ± 0.0006
Fraction of $W^- \to \mu^-\nu$	0.3510 ± 0.0005
Fraction of hadron background	0.0151 ± 0.0007
α_s^Z	0.1243 ± 0.0004
α_s^W	0.1263 ± 0.0003
k_T^{intr}	$1.57 \pm 0.14\,\mathrm{GeV}$
A_3 scaling	0.979 ± 0.026

$$\chi^2/\mathrm{ndf} = 105/102$$

$$\sigma_{\mathrm{stat}}(m_W) = 23\ \mathrm{MeV}$$

(Fit value is still blinded)

PDF uncertainties

The uncertainties are evaluated with specific prescriptions from each of the three groups[1].

At present we choose *not* to constrain the PDF uncertainty using weights or profiling[2].

Our central m_W result is an average of the three results with the individual PDF sets.

The δm_W are w.r.t central NNPDF3.1 replica
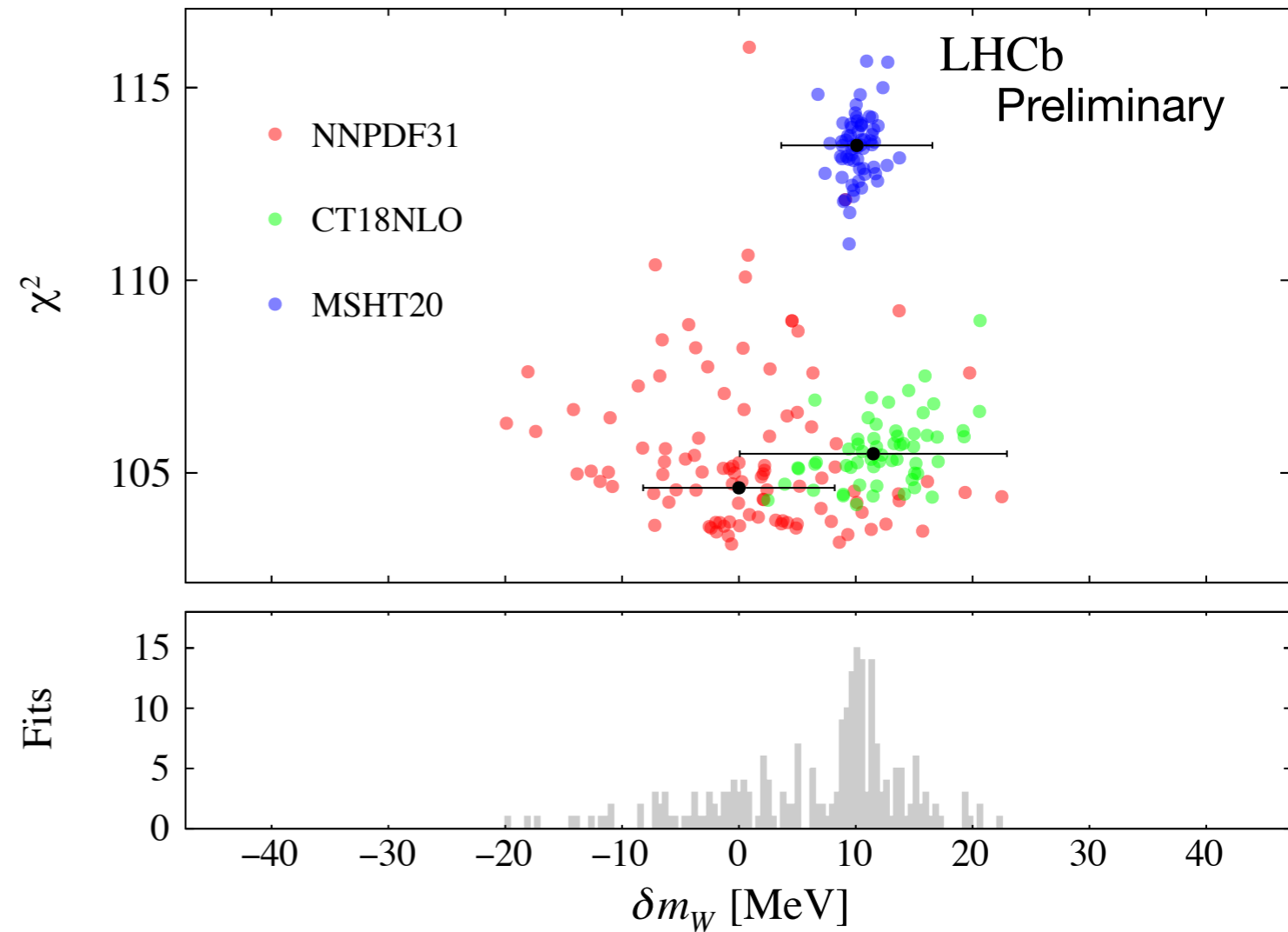
Set	δm_W [MeV]	$\sigma_{\mathrm{PDF,base}}$ [MeV]	$\sigma_{\mathrm{PDF},\alpha_s}$ [MeV]	σ_{PDF} [MeV]
NNPDF3.1	–	±8.2	±2.5	±8.6
CT18NLO	+11.4	±11.4	±1.6	±11.5
MSHT20	+10.1	±6.5	±2.1	±6.8

[1]CT18 uncertainty is rescaled to 68% C.L.
[2] Encouraging future prospects for LHCb explored in Eur. Phys.J.C 79 (2019) 6

Measurement uncertainty summary

Source	Size [MeV]	
Parton distribution functions	**9.0**	Average of NNPDF31, CT18, MSHT20
Theory (excl. PDFs) total	**17.4**	
Transverse momentum model	12.0	Envelope from five different models
Angular coefficients	9.0	"Uncorrelated" 31 point scale variation
QED FSR model	7.2	Envelope of Pythia, Photos and Herwig
Additional electroweak corrections	5.0	Test with POWHEGew
Experimental total	**10.6**	
Momentum scale and resolution modelling	7.5	Includes simple statistical contributions, dependence on external inputs and details of the methods.
Muon ID, trigger and tracking efficiency	6.0	
Isolation efficiency	3.9	
QCD background	2.3	
Statistical	**22.7**	
Total	**31.7**	

The [12 MeV] size of the transverse momentum model uncertainty is commensurate with the conclusions of the "data challenge" exercise.

Cross checks

1. **Orthogonal splits:** Five ~50:50 splits of the data (polarity, charge $\times$ polarity, etc…) all result in [m_W] differences within 2σ.

2. **Fit range:** The result is stable w.r.t. variations in the upper/lower limits.

3. **Fit freedom:** The result is stable w.r.t. variations in the model freedom (e.g. 3 independent α_s values instead of 2, etc…)

4. **W-like fit of the Z mass:** Measurements with μ^+ and μ^- agree to better than 1σ and their average agrees with the PDG value to better than 1σ.

5. **δm_W fit:** Alternative fit with the difference between the W^+ and W^- masses as another floating parameter: this parameter is consistent with zero within 1σ.

6. **Additional tests** with NNLO PDFs instead of NLO PDFs, variations in the charm quark mass, etc… affect m_W at the ≲ 1 MeV level.

7. …

Unblinding of m$_W$
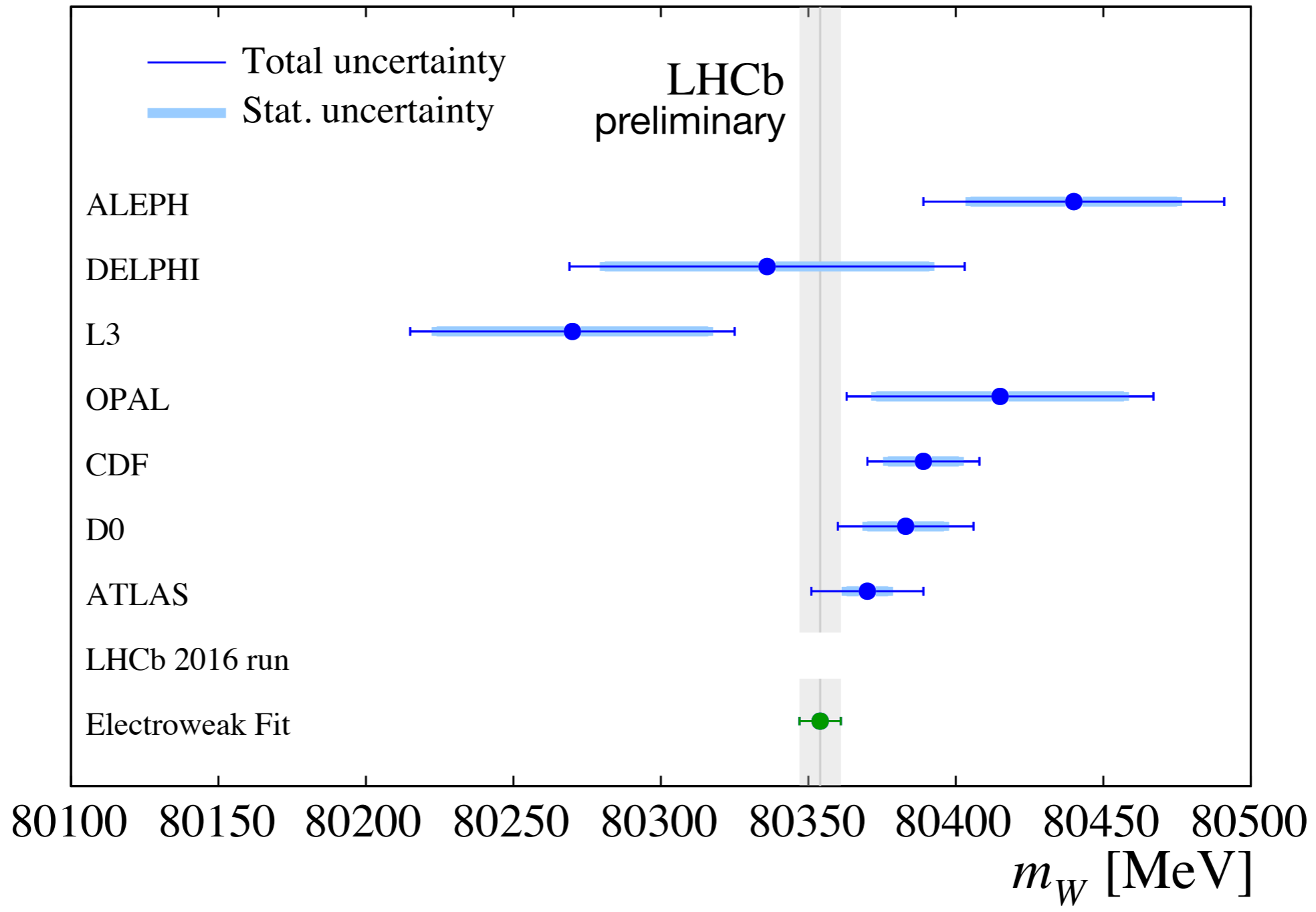
Unblinding of m_W
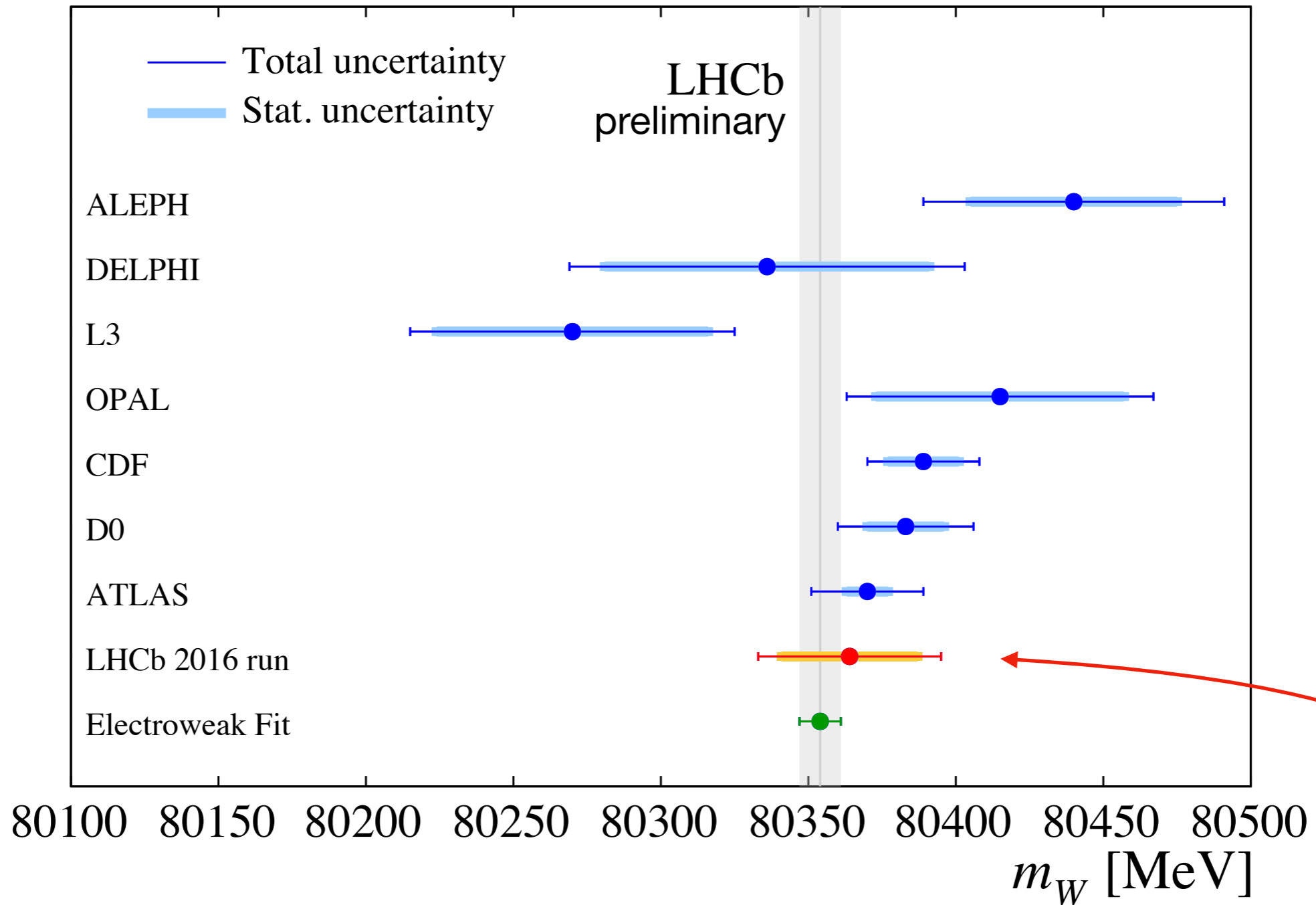
$$m_W = 80364 \pm 23_{\text{stat}} \pm 11_{\text{exp}} \pm 17_{\text{theory}} \pm 9_{\text{PDF}} \text{ MeV}$$

Prospects for LHC average

A first measurement from CMS is anticipated, while a detailed average of ATLAS, CDF and D0 is underway.

ATLAS+LHCb average under the simplest assumptions:
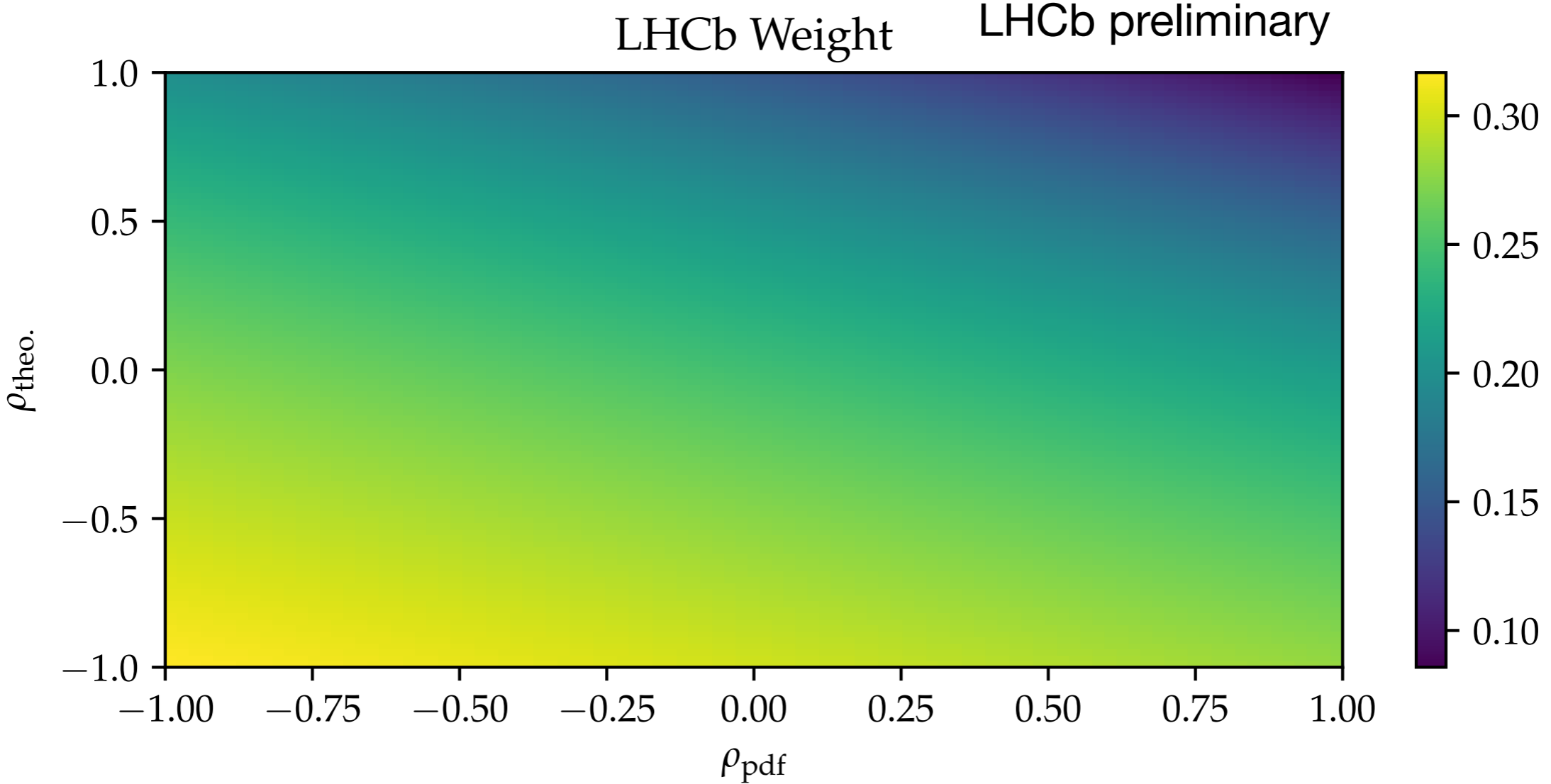
A detailed ATLAS+LHCb collaborative effort will be required to precisely determine these two correlation coefficients but it seems likely that ρ_{PDF} will be negative 1508.06954 while the (non-PDF) theory uncertainty will have a positive coefficient.

Prospects for LHC average

A first measurement from CMS is anticipated, while a detailed average of ATLAS, CDF and D0 is underway.

ATLAS+LHCb average under the simplest assumptions:
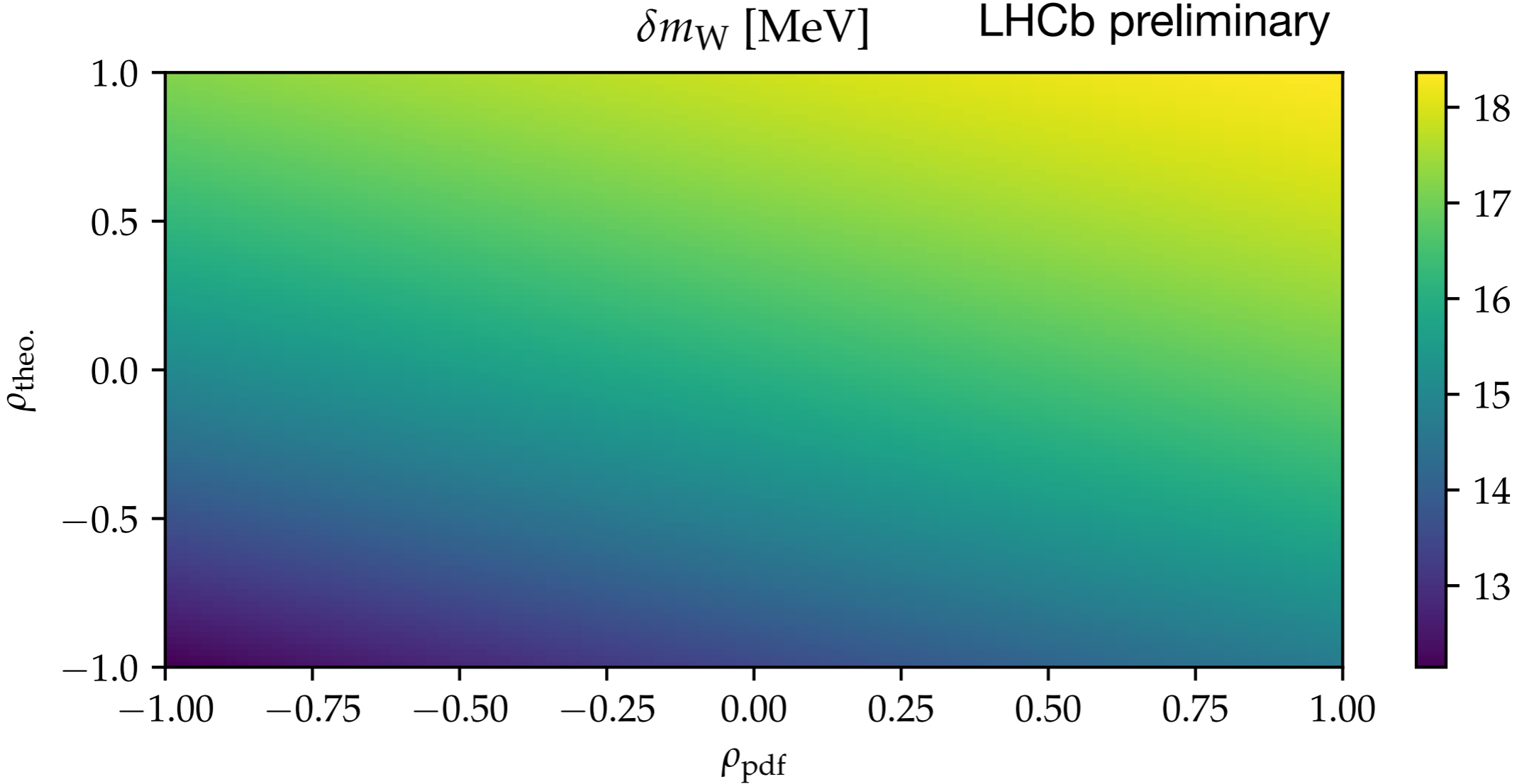
A detailed ATLAS+LHCb collaborative effort will be required to precisely determine these two correlation coefficients but it seems likely that ρ_{PDF} will be negative 1508.06954 while the (non-PDF) theory uncertainty will have a positive coefficient.

Conclusions and outlook
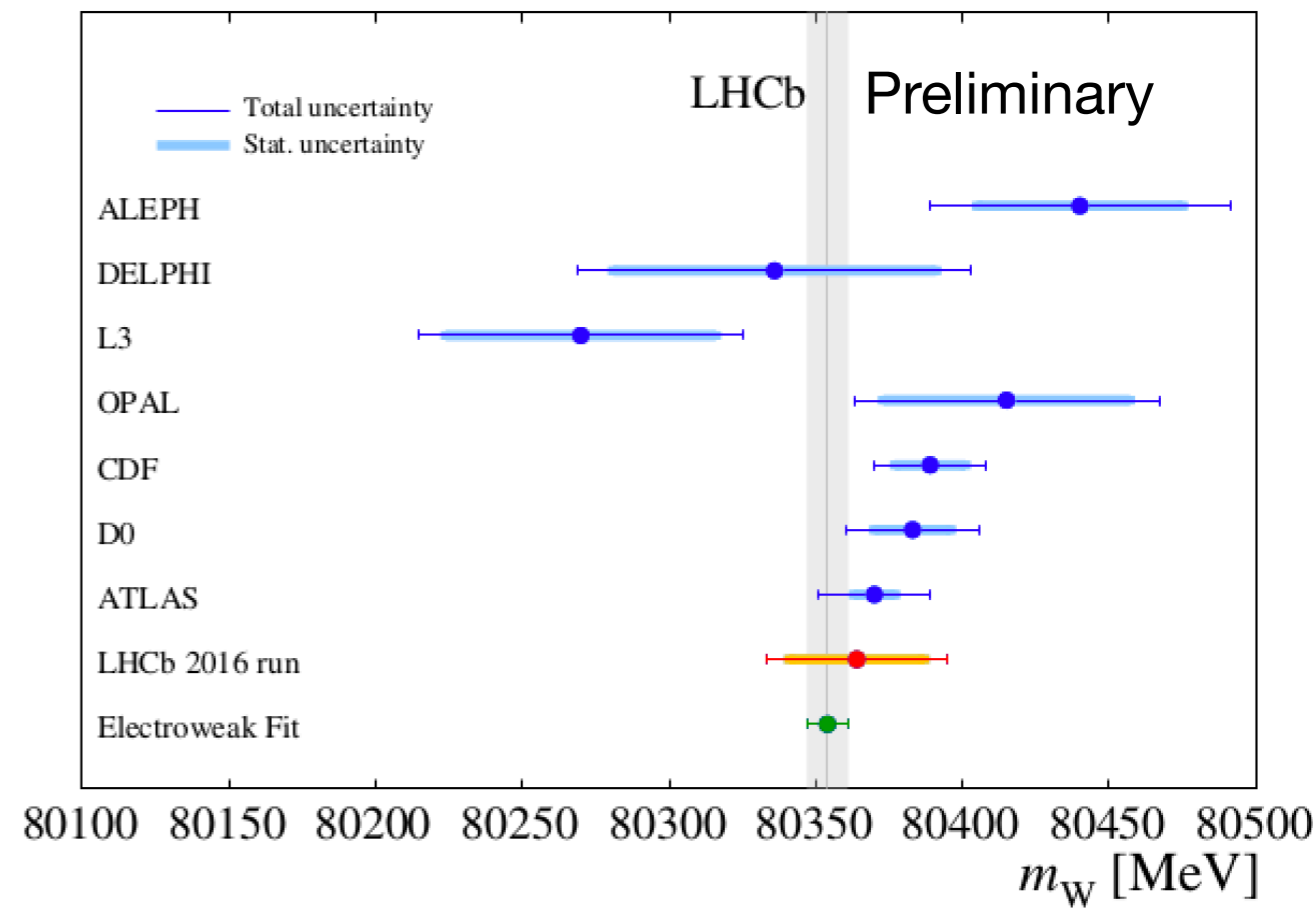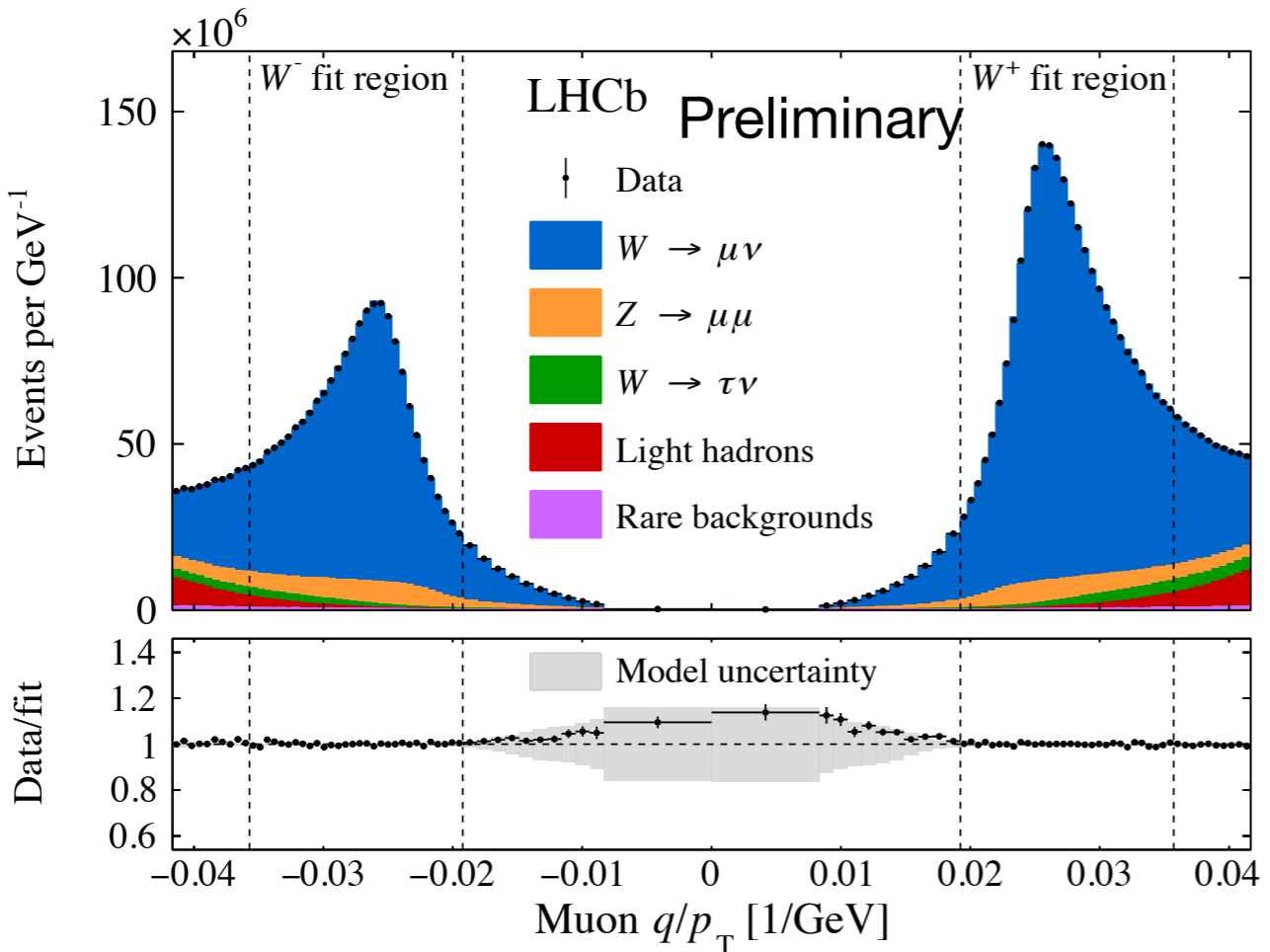
First measurement of m_W from LHCb with 32 MeV uncertainty is consistent with previous measurements and with the prediction.

A total uncertainty of $\lesssim$ 20 MeV looks achievable with existing LHCb data.

EPJC 79 (2019) 6 encourages us to upgrade to a double-differential fit.

We look forward to working with the other LHC experiments, and the theory community, to fully exploit LHCb's unique/complementary rapidity coverage to achieve the ultimate precision on m_W.

Backup slides

Custom alignment for high p_T analyses
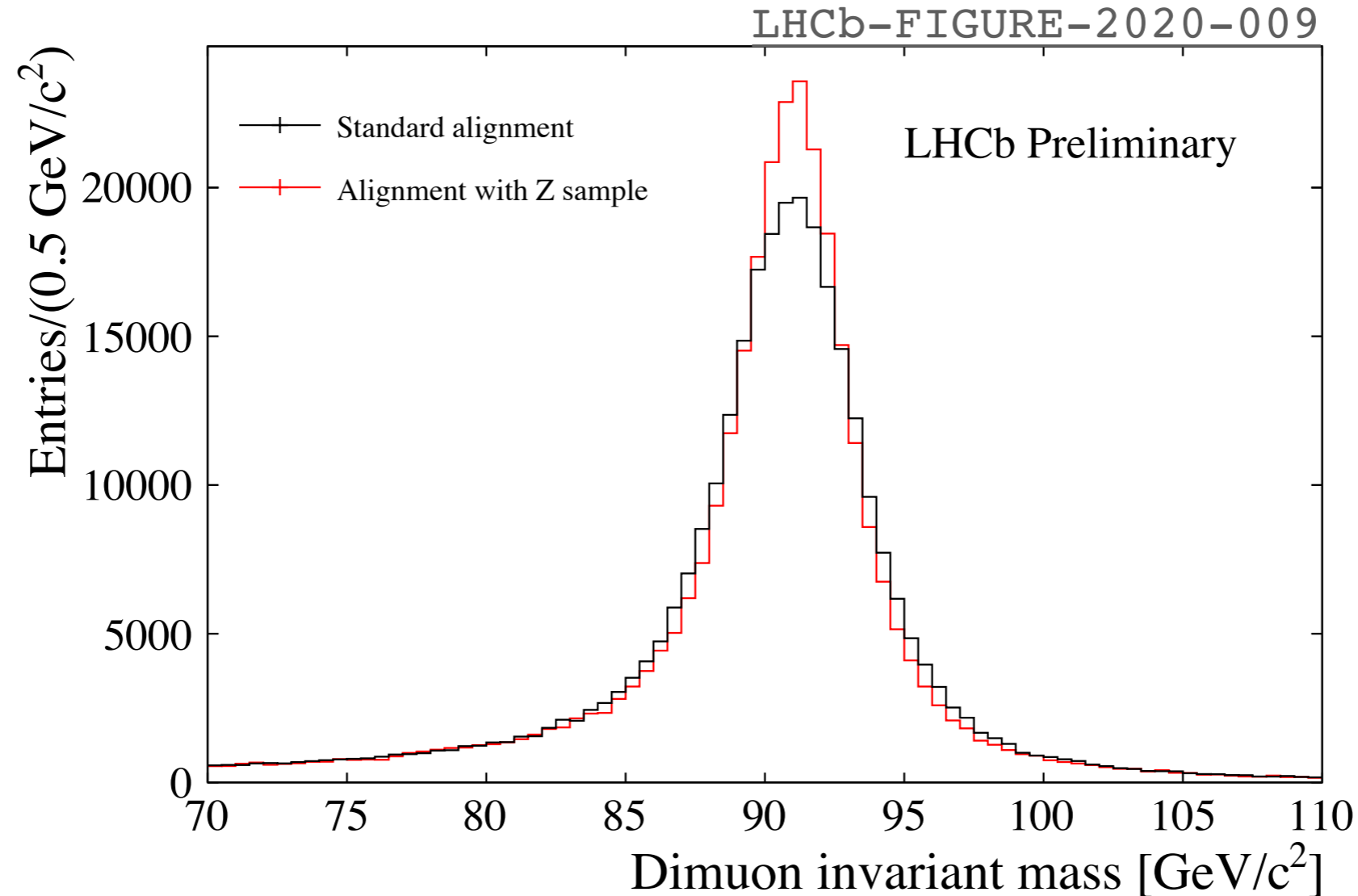
LHCb's successful real-time alignment and calibration was commissioned in Run-2 JINST 14 (2019) P04013

For the very high (up to ~1 TeV) momentum muons in EW processes the resolution could be improved with a custom alignment including mass-constrained Z candidates.

Recent study on α$_s$ [2106.10289](#)

MSHT2020 NLO $\alpha_s(M_Z^2)$ bounds of datasets
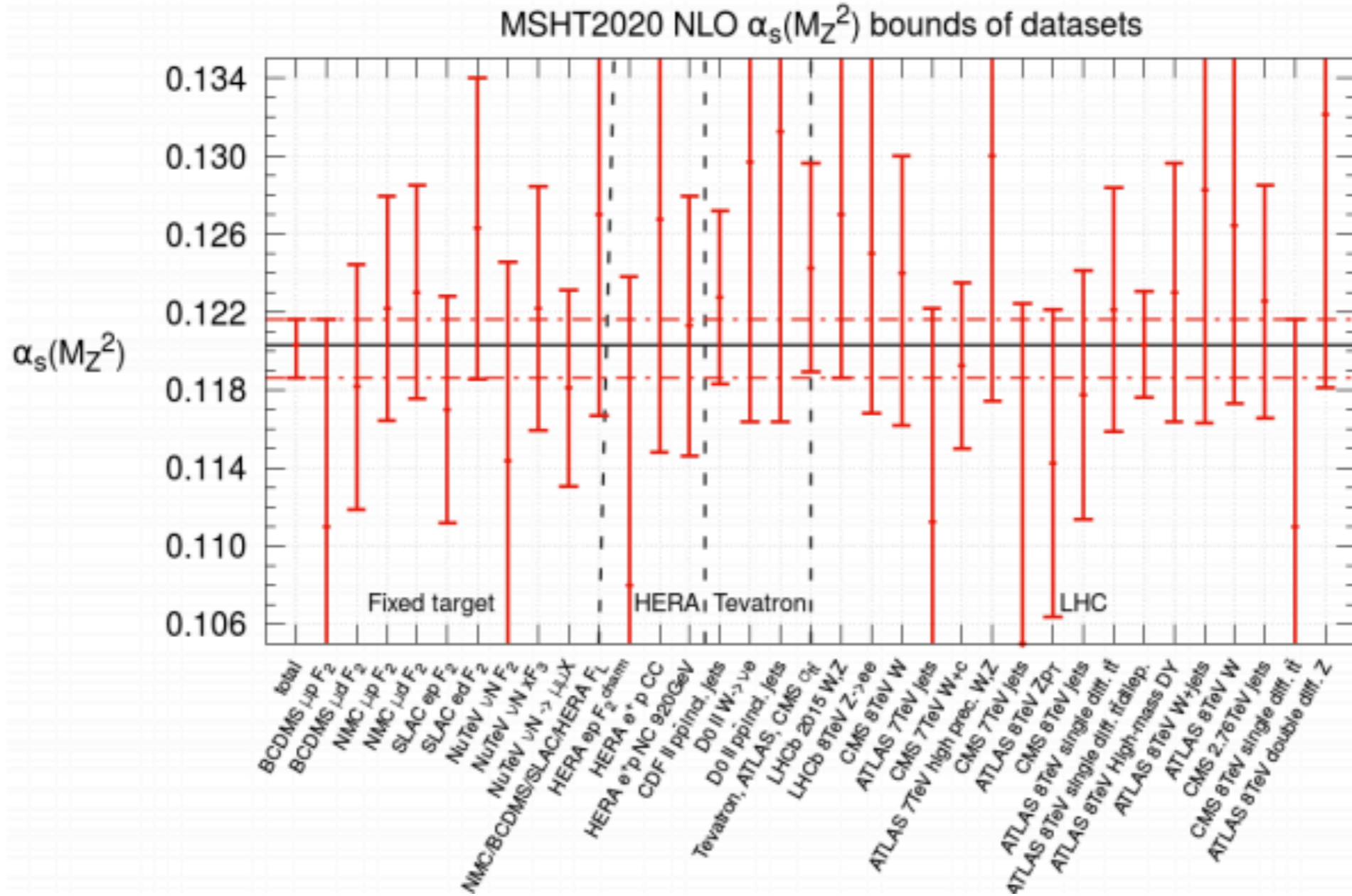
An investigation of the α_S and heavy quark mass dependence in the MSHT20 global PDF analysis

T. Cridge, L.A. Harland-Lang, A.D. Martin, R.S. Thorne

We investigate the MSHT20 global PDF sets, demonstrating the effects of varying the strong coupling $\alpha_S(M_Z^2)$ and the masses of the charm and bottom quarks. We determine the preferred value, and accompanying uncertainties, when we allow $\alpha_S(M_Z^2)$ to be a free parameter in the MSHT20 global analyses of deep-inelastic and related hard scattering data, at both NLO and NNLO in QCD perturbation theory. We also study the constraints on $\alpha_S(M_Z^2)$ which come from the individual data sets in the global fit by repeating the NNLO and NLO global analyses at various fixed values of $\alpha_S(M_Z^2)$, spanning the range $\alpha_S(M_Z^2) = 0.108$ to 0.130 in units of 0.001. We make all resulting PDFs sets available. We find that the best fit values are $\alpha_S(M_Z^2) = 0.1203 \pm 0.0015$ and 0.1174 ± 0.0013 at NLO and NNLO respectively. We investigate the relationship between the variations in $\alpha_S(M_Z^2)$ and the uncertainties on the PDFs, and illustrate this by calculating the cross sections for key processes at the LHC. We also perform fits where we allow the heavy quark masses m_c and m_b to vary away from their default values and make PDF sets available in steps of $\Delta m_c = 0.05$ GeV and $\Delta m_b = 0.25$ GeV, using the pole mass definition of the quark masses. As for varying $\alpha_S(M_Z^2)$ values, we present the variation in the PDFs and in the predictions. We examine the comparison to data, particularly the HERA data on charm and bottom cross sections and note that our default values are very largely compatible with best fits to data. We provide PDF sets with 3 and 4 active quark flavours, as well as the standard value of 5 flavours.

Possible scenarios for the ATLAS-LHC correlations
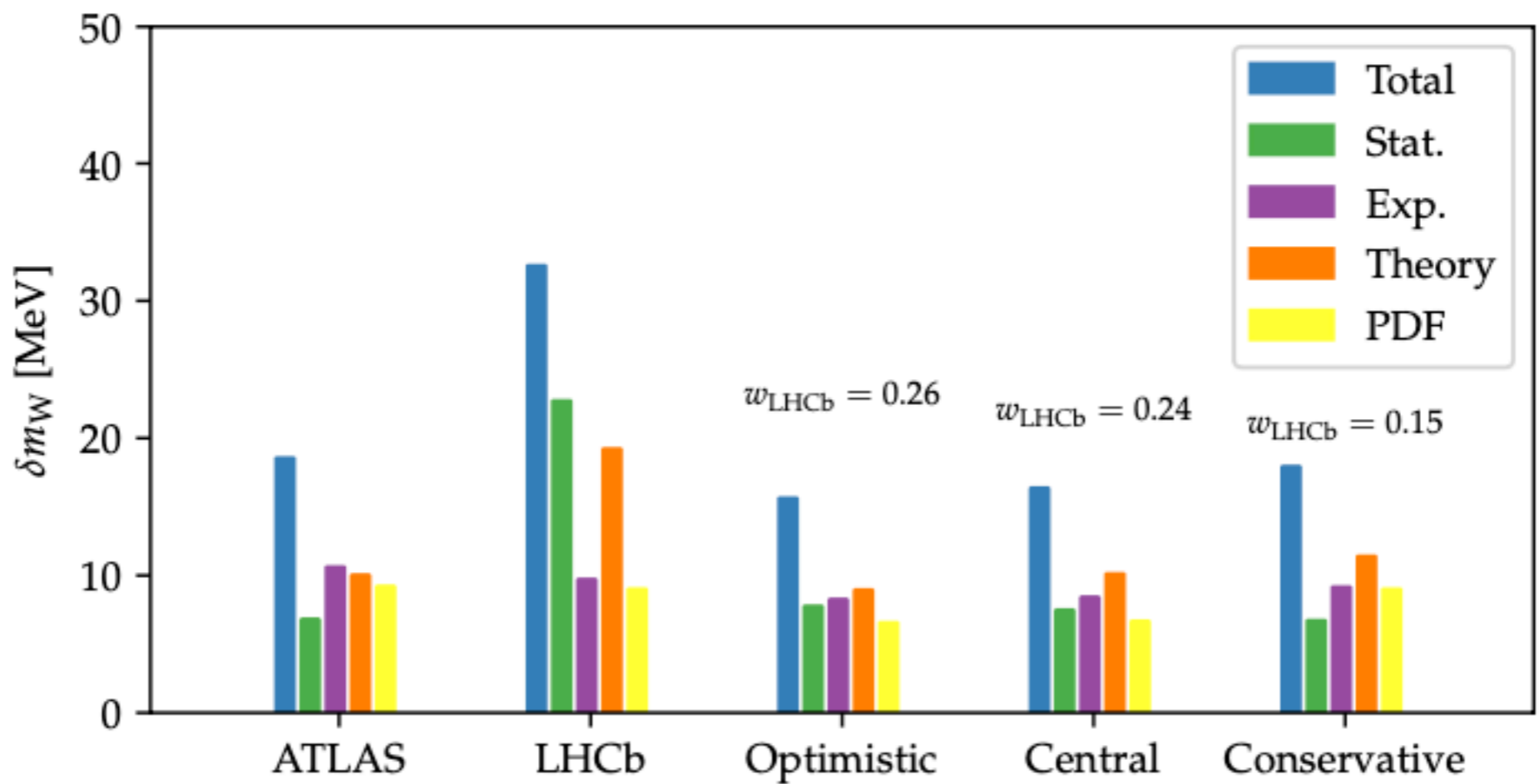
Figure 17: A breakdown of the different components of the uncertainties on the measurements of m_W at ATLAS and LHCb where additionally the combination is shown for scenarios where different assumptions of the correlation between the uncertainties due to the theoretical modelling and parton distribution functions. The weight of LHCb in the combination is indicated by w_{LHCb} and the correlation in uncertainties due to parton distribution functions is assumed to be -0.50 in the optimistic and central scenarios, and 0.00 in the conservative scenario, while the correlation on the uncertainty due to theoretical modelling is assumed to be 0.00, 0.33 and 1.00 in the optimistic, central, and conservative scenarios respectively.

Details on the ATLAS uncertainties

$$m_W = 80370 \pm 7 \text{ (stat.)} \pm 11 \text{ (exp. syst.)} \pm 14 \text{ (mod. syst.) MeV}$$

W-boson charge	W^+		W^-		Combined	
Kinematic distribution	p_T^ℓ	m_T	p_T^ℓ	m_T	p_T^ℓ	m_T
δm_W [MeV]						
Fixed-order PDF uncertainty	13.1	14.9	12.0	14.2	8.0	8.7
AZ tune	3.0	3.4	3.0	3.4	3.0	3.4
Charm-quark mass	1.2	1.5	1.2	1.5	1.2	1.5
Parton shower μ_F with heavy-flavour decorrelation	5.0	6.9	5.0	6.9	5.0	6.9
Parton shower PDF uncertainty	3.6	4.0	2.6	2.4	1.0	1.6
Angular coefficients	5.8	5.3	5.8	5.3	5.8	5.3
Total	15.9	18.1	14.8	17.2	11.6	12.9

Table 3: Systematic uncertainties in the m_W measurement due to QCD modelling, for the different kinematic distributions and W-boson charges. Except for the case of PDFs, the same uncertainties apply to W^+ and W^-. The fixed-order PDF uncertainty given for the separate W^+ and W^- final states corresponds to the quadrature sum of the CT10nnlo uncertainty variations; the charge-combined uncertainty also contains a 3.8 MeV contribution from comparing CT10nnlo to CT14 and MMHT2014.

Momentum smearing fit parameter values

$$\frac{q}{p} \rightarrow \frac{q}{p \cdot \mathcal{N}(1 + \alpha, \sigma_{\mathrm{MS}})} + \mathcal{N}\left(\delta, \frac{\sigma_\delta}{\cosh \eta}\right)$$

Parameter	Postfit value
$\alpha\ (\eta < 2.2)$	$(0.58 \pm 0.10) \times 10^{-3}$
$\alpha\ (2.2 < \eta < 4.4)$	$(-0.0054 \pm 0.0025) \times 10^{-3}$
δ	$(-0.48 \pm 0.37) \times 10^{-6}\ \mathrm{GeV}^{-1}$
$\sigma_\delta\ (\eta < 2.2)$	$(17.7 \pm 1.2)\,\mathrm{keV}^{-1}$
$\sigma_\delta\ (2.2 < \eta < 4.4)$	$(14.9 \pm 0.9)\,\mathrm{keV}^{-1}$
σ_{MS}	$(2.015 \pm 0.019) \times 10^{-3}$

Our tunes to the Z p_T data

Program	χ^2/ndf	α_s	k_T^{intr} [GeV]
DYTurbo	79.5/13	0.11800	2.330 ± 0.028
POWHEGPythia	30.3/12	0.12476 ± 0.00043	1.470 ± 0.130
POWHEGHerwig	55.6/12	0.13613 ± 0.00007	0.802 ± 0.053
HerwigNLO	41.8/12	0.13520 ± 0.00019	0.753 ± 0.052
Pythia 8, CT09MCS	69.0/12	0.12870 ± 0.00044	2.113 ± 0.032
Pythia 8, NNPDF31	62.1/12	0.12893 ± 0.00044	2.109 ± 0.032

Data challenge exercise

Data config.	χ^2_W	χ^2_Z	δm_W [MeV]	α_s^Z	α_s^W	f_{A_3}
POWHEGPYTHIA	64.8	34.2	–	0.1246 ± 0.0002	0.1245 ± 0.0003	0.979 ± 0.029
HERWIGNLO	71.9	600.4	1.6	0.1206 ± 0.0002	0.1218 ± 0.0003	1.001 ± 0.029
POWHEGHERWIG	64.0	118.6	2.7	0.1206 ± 0.0002	0.1226 ± 0.0003	0.991 ± 0.029
PYTHIA 8, CT09MCS	71.0	215.8	-2.4	0.1239 ± 0.0002	0.1243 ± 0.0003	0.983 ± 0.029
PYTHIA 8, NNPDF31	66.9	156.2	-10.4	0.1225 ± 0.0002	0.1223 ± 0.0003	0.967 ± 0.029
DYTURBO	81.5	334.3	-0.8	0.1260 ± 0.0001	0.1276 ± 0.0003	0.968 ± 0.029

Consistency between orthogonal subsets of data

| Subset	$\chi^2_{\text{tot}}/\text{ndf}$	δm_W [MeV]
Polarity $= -1$	92.2/102	–
Polarity $= +1$	97.2/102	$+57.8 \pm 45.4$
$\eta > 3.3$	115.5/102	–
$\eta < 3.3$	85.4/102	-56.6 ± 45.5
Polarity $\times\ q = +1$	97.7/102	–
Polarity $\times\ q = -1$	95.7/102	$+15.1 \pm 45.4$
$|\phi| > \pi/2$	98.8/102	–
$|\phi| < \pi/2$	114.6/102	$+65.5 \pm 45.5$
$\phi < 0$	91.7/102	–
$\phi > 0$	102.5/102	100.1 ± 45.3

Varying the freedom of the fit model

| Configuration change	$\chi^2_{\text{tot}}/\text{ndf}$	δm_W [MeV]	$\sigma(m_W)$ [MeV]
$2 \to 3$ floating α_s params	103.3/101	4.9	$\pm$ 23.1
$2 \to 1$ floating α_s param	128.2/103	-39.0	$\pm$ 21.1
$2 \to 1 \, \alpha_s$ and $1 \to 2 \, k_T^{\text{intr}}$ params	116.0/102	-14.5	$\pm$ 22.4
$1 \to 2$ floating k_T^{intr} params	103.6/101	-1.3	$\pm$ 22.7
$1 \to 3$ floating k_T^{intr} params	102.6/100	2.0	$\pm$ 22.9
Fixed $fA_3 = 1$	105.3/103	-4.1	$\pm$ 22.2
Floating QCBGD background asymmetry	103.7/101	0.2	$\pm$ 22.7

Stability w.r.t. varying the [q/p$_T$] fit range

Change to fit range	$\chi^2_{\rm tot}/{\rm ndf}$	δm_W [MeV]	$\sigma(m_W)$ [MeV]
$p_{\rm T}^{\min} = 24$ GeV	94.4/122	-2.0	19.7
$p_{\rm T}^{\min} = 26$ GeV	95.9/102	-7.8	20.9
$p_{\rm T}^{\min} = 30$ GeV	102.7/102	0.3	25.7
$p_{\rm T}^{\min} = 32$ GeV	85.0/102	18.6	30.8
$p_{\rm T}^{\max} = 48$ GeV	105.0/102	3.2	23.2
$p_{\rm T}^{\max} = 50$ GeV	102.6/102	2.0	23.0
$p_{\rm T}^{\max} = 54$ GeV	96.0/102	8.3	22.6
$p_{\rm T}^{\max} = 56$ GeV	103.4/102	13.9	22.4

Example postfit projections
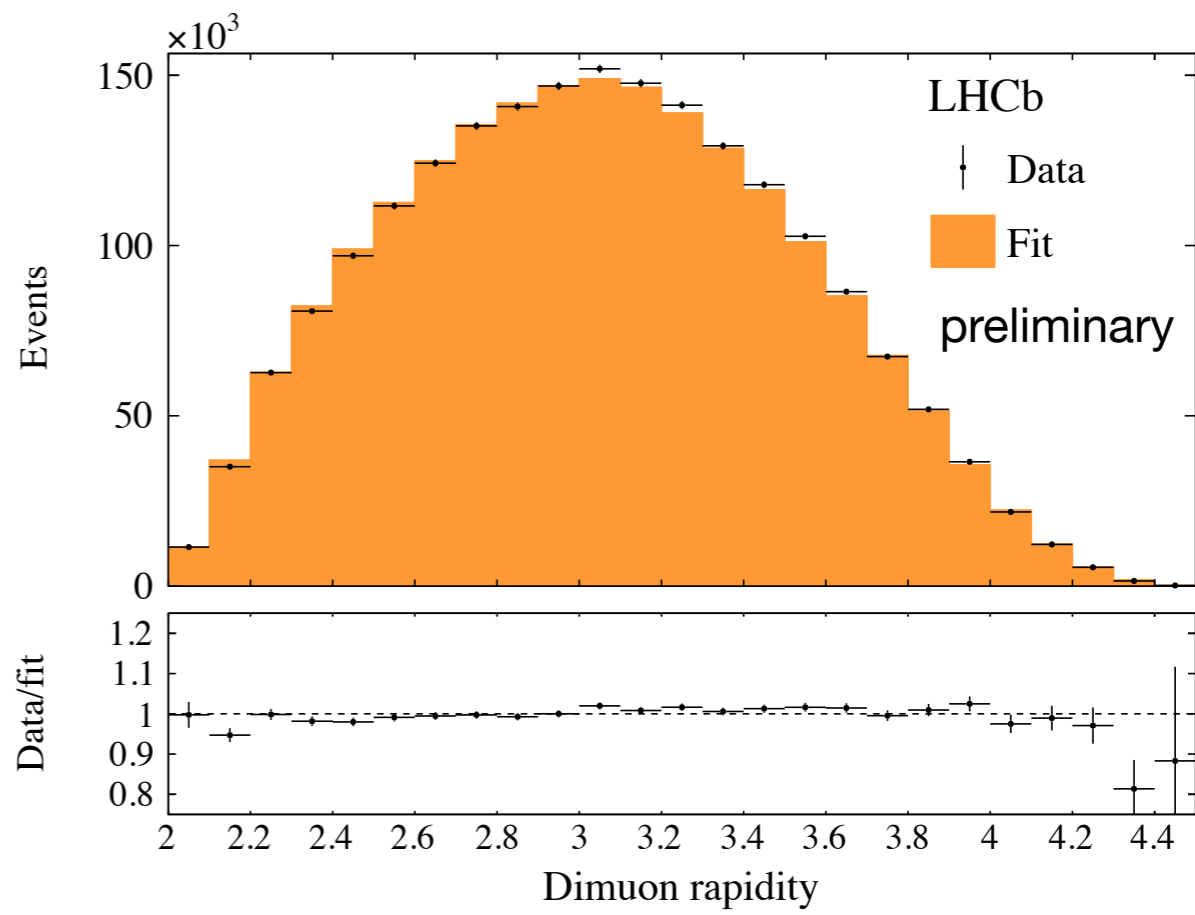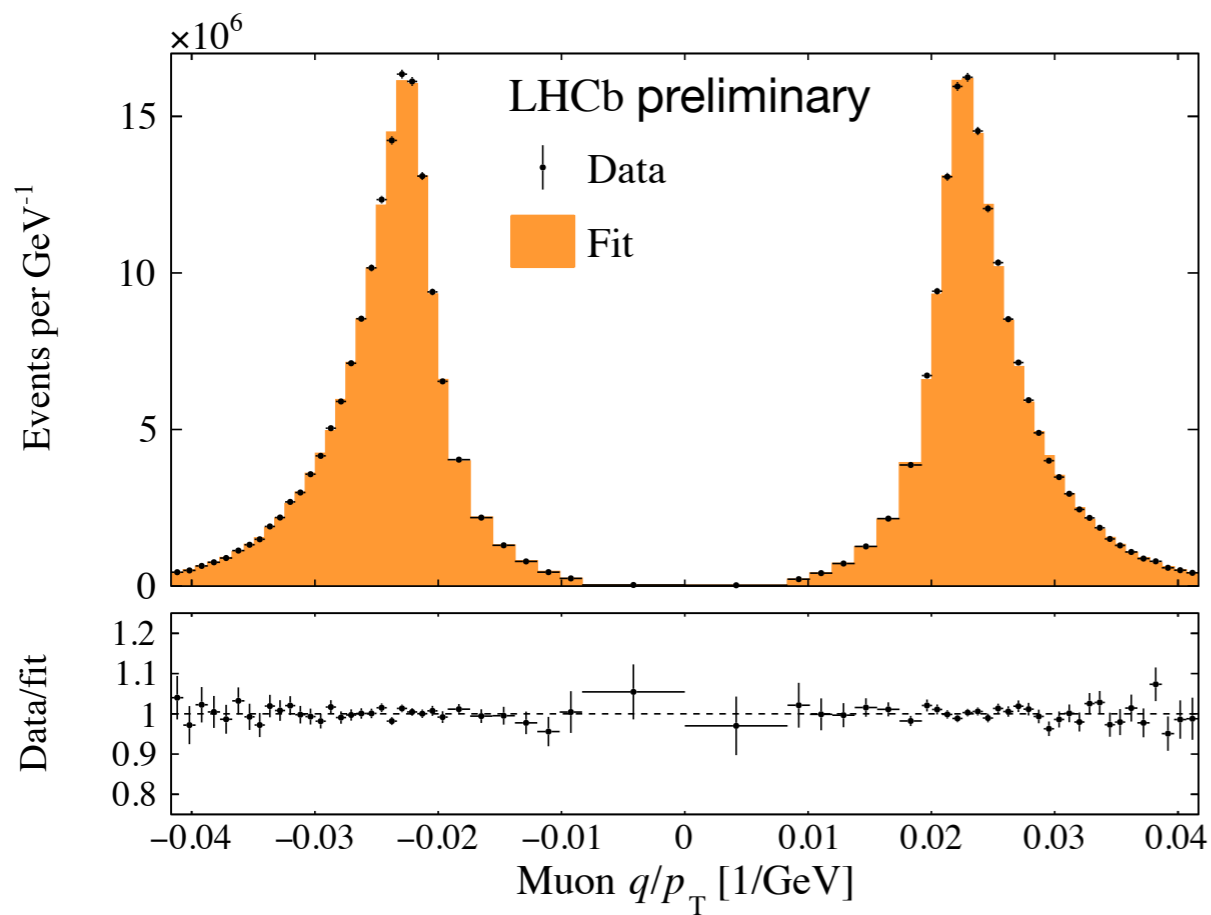
Parametric correction at high boson p_T
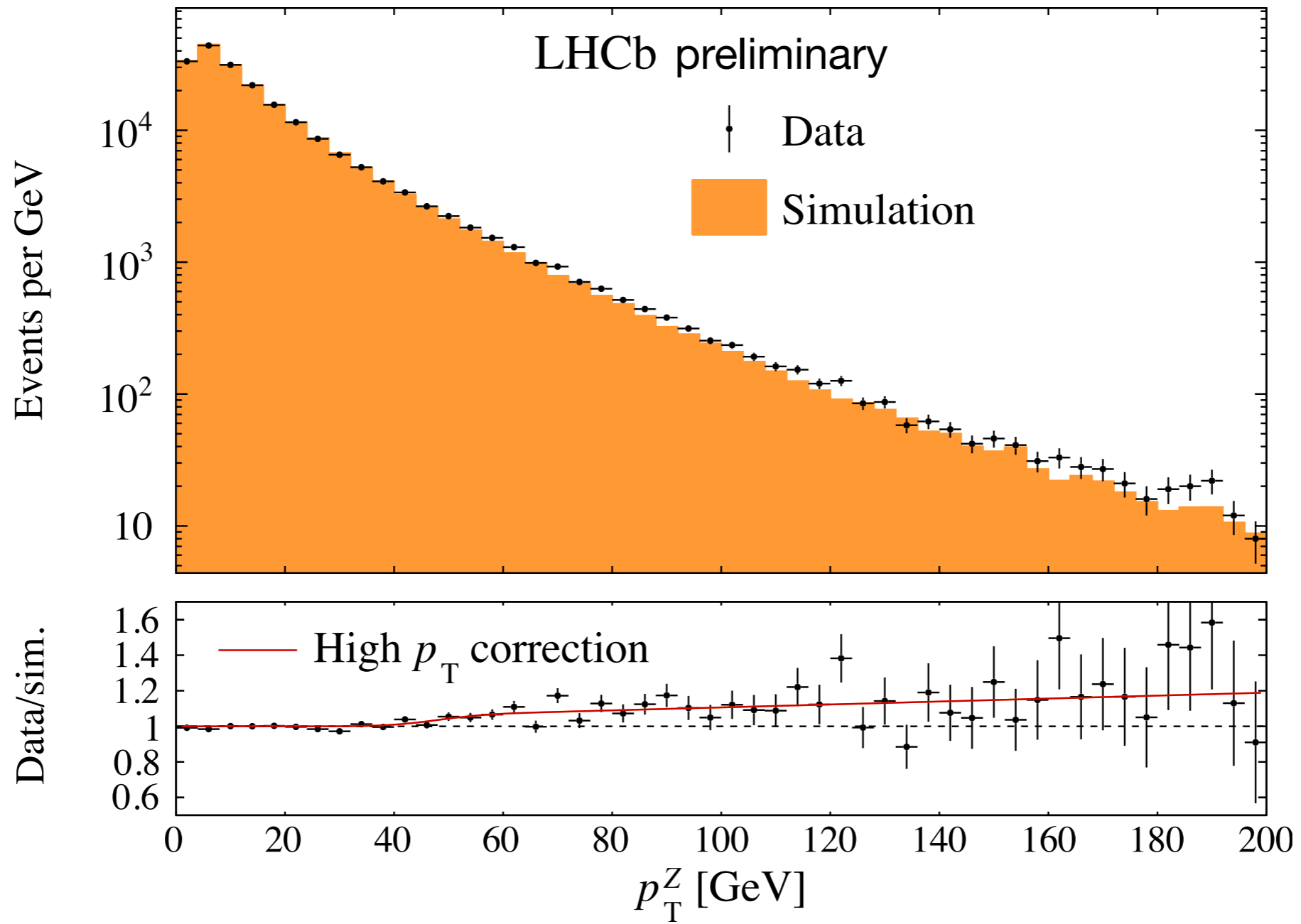
Also applied to the model of W production but with 100% uncertainty => ~1 MeV on m$_W$.